Development of a 3D Water Flow Modelling Based on Scarce Data for Arid Land Water Resources Management: Case study of Ambouli and Kourtimalei Watersheds in Djibouti

2018

Fadoumo Ali MALOW

TOKYO UNIVERSITY OF AGRICULTURE – JAPAN

THESIS DISSERTATION FOR THE DEGREE OF

PH. D. IN AGRICULTURAL ENGINEERING

DEVELOPMENT OF A 3D WATER FLOW MODELLING BASED ON SCARCE DATA FOR ARID LAND WATER RESOURCES MANAGEMENT:

Case study of Ambouli and Kourtimalei Watersheds in Djibouti

Fadoumo ALI MALOW

Supervisor: **Professor Dr. Sawahiko SHIMADA**

Advisors: **Professor Dr. Hiromu OKAZAWA**

Professor Dr. Naomasa HONDA

Associate Professor Dr. Ayako SEKIYAMA

Professor Dr. Hiroyuki TOSAKA

March 2018

ABSTRACT

Water shortage and groundwater degradation have become two primary environmental concerns to Djibouti since the 1990s. Due to semi-arid to arid climatic conditions the mean annual precipitation averages only 150 mm in a very erratic uneven way. The country, especially the capital city, has to face continuously difficulties in its water supply which is derived by 95% from groundwater. The economic development programs and population growth in Djibouti city has increased groundwater demand leading to an overall overexploitation of the resources and water quality degradation. Future water requirement is likely to increase more than the present production rate.

Understanding the hydrogeological system is fundamental for a sustainable water resources management. However, in Djibouti, the available information on water resources is scarce and insufficient. The present work focused on case study of watersheds in Djibouti (Ambouli and Kourtimalei) by the setting up and calibrating of numerical hydrologic model GETFLOWS in effort for sustainable management. Despite the lack of information, the model was able to reproduce correctly the main behavior of the system with a reasonable accuracy for both surface and subsurface level.

In Kourtimalei watershed, a rainfall-runoff simulation was run with GETFLOWS, and calibrated the model by using both water levels observations data, and then evaluated the results with satellite derived datasets. GETFLOWS model was able to reproduce the rainfall-runoff process of the watershed fairly with RMSE of 0.40 m and a Kappa coefficient higher than 0.80.

In Ambouli watershed, good agreement between simulated and observed groundwater heads with r^2 of 0.9 is obtained. The transient groundwater flow simulations reflected the observed drawdown of the last 40 years and show the formation of a depression cone in an intensively pumped area. However, some additional improvements should be made for the model to increase in the representativeness of the system. In the future this tool can be used as part of an integrated watershed management tool.

日本語要約

アフリカ大陸東北部の「アフリカの角」に位置する国々は、2007 年から続いた大干ばつによる貧困や飢餓の危機に常にさらされている。中でもジブチ共和国は、地溝帯の陸部北端に位置する立地条件の影響で国土の大部分を玄武岩で覆われた地表面環境であることに加え、年間降水量が 150 mm 程度、夏季の最高気温が 40℃を上回る最も自然環境の過酷な国である。流水河川は存在せず、ワジ（涸れ川）のみ存在し、水資源はほとんど地下水に依存している（年間消費水量 21,700,000 m^3 の 98%）。このような環境下のジブチにおいては降雨に依存した作物栽培は成立せず、ワジ周辺において得られる浅層水が農業・畜産・生活用水として主に利用されてきた。水資源不足・汚染の問題は 1990 年代からジブチにおける課題となってきた. しかし、このような水資源の賦存量や水循環は把握がなされていないのが現状である。

本研究では乾燥地水資源管理を目的とし、気象データ・GIS データを駆使し地質の水文地質パラメータをトライアル・アンド・エラーにより決定することにより、不十分なデータ条件下にありながら、アンブリ・ワジ（Wadi Ambouli）流域（643 km^2）およびクルチマレ（Kourtimalei）集水域（40.6 km^2）における 3D 水循環モデルを構築し、高い精度で水循環を再現できることを検証した。水循環シミュレータには、表流水流れにマニングの平均流速公式、地下多孔質媒体中の空気・水 2 相流れに一般化ダルシー則を用いた統合型水循環シミュレータ（GETFLOWS）を採用した。標高図（Aster-GDEM，ALOS-World3D-5m）、地質図（ORSTOM 1985）、井戸・ボーリングデータ（Ministry of Agriculture, Fishery and Livestock in Charge of Marine Resources, Djibouti）をベースモデルとし降雨・気温（Meteorology Agency Djibouti および実測データ）用いて、初期化・最適化・再現シミュレーションを行った。トライアル・アンド・エラーにより、沖積砂質土（Alluvial Fan）および玄武岩石被覆地（Basalt Rock）におけるマニングの粗度係数（n）はそれぞれ、0.040，0.027 と決定され、沖積層（Alluvium Deposit）および玄武岩層（Gulf, Stratoid, Dalha, Somali Basalts）の絶対浸透率（K）はそれぞれ、1.37×10^{-10} m^2（初期値同値）、0.9～3.5×10^{-6} m^2 と決定された。結果検証は、Wadi Ambouli 流域ケースにおいては、算出される定常時の地下水位値（m）と現地井戸・ボーリング孔での実測データとの比較、Kourtimalei 集水域ケースにおいては、2013 年 8 月～12 月の雨量計による実測雨量イベントに対する農業用ため池の面積のシミュレーションと時系列衛星画像（Landsat-8）との比較により行った。数値解析の結果、定常状態における地下水動態が推定可能（地下水位 RMSE：11.37 m）であること、降雨イベントベースの流出動態が高精度で推定可能（ため池水位 RMSE：0.40 m, $\kappa>0.8$）であることを示した。さらにジブチ・シティ周辺の取水地点における 1960 年代からの地下水揚水量（245 m^3 day^{-1}）を加味し、地点における ca. 1.5 m/40yr の地下水低下減少を高精度（RMSE：0.15 m）で推定することに成功した。また、Ambouli 流域の各玄武岩帯水層内に蓄積されている地下水賦存量の推定分布図を示すことが可能となった。これら得られた研究成果は、ジブチ国の今後の水資源管理に資する技術として有用であり、他の乾燥地での広域水循環把握にも適用可能である。

ACKNOWLEDGMENT

I have the greatest appreciation for my first supervisor Dr. Sawahiko Shimada who hosted me in his team and helped me to define the good development of the Ph. D. work during the field work in Djibouti as well as during all my stays in the Tokyo University of Agriculture, Japan. Above all I am indebted to his unceasing support and guidance and encouragement throughout my study period and thesis time. I really appreciate his constructive criticism and valuable advice which helped me to develop research skills.

I have also the greatest appreciation for Dr. Toyoda and Dr. Sekiyama for their valuable support and guidance during my research period in the laboratory.

I have also benefited a lot from discussions I had with Mr. Toru Yoritate and Dr. Tosaka from which I gained a deeper insight and understanding into the governing factors of groundwater occurrence and movement. They taught me so many of the aspects in groundwater modeling principles and I am grateful for his critical comments during the thesis preparation time.

I acknowledge the support during my laboratory work to Mr. Aurelien Hazard and Ms. Nobuko Kakizawa. It is also my pleasure to thank all GET Corp. staff for their help. This work would not have been achieved without them.

I also wish to express my appreciation to all my class mates for their friendship, support, socialization and help each other in times of pressure and stress.

Finally, I owe special gratitude to all my family members and friends back home for always being there for me.

Thank you all

TABLE OF CONTENTS

CHAPTER IV: NUMERICAL MODELLING

CHAPTER V: USING GETFLOWS FOR SURFACE WATER FLOW: APPLICATION ON KOURTIMALEI

CHAPTER VI: DEVELOPMENT OF 3D NUMERICAL MODEL OF AMBOULI WATERSHED

CONCLUSIONS AND PERSPECTIVES

List of Tables

List of Figures

CHAPITRE I:

GENERALE INTRODUCTION

CHAPITRE I:
GENERALE INTRODUCTION

1.1 BACKGROUND AND MOTIVATION

The Republic of Djibouti (23,200 km² and 520,000 inhabitants) is located in the Horn of Africa. The arid climate regime to semi-arid, low rainfall (on average 150 mm yr^{-1}) and the virtual absence of surface water has led the country to exploit intensive groundwater. The hydrographic network is formed essentially by many temporary streams (wadis) that flow only during periods of high rainfall. There is virtually no surface water. Thereby, the country's water supply is based on the volcanic aquifers that represent large potential reservoirs that may contain the necessary water resources. Indeed, volcanic rocks cover most of the territory (80%), the formations of sedimentary remains of small extent. These volcanic aquifers are intensely exploited, and this overexploitation, by the lack of knowledge of hydrodynamics, has led to the degradation of water quality and the lowering of the water table levels, which is not offset by the low recharge amplitude.

The country derives most of its water needs (80%, 17.5 Mm^3 yr^{-1}) from fractured volcanic aquifers. The lack of knowledge about the hydrogeology of these reservoirs has created many problems of exploitation and management of resources. Signs of overexploitation are seen mainly on water points of the basaltic aquifer of Djibouti city by salinization. Because of this scarce water availability and poor soil, only 0.04% of the land in Djibouti is arable. Over 50% of the land is permanent pastures used for livestock, but scarce water availability and overgrazing has contributed to significant land degradation and desertification. This barren landscape and limited water supply provides little space for agricultural development – which only supplies 3% of national GDP (Aquastat FAO, 2007).

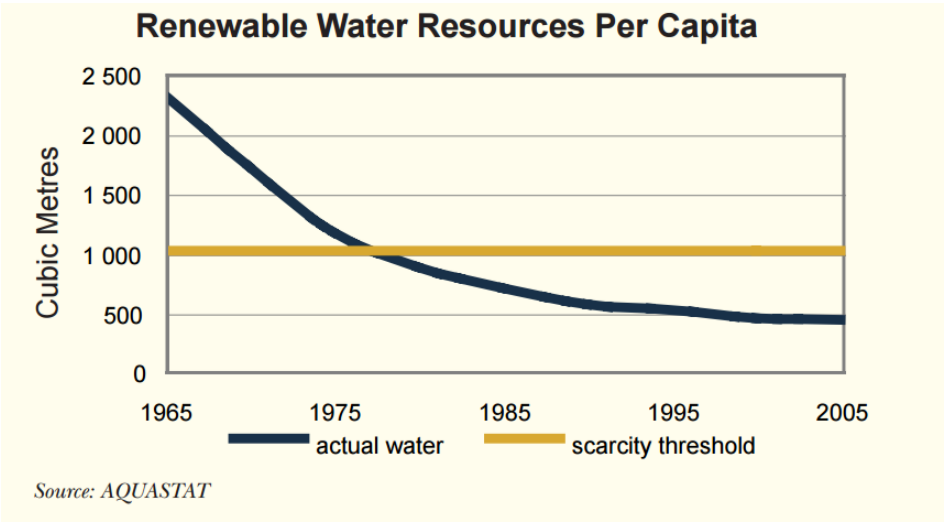

Figure 1.1: Renewable water resources per capita

To remedy such a situation and respond effectively to the different water needs of the country, the National Commission for Water Resources has drawn up a Master Plan for Water in 2000, which includes a number of major programs particularly concerning the supply of drinking water to the city of Djibouti, which groups nearly 83% of the population and the main economic activities. A Secretariat Water Technique, responsible for coordinating the actions undertaken was created. Work presented here is part of a contribution to the objectives set out in the Scheme Director of Water, and particularly that of studying the watershed of Djibouti. Indeed, the basaltic aquifer of Djibouti located in coastal zone is sheltered in basaltic formations from the opening of the Gulf of Tadjourah. This aquifer supplying the capital is the most exploited of the country. The hydrogeological study of this aquifer is therefore of huge importance for the Republic of Djibouti (RDD), faced with problems of availability and quality of the water. The Technical Secretariat for Water comprises three main bodies working on the water resource of the country. The CERD (Center of Studies and Research of Djibouti) works on the research nationwide through its Hydrogeology/Hydrology laboratories and of Hydrochemistry. ONEAD

(National Office of Water and Sanitation of Djibouti) is the operator of underground aquifers, responsible for supplying drinking water to urban centers. The Department of Water, Ministry of Agriculture, Livestock and Sea, responsible for MAEM-RH, is responsible for ensuring the water supply of rural populations.

At the regional level, there is a great similarity of geological formations, essentially basaltic, whose hydrogeology is still poorly known. In addition, it is necessary note that the world literature provides little information on the hydrogeology of volcanic media. The study proposed here is therefore of particular interest for the management and protection of regional volcanic aquifers.

1.2 RESEARCH OBJECTIVES

The work undertaken in this project aims to characterize watershed, improve geological and hydrogeological knowledge of fractured medium, to understand the processes of recharge and flow in arid condition, to characterize the degree of heterogeneity, determine the hydrodynamic specificities of the aquifer. Ultimately, the thesis aims to develop a numerical tool for sustainable management of the water resources of this reservoir.

1.3 STRUCTURATION OF THE THESIS

This thesis is structured in 6 chapters including the introduction and the general conclusion.

Chapter I relate to a general introduction to the thesis

Chapters II provides a general overview of knowledge both nationally and regionally study. It describes the geology as well as the hydrogeological role of geological formations.

Chapter III stresses the review of previous studies in the area and literature review related to challenges facing the water resources management are discussed

Chapter IV: Numerical modeling, this chapter is mainly designed to discuss the code selection, model design, model calibration and analysis

Chapter V: Development of 3-D model pf Kourtimalei watershed. The main task of this chapter is development of 3D model of the area in order to investigate the surface flows circulation during an event of rainfall-runoff.

Chapter VI: is specific to the studies conducted as part of this work for the Ambouli watershed. Development of conceptual model then 3D model, results and discussion, Illustration and discussion of the modeling results are presented in this chapter

Chapter VII: Conclusions and recommendations will be made on the basis of the analysis result. In this final chapter, matters which cannot be addressed fully or partially are out lined and limitation of the research and possibilities of further research are indicated

CHAPTER II:

HYDROGEOLOGY OF DJIBOUTI: REVIEW OF THE LITERATURE

CHAPTER II: HYDROGEOLOGY OF DJIBOUTI: REVIEW OF THE LITERATURE

INTRODUCTION

The Republic of Djibouti is an interesting territory from the geological point of view and tectonic, due to the activity of the East African rift. The water resource is limited because of semi-arid climate. The case of the basaltic aquifer of Djibouti, the most exploited of the country, provide an overview of the potential degradation of groundwater in the event of uncontrolled exploitation. In this chapter a general description of the geology and water resources of the country is carried out.

TOPOGRAPHY

Territory of 23 000 km², the Republic of Djibouti (RDD) is contained in south of the Afar triangle geological zones where Africa, Arabia and Somali tectonic plates contact each other. In the Afar triangle zone, the Great Rift Valley was formed by the expanding tectonic plates Somalia to the southeast, Eritrea to the north and Ethiopia to the rest of its western frontage. The north-east it is bounded by the Red Sea and Bab El-Mandeb Strait, to the east by the Gulf from Aden which extends to the west by the Gulf of Tadjourah and Goubbet-El-Kharab (Figure 1-1).

From a morphological point of view, several sets can be recognized (Figure 1.1): east of large coastal plains, formed mainly of alluvial deposits (plain coastal Tadjourah) and coral reefs (Obock coastal plain); to the western region, made up of horsts (Dakka, Yager)

whose altitude is often beyond 1,000 m and grabens filled with recent lacustrine sediments (Asal, Gaggadé, Hanlé, Gobaad, Alol). The upper level of filling of these ditches decreases from Southwest to Northeast and goes from +250 m in the basin of Lake Abhé (Gobaad) to -155 m in the depression of Asal.

Between these two regions, there is a relief of basaltic plateaus (Dalha, Mak'arrassou) and rhyolitic massifs that often rise to more than 1000 m (Day, Mabla, Ali Sabieh and Moussa Ali which culminates at 2,021 m). This N-S mean axis is split in two by the Gulf of Tadjourah whose bottom rises progressively from -1,500 m to the East (Obock pit) to -200 m in the west (Goubet).

GEOLOGY

Rocks found in the Republic of Djibouti result from volcanic activity related to the expansion of the tectonic plates of the region. Essentially constituted of basalts and some rhyolitic formations, the volcanic rocks cover the major part of the territory. The geographical distribution and ages of volcanic series trace the chronology of tectonic plate movements of the latter 25-30 Ma (Figure 1-2). At the beginning of the expansion, the first break-up movements of the Arab-Nubian massif, Miocene inferior, are accompanied by basaltic emissions (Adolei basalts). These basalts cover the Mesozoic sedimentary basement. At this stage, follows a period slow expansion, marked by the thick rhyolitic series of Mabla (15 Ma). After a phase of erosion marked by conglomerates and a sometimes preserved paléorelief, the activity volcanic resumed in the late Miocene with the establishment of the basaltic series of Dalha (3.4 - 9 Ma) which rests with angular discordance on Mabla rhyolites.

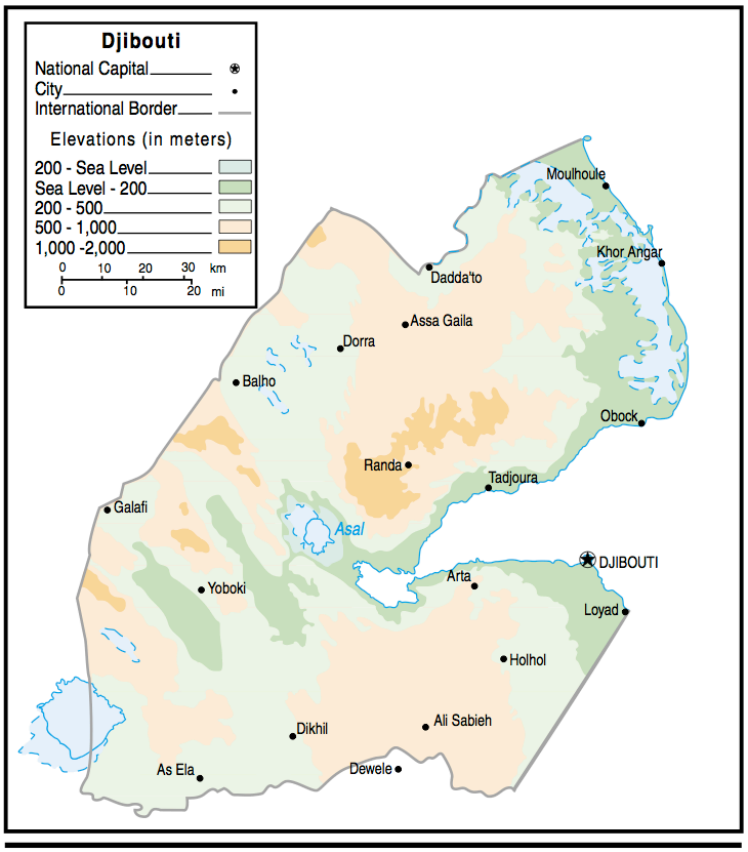

Figure 1.1: Topography and Drainage of Djibouti

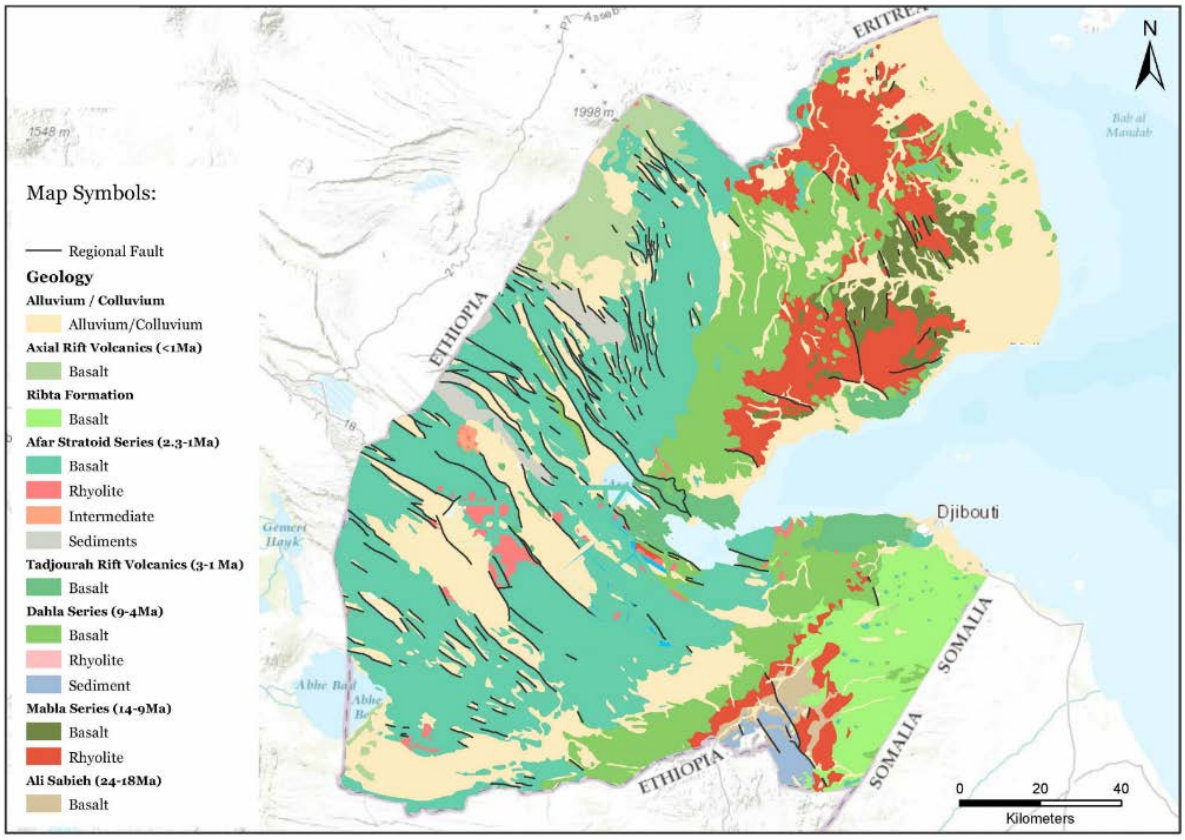

Figure 1.2: Geology of Djibouti

At the same time, Somali basalts are deposited in the south-east of the Republic of Djibouti. (Barberi and Varet 1977, Arthaud et al 1980). Between 3.4 and 1.5 Ma, the Stratoid basalts and the basalt of the Gulf are set up with the opening of the Gulf of Tadjourah. The recent volcanic formations are located on the active rifts of Asal (center of the country) and Manda Inakir (in the north-west of the country) (Audin et al., 1990).

Geodynamic evolution is determining for sedimentation: the formation of sedimentary basins is of origin tectonic. Once in place, their sedimentation is mainly governed by the climatic factors. Sedimentary formations are less widespread on the surface than volcanic rocks. They are found in large sedimentary basins (Gobaad, Hanle, Gaggadé ...), along the main wadis and in areas of alteration on the plateauxbasaltic. The north coast of the Gulf of Tadjourah, the coast between Obock and Doumeira and the plain coastal areas of Djibouti are sedimentary.

WATER RESOURCES

In Djibouti, the renewable water resources are estimated at 300 Mm^3 yr^{-1}. The rivers are not perennial because of the low rainfall, but contribute to the supply of groundwater (only the Djibouti aquifer is currently being followed). In general, flow rates are low with a salt content between 1 and 1.5 g L^{-1}. Only about 5% of the precipitation is likely to seep and recharge the shallow (wadi sediment) or deep aquifers (basaltic aquifers). While 83.5% of rainfall evaporates to the air, the rest flows surface (6%), penetrates into sub-surface (5.5%) and ground (5%). Water volume penetrating into sub-surface and ground is roughly estimated to be 34 5Mm^3 yr^{-1}. (= 11.5% of total rainfall). This would be 3,000 Mm^3 in volume and 130 mm in intensity of the mean annual rainfall in Djibouti.

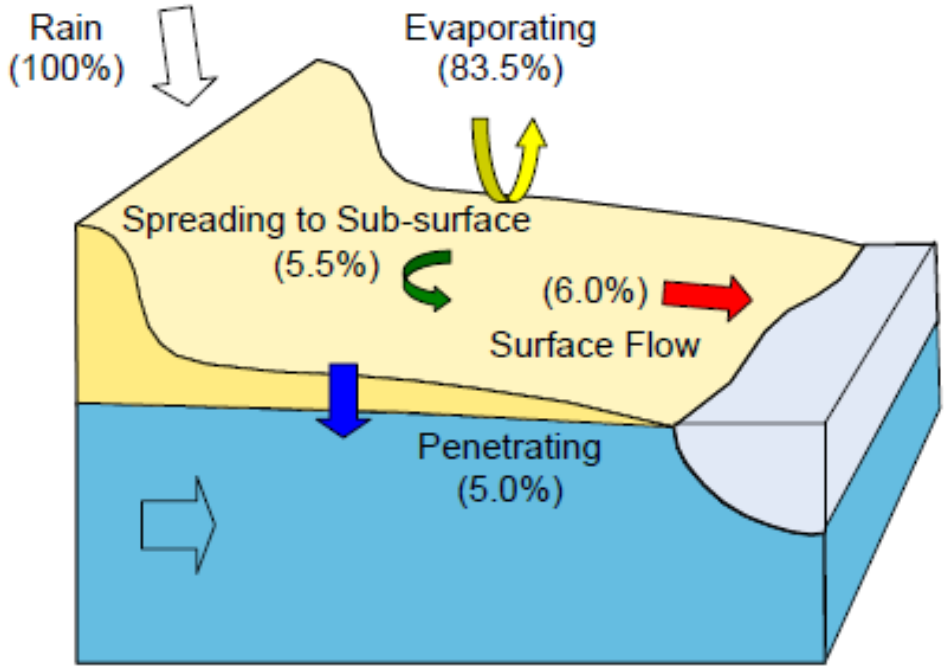

Figure 1.4: Conceptual Figure of Rainfall and Outflow

SURFACE WATER

In Djibouti, there are no permanent watercourses except for a few waterfalls located at high altitude in the Goda Mountains. All wadis draw a dense hydrographic network. These are not sustainable, due to the low rainfall, but contribute to the supply of groundwater. Because of the slope relatively strong and of the edaphic context, the hydrology of most wadis is present in the form of flash floods and very limited in time, causes spectacular floods that cause damage to the road building and the environment in general. In all, the hydrographic network is subdivided into two sub-networks:

• Wadis that throw their waters into the depressions of the interior (flow endoreic)

• Flows that pour into the bitter (exoreic flow) with the line of north-south sharing of direction through Lake Asal and Goubet.

The hydrographic network covers about 53 watersheds, almost half to a catchment area of

less than 100 km^2. Runoff that represents only 6% of the rainfall is characterized by a strong power because of the bare state of the ground surface and especially important slopes. The runoff can represent large volumes of water discharged at the time of torrential floods. The floods are very abrupt and are only generated with rainfall more than 10 mm high.

Surface water resources are still underutilized. However, it has been demonstrated even in the absence of reliable hydrometric data that the mobilization of this water resource is not as easy and more expensive that we can think at first sight. The rivers are too violent (energy kinetics / power) and too much sediment to allow what a mobilization solution. The conditions of flow of surface water, in torrential regime, make particularly difficult the use of surface water. The impounded water volume varies every year depending on the amount of rainfall.

GROUNDWATER

In Djibouti, Two main types of aquifer system are encountered in RDD: aquifers Sedimentary rocks and aquifers of volcanic formations (Figure 1.6). Aquifers sediments include inferoflux aquifers and alluvial plains aquifers. The aquifers of the volcanic formations are divided into two groups. The aquifers of low extent (<2,000 km² area) and the regional aquifer hosted by basalts Stratoids, covering more than 9,000 km² of the country. Inferior water aquifers (invisible at scale of the map of Figure 1.7) are located only in the alluvial wadis. Those are

subflows of superficial streams.

Their width is between a few tens to a few hundred meters and their length can exceed several tens of kilometers. The thickness of the inferoflux aquifers generally

remains of the order of a few tens of meters. These aquifers are exploited in the rural environment by over 700 large diameter wells, and some cased wells for domestic use and agriculture, totaling 4.2 Mm^3 yr^{-1}. This intensive pumping especially in areas agriculture, representing more than 70% of rural needs, leads to over-exploitation of this resource. The aquifers of the alluvial plains, including the aquifers of the Sedimentation and coastal plains cover 22% of the territory. Their area varies from 40 km² to 1,500 km² and their thickness between 40 m and 300 m. Twenty boreholes pump these tablecloths 1 Mm^3 yr^{-1} in rural areas and for the food of the cities of Tadjourah and Obock. The alluvial layer of Tadjourah would be largely fed by a stream underground from the volcanic massif upstream (Houmed-Gaba et al., 2006).

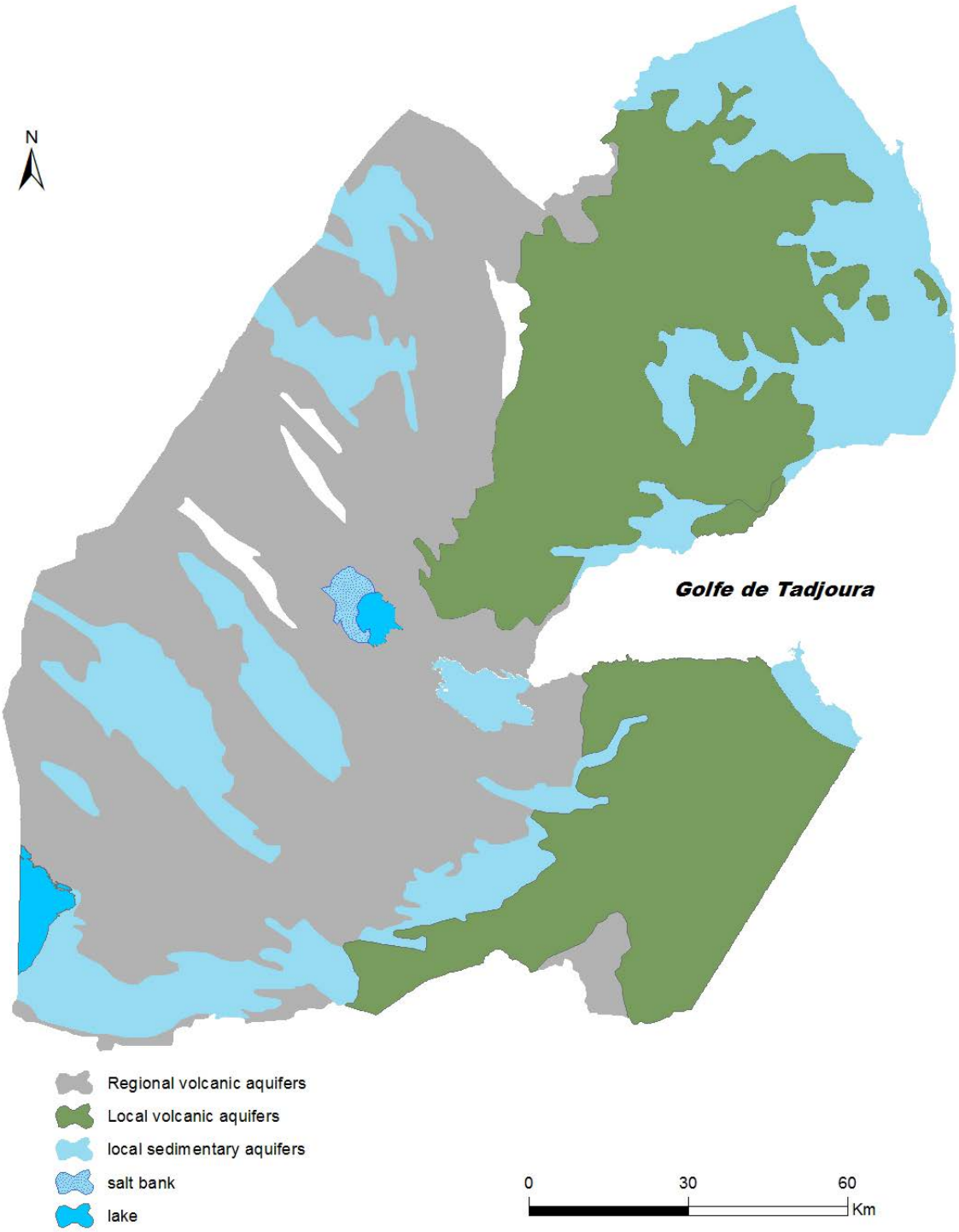

Figure 1.6: Type of Aquifer in Djibouti

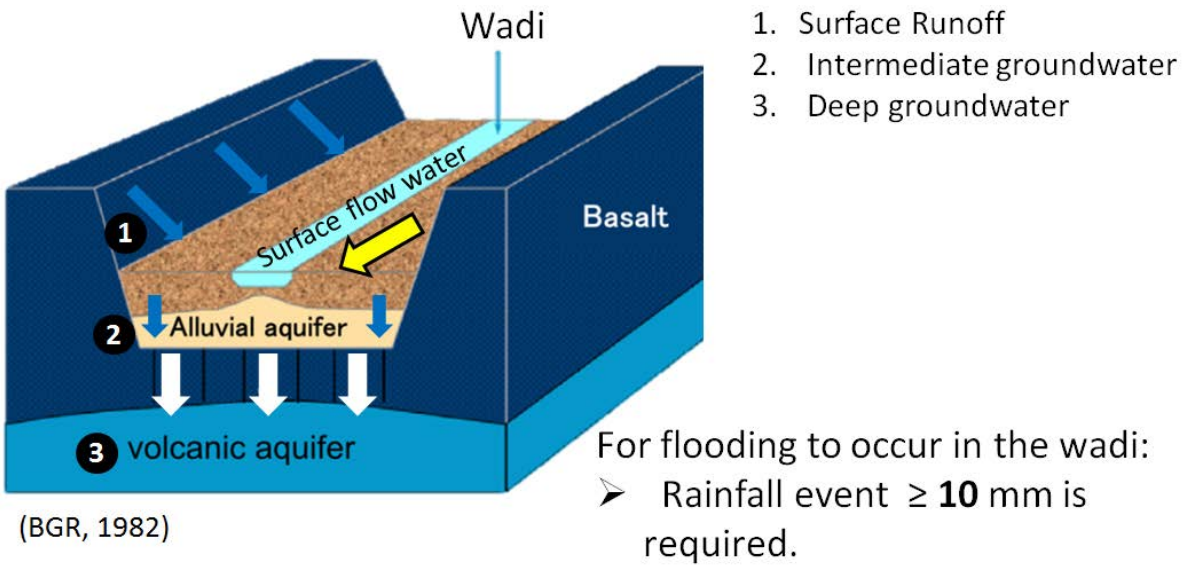

Figure 1.7: Hydro-geological processes

Aquifers of small volcanic formations (<2000 km²) are localized recharge through the wadi beds (Jalludin and Razack, 1994). These aquifers Volcanic are local extension. Their thicknesses often exceed 200 m. The hydrothermal circulations that settle in these formations eventually clog, completely or in part, cracks with deposits of calcite and silica, which decreases considerably the permeability of these aquifers. This is how Adolei basalts, the most ancient volcanic formations of the country are also the least permeable. From Local volcanic aquifers Basalt aquifer of the Gulf and Somali is the most intensively exploited at 36,000 m^3 d^{-1}. This aquifer supplies the city of Djibouti. The Stratoid volcanic series cover more than 9,000 km² of the country's surface. She is carpeting practically all the hinterland and continues in Ethiopia beyond the river regions Awash. These contemporary volcanic rocks of the Gulf basalt can go up to1,300 m thick and occupy most of the Afar depression. Because of its dimensions considerable, it was recognized that this volcanic unit formed the regional volcanic aquifer.

Preliminary studies suggest that this aquifer is fed by a flow underground from the

Awash River in Ethiopia (Houmed-gaba et al., 2002).

An aquifer exists in cracks and fissures of wide spreading volcanic rock (basalt and Rhyolite) and also in the layer of scoriae and/or fracture zone of fault. Cracks in the volcanic rock are formed during the cooling stage of erupted rock and by the movement of the rift valley. Along the wadi, where surface flow water after rain come, pervious sand and gravel deposit layer is formed and it is an aquifer of surface water.

Djibouti has scarce rainfall and high rate of evaporation. Therefore, rainfall cannot supply much water to aquifer in the rock foundation. If salty ingredients are accumulated by repetition of the evaporation, the salinity of the water in the aquifer increases. Under these natural conditions, development of abundant volume of the water in the aquifer is not easy for drinking. Most wadis flow to low elevation inland lakes. Salt is accumulated in the inland lakes by repetition of impoundment and evaporation.

METEOROLOGY

The country is mainly a stony semi-desert, with scattered plateaus and highlands. The climate in Djibouti is hot and humid year-round. It is characterized as typical arid type with fluctuating and low rainfall and continuous high temperature in summer. Meteorological observation had been conducted at 38 stations in the whole country since 1936. However, the meteorological data of most stations had not been collected after the early 1990s. The meteorological observation has been continued only at Djibouti airport. The installation of meteorological observation stations was started again on the whole country in 2013, and collecting and compiling of the meteorological data were restarted.

The meteorological data of Djibouti reveals the fact that annual precipitation during the period of 2007 to 2010 was drastically low 50 mm more or less, which is around one third of the past annual mean precipitation.

Table 2-1 Annual Precipitation in Djibouti (2000 – 2014) Unit: mm

year	2004	2005	2006	2007	2008	2009	2010	2011	2012	2013	2014
Precipitation	207.6	96.2	182.5	33.8	66.5	33.5	55.5	88.8	--	52.6	---

. The maximum temperature rises over 40°C, and the minimum relative humidity is below 40% during summer season (June to August). The maximum wind speed rises in these months as well. In contrast, the temperature drops, and relative humidity rises during the winter season (October to April)

Table 2-2 Temperature C^0 min, max average-Djibouti-Ambouli in Djibouti (1953 – 1999)

	Jan	Feb	Mar	Av	May	Ju	Jul	Aug	Sep	Oct	Nov	Dec	Annual
T min	19.1	19.5	20.9	22.7	24.1	26.4	27..7	27.1	25.9	22.5	20.7	19.4	23.0
Tmax	30.0	30.7	32.6	34.7	39.1	44.0	44.0	42.4	35.9	32.6	30.5	36.7	36.7
T ave	24.5	25.1	26.7	28.7	31.6	35.2	36.2	35.6	34.2	29.2	26.6	24.9	29.9

CONCLUSION

Understanding the particular environmental settings of the country is critical for understanding the challenges of the water resources questions. The Djibouti aquifer has been the subject of many studies since the first note preliminary report on water resources in the Djibouti region of NEYRPIC (1953). In the beginning, the extension of the

exploitation areas was always preceded by more or less extensive, but limited to the targeted area. As a result, we have today a mass of fragmentary information, difficult to find and to regroup. It's very late in the nineties that the Djibouti aquifer began to be studied as a whole. It is true that the authors quickly realized the complexity of this aquifer system. It is difficult to recognize the outlines.

REFERENCES:

Arthaud F., Choukroune P., Robineau B., 1980a. Tectonique, microtectonique et évolution structurale du golfe de Tadjourah et du Sud de la Dépression Afar (République de Djibouti). Bulletin de la Société Géologique de France, t.XXII, n° 6, p. 901-908.

Audin J., Vellutini P.J., Coulon C., Piguet P., Vincent J., 1990. The 1928-1929 eruption of Kammourta volcano – Evidence of tectono-magmatic activity in the Manda-Inakir rift and comparison with the Asal rift, Afar depression, Republic of Djibouti. Bull. Volcanol., 52p.

Barberi F., Varet J., 1977. Small scale plate tectonics implication: volcanism of Afar. Geol. Soc. of Am. Bull., 88, 1251-1266.

Daoud M.A., 2008. Dynamique du rifting continental de 30 Ma à l'actuel dans la partie Sud-Est du triangle Afar. Tectonique et magmatisme du Rift de Tadjourah et des domaines Danakil et Ali-Sabieh, République de Djibouti. Thèse de Doctorat, Université de Bretagne Occidentale, 157p.

Houmed-gaba A., Jalludin M., Razack M., 2002. Modélisation préliminaire de l'aquifère volcanique régionale de la région de la plaine de Hanlé. République de Djibouti. Revue Science et Environnement volume 16/02-CERD, p.7-21.

Houmed-gaba A., Jalludin M., Razack M., 2006. L'aquifère côtier de Tadjourah : Synthèse des connaissances et modélisation en vue de la gestion des ressources en eau (République de Djibouti). Proceeding International Conference, GIRE3D, Marrakech, p.23-27.

CHAPTER III:

GROUNDWATER AND THE CHALLENGES FOR THE FUTURE WATER SUPPLY OF DJIBOUTI CITY

CHAPTER III: GROUNDWATER AND THE CHALLENGES FOR THE FUTURE WATER SUPPLY OF DJIBOUTI CITY

3.1 INTRODUCTION

The country continuously has to face difficulties in its water supply which is mostly derived from groundwater. 29.4 Mm^3 per year are produced from volcanic and sedimentary aquifers of which 5.7% is used by the rural population and for cattle farming, 42.5% for irrigation and 51.7% for urban areas. Given the problems of falling water tables, water quality degradation and high TDS contents, alternative solutions have been used, i.e., surface water and desalination of high TDS-content aquifers. Nevertheless, the economic development programs and population growth in the future will likely continue to increase groundwater demand over the next years. To fulfil the demands for water over the next years, the production rate must increase more than the present production rate. That is why for the sustainability of ground-water resource, y management and protection of the aquifer systems should be implemented and not just the search for new groundwater resources.

3.2 HISTORY OF WATER PRODUCTION

The country has 371 wells (55 boreholes for Djibouti and 25 for the rest of the

country) of which only a hundred are effectively exploited for urban and rural water supply (ONED, 2004; BGR, 1982; MAEM-RH, 1997). The remaining wells are abandoned, unproductive or characterized by high TDS. The total number of water wells is set to increase given the current water resource projects. The best yields are obtained in recent sediments, and basalts (Figure 3.2).

The aquifer that supply the city of Djibouti, in which are located thirty boreholes is, of far, the most exploited of the country. The exploitation of this aquifer, with the help of boreholes, has begun in 1962 with the first three holes E1, E2 and E3. Previously the small town that was Djibouti drew its water from a network of underground drainage galleries that captured the waters rain runoff and underflow waters of wadis (Neyrpic, 1953; Hauquin, 1978, Rayalleh, 2004). Thus around 1960, two million m^3 of water per year fueled Djibouti. With the increase of the population and the increase of the number of drillings according to the needs the exploitation reaches 16 million m^3 for the year 2015 (Figure 3.1). This volume is insufficient to cover all the needs of the city, according to the projected needs study in the city of Djibouti by Lavalin-Tractebel (1993) on behalf of ONEAD on the basis of the 1991 population census. The needs of the city will increase to 25 Mm^3 in 2025

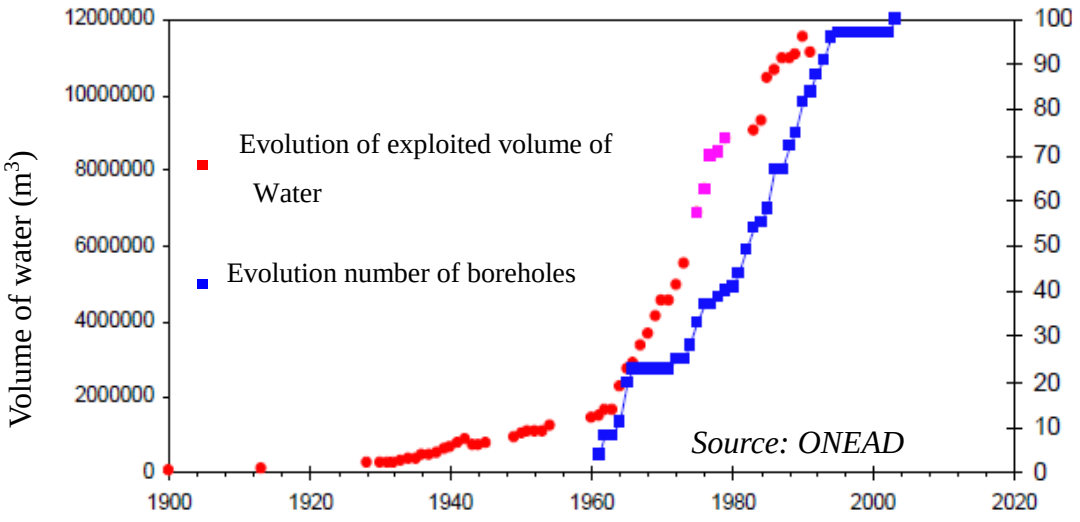

Figure 3.1: Evolution of production Djibouti aquifer (ONEAD, Dir Eau, CERD)

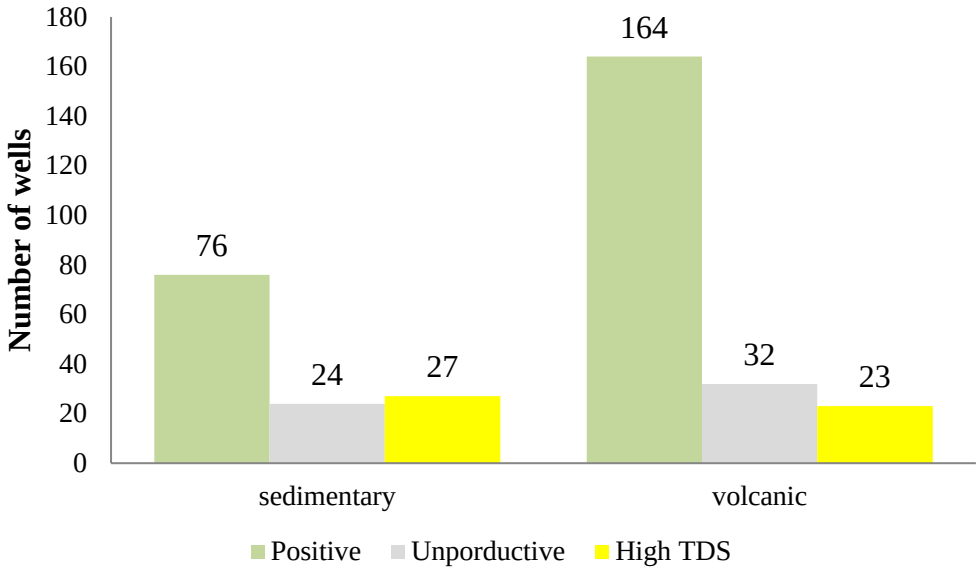

Figure 3.2: Success rates in sedimentary and volcanic aquifers

3.3 FUTURE WATER NEEDS CHALLENGES

Given the difficulties of the Republic of Djibouti to ensure fresh water supply for the different sectors today, the volumes needed for the next ten years raise questions over which water resources can be developed. Concerning the water supply of the towns, the study by Lavalin-Tractebel (1993) projects the demand for water until 2015, based mainly on the growth rate, i.e., 3%. The greatest need concerns the town of Djibouti with 25 Mm^3/y. it was proposed as solutions for this situation the seawater desalination and the construction of a dam for surface water impoundment (BCEOM, 2005). Another option for the town of Djibouti is exploitation of the Stratoid basalt regional aquifer but this will demand significantly more time than the previous solutions as the aquifer potential has not

yet been evaluated. Secondly, groundwater from the regional aquifer contains an excess of fluoride according to the WHO standards (BGR, 1997). The total needs for the urban zones in 2030 will be 28.5 M m^3 y^{-1} (Figure 3.3).

Water supply in the rural areas also remains a major problem. In 2030, the livestock water needs will have increased by around 12% without taking into account the needs arising from the cattle exportation project near Djibouti. Rural community needs and the demand from livestock would be 3.2 Mm^3 y^{-1}. compared to the total production the seawater demands remain below 6.5%. Nevertheless, these volumes are not negligible and will require the creation of new shallow and deep wells. Surface water exploitation represents an increasingly realistic option for the rural water supply.

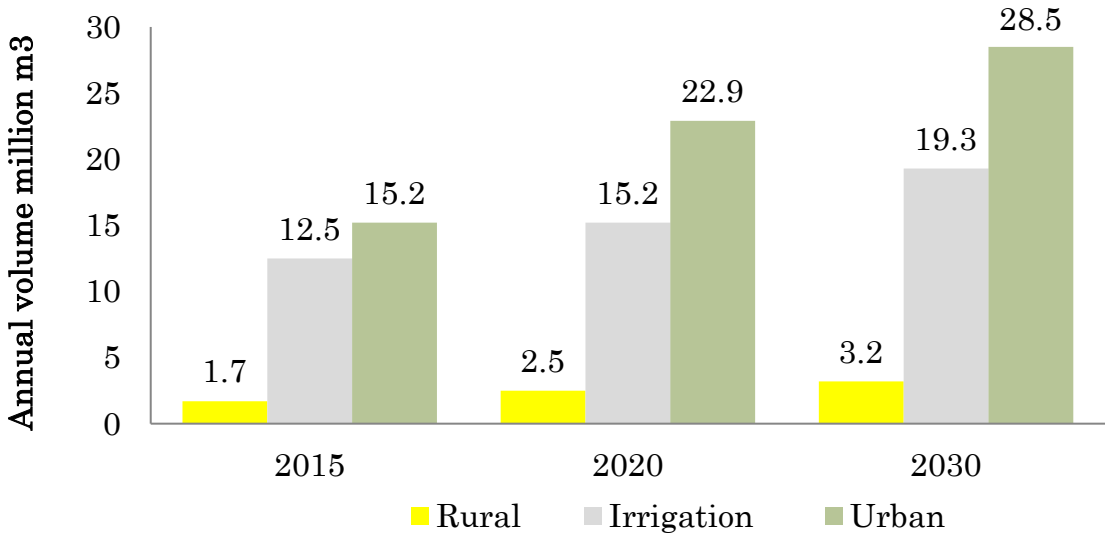

Figure 3.3: Water needs: Per sector

Although the agricultural sector is relatively limited, it represents an important component of the water demand with more than 12 Mm^3 y^{-1} used to irrigate 10 km^2. The additional needs of this sector over the next ten years depend on further extensions of the irrigated areas. The current production of 12.5 Mm^3 y^{-1} might, therefore, reach 19.3 Mm^3 y^{-1} by

2030 (Figure. 3.3). Such a large increase in the withdrawal of water for irrigation would definitely intensify the exploitation of some aquifers and new aquifers would have to be tapped, for instance in the area of Bissidourou or the Hanlé plain.

The estimated total needs for 2030 is 51 Mm^3/y. Hence, the production must be increased by 21.5 $Mm^3\ y^{-1}$ compared to the production of 2015. As a consequence, the Republic of Djibouti will have to double its total production by 2030.

The mean annual production rate increase for the town of Djibouti calculated since 1960 is 0.3 $Mm^3\ y^{-1}$. For the period 1977 to 2005 and for the whole country, the mean annual production rate increase was estimated at between 0.55 and 0.7 $Mm^3\ y^{-1}$. To achieve the objective of securing a water supply in 2030 without any shortage, the Republic of Djibouti will have to maintain a production rate increase of 2.17 $Mm^3\ y^{-1}$. This objective represents a serious challenge both scientifically and financially given that in the next few years, the mean production index might be multiplied by a factor of between 3 to 4

However, when these rates are calculated separately for the town of Djibouti, the rural areas and for irrigation, it appears that they are dominated by the town of Djibouti, 1.18 $Mm^3\ y^{-1}$, due to its size and its current water deficit which is estimated to be between 3 and 5 $Mm^3\ y^{-1}$. Irrigation takes second place with 0.68 $Mm^3\ y^{-1}$. The mean annual production rates for the rural areas (populations and livestock) and the other towns are similar, i.e., 0.15 $Mm^3\ y^{-1}$.

About 1.5 $Mm^3\ y^{-1}$ needed by the rural communities and their livestock might be covered by groundwater but over 70%, the remainder could be supplied by surface water. The surface water exploitation infrastructures are already operational in the northwestern part of the country and similar ones would be useful in other silty plains. Carrying out preliminary hydrological studies is essential prior to building such infrastructures.

By 2030, the agricultural sector will require an extra 6.84 $Mm^3\ y^{-1}$ for irrigation. According to the projected programs, these volumes would be provided by ground-water.

The additional water needs for Djibouti town will reach 11.8 Mm^3 y^{-1}. The Gulf basalt aquifer may not be exploited for this extra volume as it is already overexploited. The additional needs until 2010, 6.8 Mm^3 y^{-1} may still be covered by groundwater. These groundwater resources will require new hydro-geological studies of the upper part of the aquifer and its western zones as well as of its adjacent aquifers. If the projected dam and desalination are operational, they would cover the water needs of Djibouti town and contribute to reduce the pressure on the Djibouti aquifer

3.4 CLIMATE CHANGES CHALLENGES

Warming of the climate system is unequivocal, as is now evident from observations of increases in global average air and ocean temperatures, widespread melting of snow and ice and rising global average sea level. Given the global situation concerning the rapid change of the climate conditions, the country has to pay an extra careful attention to its impact on the already scarce water resources. According to the Koppen-Geiger world climate classification,

The climate of the Republic of Djibouti is defined as a hot desert (BWh) . Hot conditions prevail year-round with monthly average temperatures ranging from 25.4°C in January to 36.8°C in July, while rainfall are very scarce all year-long with monthly total precipitation below 10mmfrom May to August and between 10 and 28mm the rest of the year (Figure 3.3). As in many arid regions, annual rainfall is significantly irregular and extreme rainfall can be observed in a number of years.

With yearly precipitation ranging between 29 and 66mmbetween 2007 and 2011, the last 5-year period (average rainfall of 44 mm) has been the driest ever recorded since 1980 with precipitation amount as low as 27% of the long-term mean (1981–2010). Such large rainfall shortages were recorded elsewhere in the neighbouring countries of the Great Horn of Africa and partly explain recent food insecurity in the country and the large

migration fluxes towards Djibouti City. The conjunction of a very dry period with the absence of extreme daily rainfall events and limited access to risk knowledge increases the settlements in flood-prone areas and contribute to flood vulnerability.

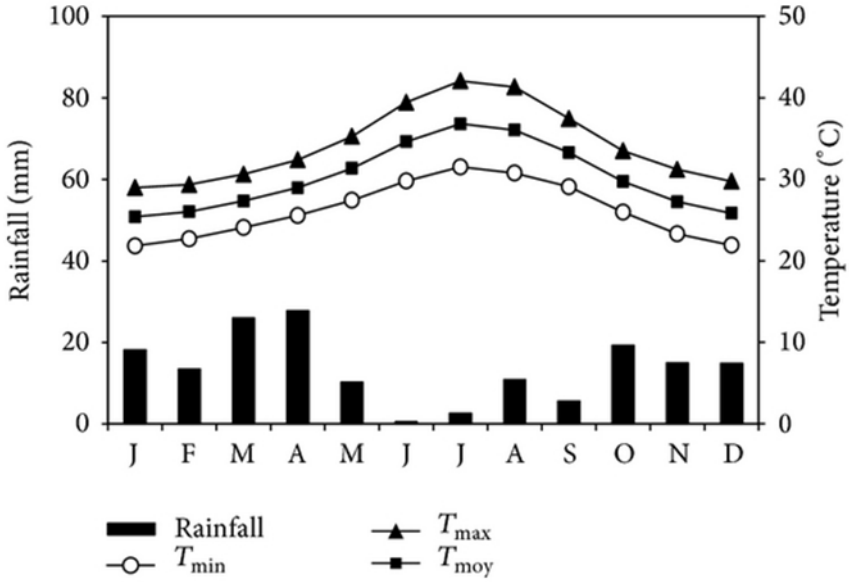

Figure 3.4: Monthly distribution of rainfall and temperature in Djibouti city (1980-2011)

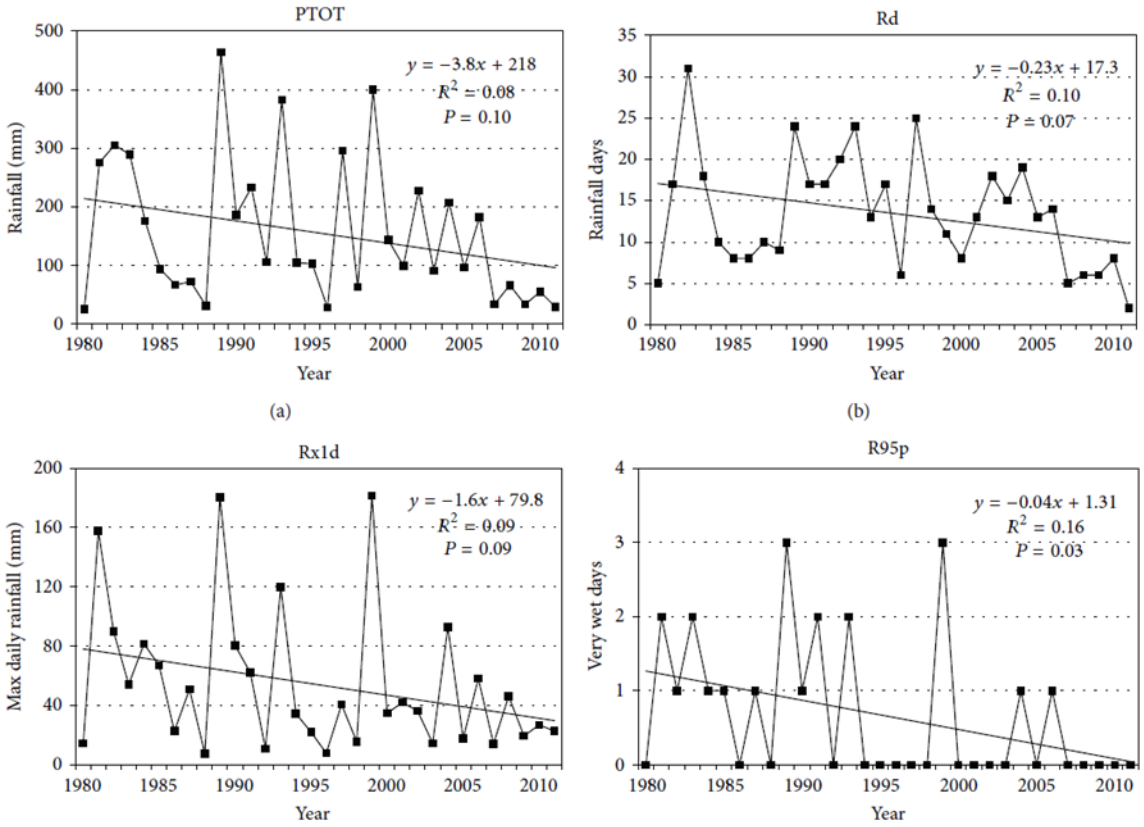

Figure 3.5 Evolution and trends of Total precipitation (PTOT), Rainy days (Rd), Daily rainfall (Rx1d), and Wet days (R95p)

Local authorities have now to challenge two rainfall related hazards: the current drought impact and the effects of future exceptional rainfalls with probable large damages in recent settlements.

With an average mean temperature of 31.0°C, the 2007–2011 periods has been the hottest 5-year period ever recorded since 1966, 0.9°C warmer than the long-term mean (1971–2000). Extremely warm nights and days have become much more frequent than in the past while extremely cool nights and days tend to disappear with an average mean temperature of 31.0°C, the 2007–2011 period has been the hottest 5-year period ever recorded since 1966, 0.9°C warmer than the long-term mean (1971–2000).

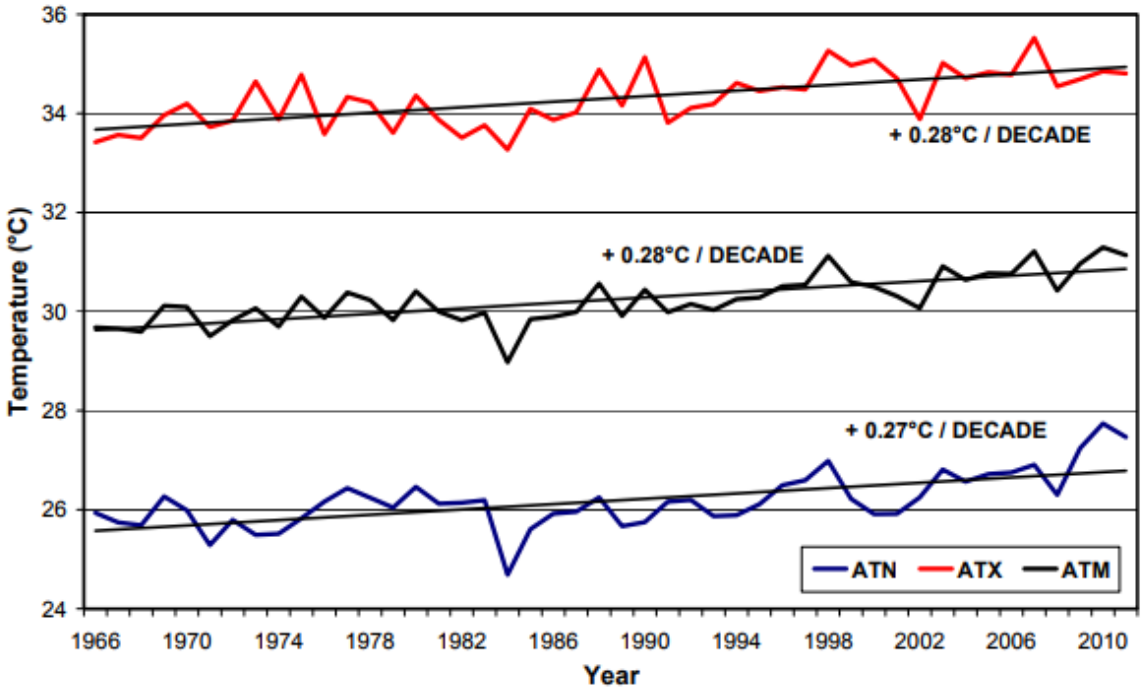

Figure 3.6: Evolution in annual average minimum, maximum and mean temperatures (ATN, ATX and ATM)

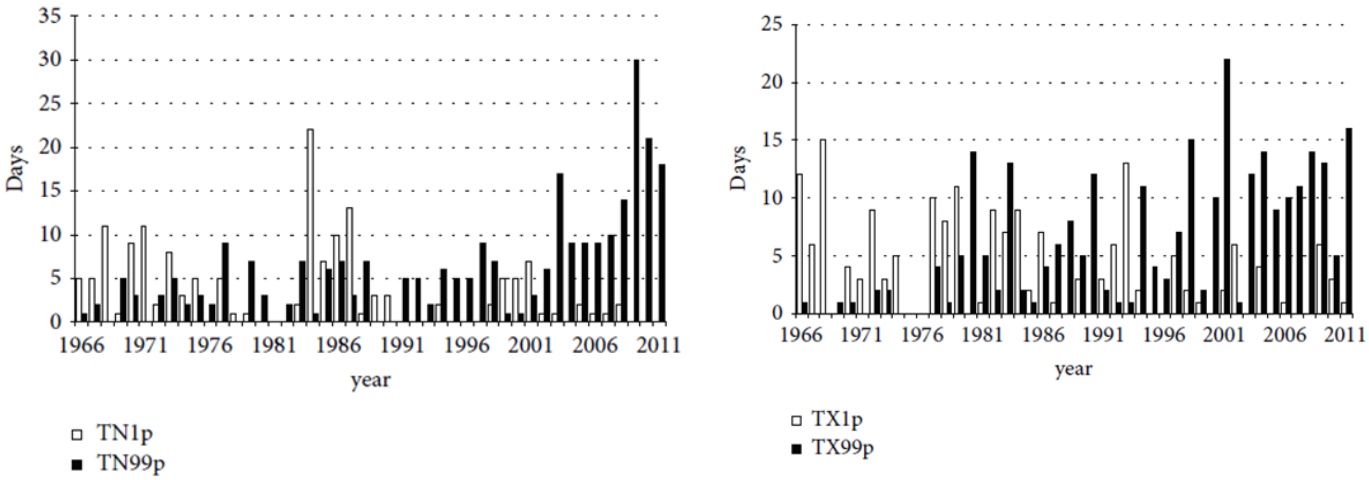

Figure 3.7 (Left) extremely cool (TN1p) and warm (TN99p) nights. (Right) extremely cool (TX1p) and warm (TX99p) days in Djibouti City (1966–2011).

Extremely warm nights and days have become much more frequent than in the past while extremely cool nights and days tend to disappear. These trends observed in the bordering countries clearly have an impact on human health that needs to be managed by national authorities.

3.5 CONCLUSION

Water supply in the Republic of Djibouti from volcanic and sedimentary aquifers currently represents 29.4 $Mm^3 y^{-1}$. This intensive groundwater withdrawal that started in the 1960s results in over exploitation of several aquifers: water table lowering and deterioration of the water quality by seawater intrusion and upwelling of high TDS groundwater. Given the current climatic conditions Future need in water supply exceed sustainable production. In this situation, it is essential to apply the measures recommended by the Master Plan for water resources for the management and protection of groundwater resources. Evaluations of the groundwater resources would be useful to manage adequately the aquifer systems. New hydrogeological studies must, therefore, be undertaken to pursue these objectives and to develop new groundwater resources for urban and rural needs. At the same time, a complete economic analysis is necessary to better define the new water requirements.

References:

BGR (1997) Forages de reconnaissance dans la région de Hanlé. ONED CoopérationHydrogéologique Djibouto-Allemande Rapport

Hauquin J.P., 1978. La nappe côtière de la région de Djibouti. Géologie et Hydrogéologie. Thèse de Doctorat. Université de Bordeaux III, p86.

Jalludin, M.1997. Hydrogeological features of the Afar Stratoid basalts aquifer on the Djiboutian part. International Symposium on flood basalts, rifting and paleoclimates in the Ethiopian rift and Afar Depression, Addis Ababa, Djibouti, 3–14/02/1997.

Lavalin et Tractebel (1993) Plan Directeur d'alimentation en eau potable des centres urbains. ONED2 vol

MAEPH (1997) Ministry of Agriculture, Livestock and Fisheries, in charge of Hydraulics (1997) Inventory of boreholes Report

NEYRPIC, 1953. Preliminary note on the water resources of the Djibouti region and the food of the city. Ets. Neyrpic, Grenoble Beauvert, p39., Rural Engineering of Djibouti. In

ONED (2004) Activity Report for the year 2004. National Water Board of Djibouti

Pierre Ozer and Ayan Mahamoud, "Recent Extreme Precipitation and Temperature Changes in Djibouti City (1966–2011)," Journal of Climatology, vol. 2013, Article ID 928501, p8, 2013.

Rayaleh H.O., 2004. La gestion d'une pénurie: l'eau à Djibouti. Thèse de doctorat, université d'Orléans, p315

CHAPITRE IV:

NUMERICAL MODEL

CHAPITRE IV: NUMERICAL MODEL

4.1 Introduction

Given their predictive capability, simulations models are often the only viable means of providing input to management decisions as they can forecast the behavior of a natural system, the likely impacts of a particular water management strategy. GETFLOWS is the numerical model of choice for the studies of the Ambouli and Kourtimalei catchments. This model is a 3D general-purpose computer model program able to simulate fully coupled surface-subsurface fluid flow, solute, and heat transport (Tosaka et al., 2000, 2010). A brief overview of the governing flow equations is presented here.

4.2 Overview of simulation modelling:

The sustainability of groundwater resources is a critical issue and their management is a challenging task given the growing water demand and shrinking resources. (Gleeson et al., 2012). In Djibouti, groundwater is not adequately managed to ensure its long-term sustainability (Houmed et al., 2008). In fact, groundwater depletion and sea water intrusion problems are both prevalent in Djibouti town (Jalludin et al., 1994; Houmed et al., 2008).

Groundwater models can be powerful tools to help analyze number of ground water related problems. It has become a commonly used tool for hydrogeologists to

perform various tasks. The most common categories of problems for groundwater modeling include basic understanding of groundwater system, estimation of aquifer properties, understanding the pas-present hydrologic condition and forecasting the future (Reilly and Harbaugh, 2004). The rapid increase of computing power of PCs and availability of user friendly modeling systems has made it possible to simulate large scale regional groundwater systems (Zhou et al., 2011). In recent years, research on the development and application of groundwater flow and transport models has increased significantly. It was used for understanding the groundwater dynamics and to improve the water management resources in the Federal District of Brazil by Gonçalves et al (2013). Groundwater flow model have been demonstrated in studies of groundwater management in arid areas (Wu et al., 2011; Gräbe et al., 2012). In china, Sun et al (2011) analyzed the groundwater drawdown at Nankou site of Beijing plain. In Djibouti Jalludin and Razack (1994) developed a 2D model of the Djibouti aquifer to understand the hydrologic conditions of the system.

4.3 Brief overview of GETFLOWS simulator

The characteristic feature of the GETFLOWS simulator is to formulate the terrestrial water circulation system as the multi-phase and multi-component fluid system and to simulate the fully-coupled surface water and subsurface fluids. The GETFLOWS simulator can synthesize the various interactions between surface and subsurface environment, which includes solute, heat and sediment transport.

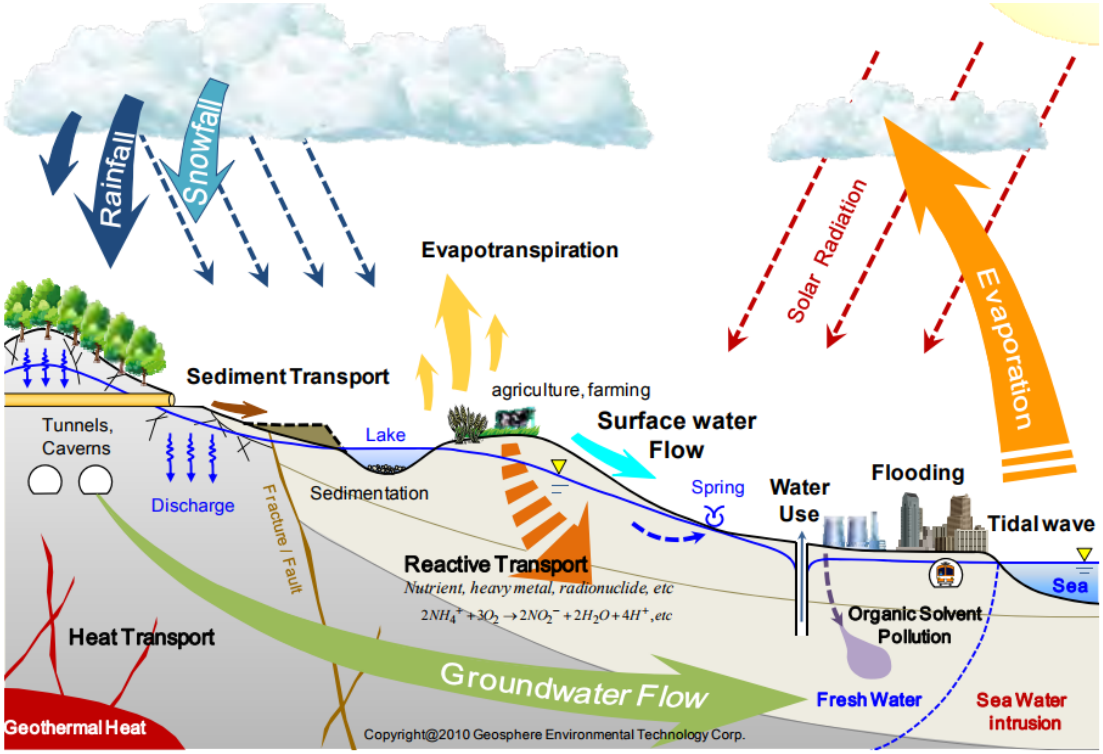

Figure 4.1: Conceptual model of terrestrial fluid-flow in GETFLOWS

(Cited from: GET Corp.)

The GETFLOWS model can simulate the terrestrial fluid-flow in geosphere for the various types of water related problems such as groundwater flow, runoff, flood/inundation, surface water and subsurface fluid coupled flow, contaminant transport and heat transport. It include features such as :

- Three dimensional corner-pointed finite difference simulator
- Isothermal, non-isothermal multiphase and multi-component fluid flow (water, gas, miscible and immiscible liquid etc.)
- Fully-coupled surface water and subsurface fluid
- Distributed, dynamic land surface conditions(land use, air temperature, precipitation, water body, man-made structures)
- Directional permeability (heterogeneity)
- Stress-dependent soil/rock properties
- Upstream weighted fully-implicit Newton-Raphson scheme with Successive Locking

Process(SLP) for the strong nonlinearity of fluids

- Matrix solver by preconditioned conjugate residual (PCR) algorithm
- Domain decomposition on parallel computers

4.4 Generalized Flow Equation for Surface and Subsurface Flows

The numerical modelling approach GETFLOWS, a general-purpose computer model program, address problems that may initiate a hydrologic study involving groundwater flow model (Tosaka et al. 2000; Mori et al., 2015). It is a physically based model that solves flows in a fully unified way by employing generalized flow formula that gives a common numerical description of the surface and subsurface without decoupling them. In GETFLOWS flows is solved in a unified way by using a generalized flow formula which uses common numerical description of the surface and subsurface. GETFLOWS traces the dynamic behaviour of surface water flow by solving nonlinear partial differential equation; the linearized-diffusion-wave approximation equations (Tosaka et al., 2000). In this modelling study, the fluid movement is simulated by using the governing equation for air/water two-phase fluid flow under an isothermal condition based on the generalized Darcy's law. It can be expressed by the following mass conservation equation:

$$-\nabla(\rho_p u_p) - \rho_p q_p = \frac{\partial}{\partial_t}(\rho_p \emptyset S_p) \qquad (1)$$

Where u_p is the fluid flow velocity (m s^{-1}), ρ_p is the fluid density (kg m^{-3}), q_p is the production and/or injection rate (m^3 m^{-3} s^{-1}), $\emptyset$ is effective porosity (-), and p is a subscripts representing the each fluid phases (i.e., w = water, a = air). The first term on the left-hand side of Equation (1) is the flow term, which is expressed by different average flow formula depending on surface and subsurface environment; Manning's law for the surface water flow (equation (2)) and Darcy's law for the subsurface fluid flow (equation (3)).

Manning's Surface water flow

$$u_w = -\frac{R^{2/3}}{n_l}\sqrt{\left|\frac{\partial h}{\partial l}+\frac{\partial Z}{\partial l}\right|}\ sgn\left(\frac{\partial h}{\partial l}+\frac{\partial Z}{\partial l}\right)$$

$$u_a = -\frac{\mathrm{K}k_{r,a}}{\mu_a}\nabla(P_a+\rho_a g Z) \qquad (2)$$

$$l = (x, y)$$

n_l Roughness coefficient of Manning ($m^{-1/3}$ s)

$R^{2/3}$ Hydraulic radius is (m),

h Water depth (m)

Z Elevation (m)

sgn Represents a sign function

l Direction

Darcy's law of Underground water flow

$$u_p = -\frac{\mathrm{K}k_{r,p}}{\mu_p}\nabla\left(P_p+\rho_p g Z\right) \quad (3)$$

K Absolute infiltration rate (m^2)

$k_{r,p}$ The relative permeability represented by the non-linear function of the saturation (-)

μ_p Viscosity coefficient (Pa · s),

P_p Fluid pressure (Pa)

g Gravitational acceleration (m / s^2)

Z Elevation (m)

Surface water and infiltrated underground water are in constant interchange however the difference velocity of surface flows and subsurface flow flows is very large. Hence the flow formula is different too. In GETFLOWS, interchange phenomena between surface and subsurface fluids such as water and air (for example, permeation by a body of water or by rainfall and the infiltration or exfiltration of air that accompanies it) are also modeled. The amount of flow passing between the two sites is calculated from the following formula:

$$u_p = -\frac{K_{12} k_{r,w12}}{\mu_w} A_{12} \frac{P_{w1} + \rho_w g(dz_1 + dz_2) - P_{w2}}{dz_1 + dz_2} \quad (4)$$

P_{g1}	Pressure (Pa)
h	Surface water depth (m)
H1 2	Heights of grid
K1	Permeability surface (m^2)
K2	Permeability subsurface (m^2)
$k_{r,w12}$	Relative permeability of water
A_{12}	Area of the grid
P_{w12}	Fluid pressure (Pa)
g	Gravitational acceleration (m / s^2)

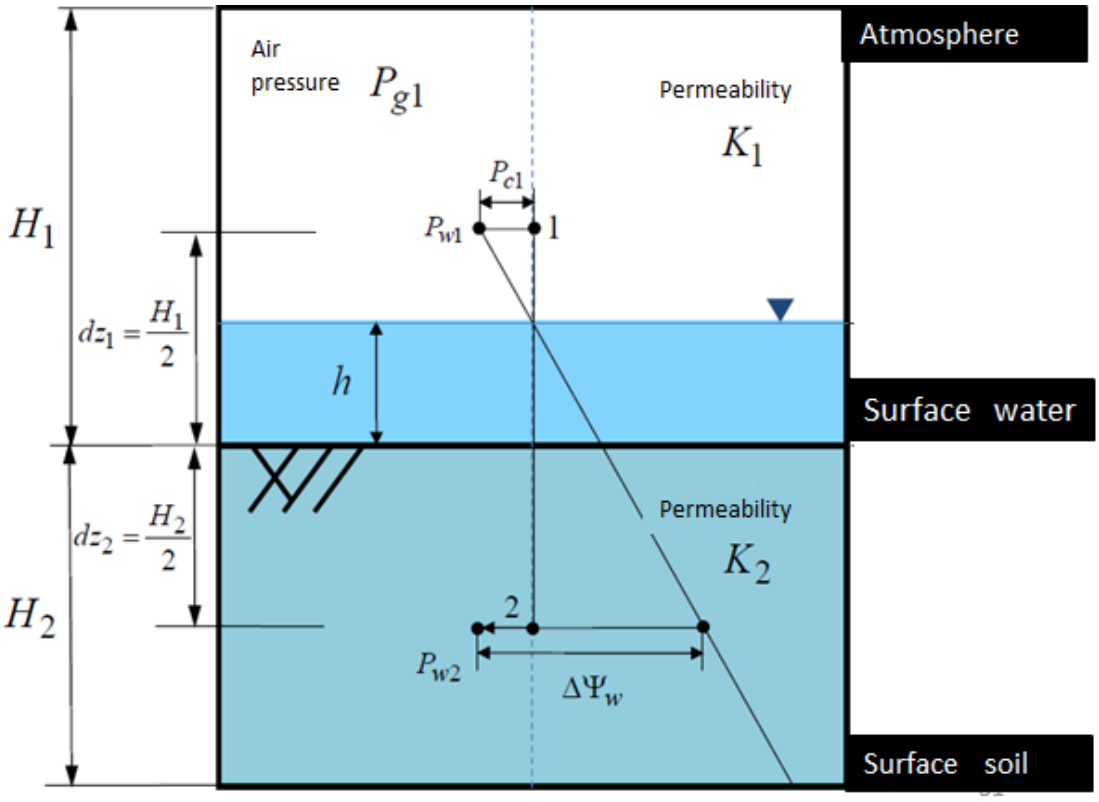

Figure 4.2: Interchange between surface water and groundwater

(Cited from: GET Corp.)

GETFLOWS solves the saturated, unsaturated subsurface flow and surface flow in a continuum approach within a single matrix. Nonlinear interactions between all components of the system are simulated without a priori specification of the coupling between surface and subsurface flow. Therefore, streams formations are purely based on hydrodynamic principles governed by recharge, topography, hydraulic conductivity and flow parameters when water is ponded due to surfaces flux exceeding the infiltration capacity of the soil (Horton, 1933) or due to excess from subsurface soil saturation. Plus, underground water converges to topographic depressions and depending on recharge and laterals flows; unsaturated zones may be shallow or deep.

4.5 Numerical methods

4.5.1 Discretization and solution procedure

Spatial discretization of the target system is represented basically by a general Cartesian grid (rectangular lattice) and irregular corner-point differential grid system. The corner-point differential grid is designed to realize spatial representations of complex terrain, geological structures, and man-made structures represented by atypical differential grid based on a structured grid system of orthogonal divisions (Wadsley, 1980; Ponting, 1989; Ding, 1995). In geometry, a corner-point grid is a tessellation of an Euclidean 3D volume where the base cell has 6 faces (hexahedron). A set of straight lines defined by their end points define the pillars of the corner-point grid. The pillars have a lexicographical

ordering that determines neighbouring pillars. On each pillar, a constant number of nodes (corner-points) are defined.

A corner-point cell is now the volume between 4 neighbouring pillars and two neighbouring points on each pillar. Each cell can be identified by integer coordinates (*i*,*j*,*k*), where the *k* coordinate runs along the pillars, and *i* and *j* span each layer. Data within the interior of such cells can be computed by trilinear interpolation from the boundary values at the 8 corners, 12 edges, and 6 faces. Corner-point grids are supported by most reservoir simulation software, and has become an industry standard. (Aarnes et al., 2006).

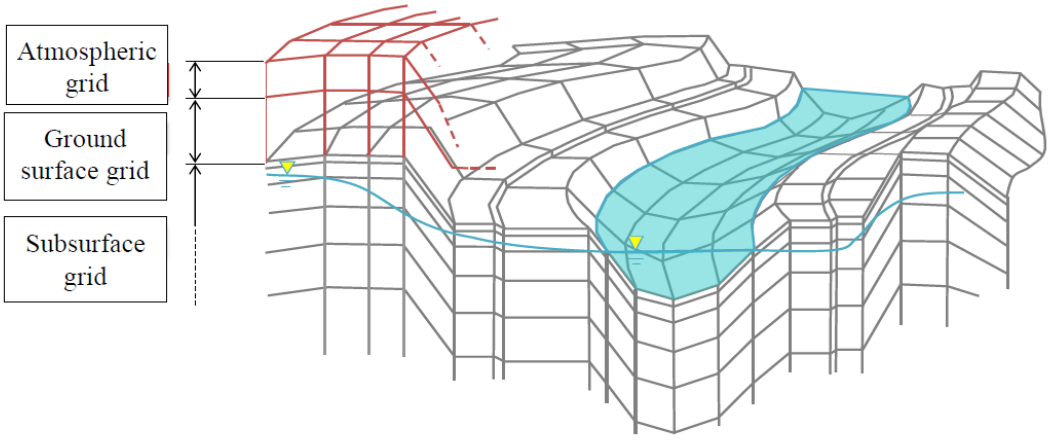

Figure 4.3: 3D grid system (Cited from: GET Corp.)

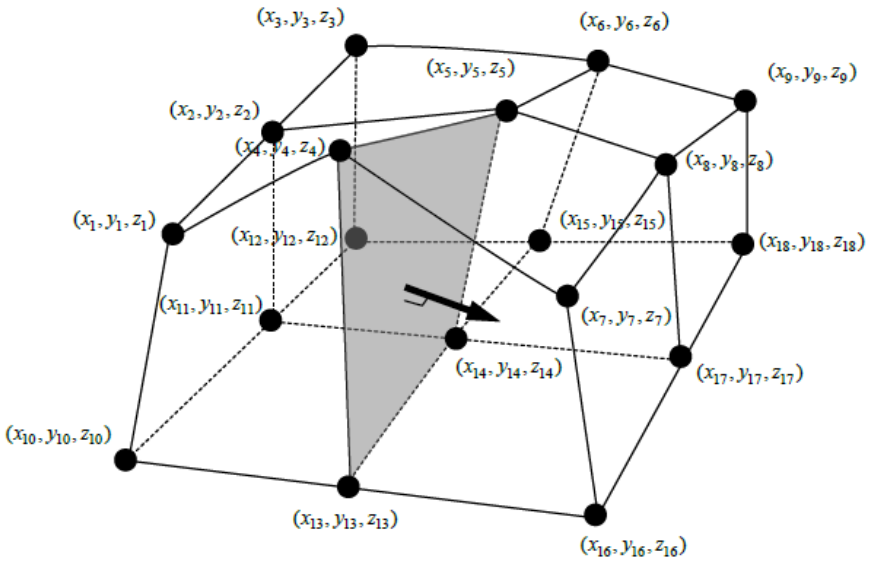

Figure 4.4: Corner point difference grid (Cited from: GET Corp.)

In GETFLOWS, the top layer of grid-block system is called atmospheric layer and the second layer is the surface layer. Usually the atmospheric layer has huge capacity and maintains standard pressure condition. The distributed precipitation condition is assigned into the surface layer. The surface water flow is represented in this layer. The interaction of surface water and groundwater such as infiltration and groundwater discharge is simulated as the water flux between surface layer and the next third layer.

Most natural phenomena are nonlinear, with the flow of rivers and multi-phase flow being typical examples. Nonlinear problems must be solved by iterative methods, such as Newton's method. To allow simultaneous and fully implicit solutions to problems in the case where there are multiple state quantities (unknown quantities), GETFLOWS applies Newton's method based on a block matrix. Numerical solutions are obtained by employing an integral finite difference method for spatial and a fully implicit method for temporal variances to discretise the above governing equations. A parallel matrix solver can be applied to large-scale watershed problems (Tosaka et al., 2000; Mori et al., 2015). This method uses a pre-processing method called nested factorization as the

pre-conditioner (Appleyard, 1983). Moreover, the implementation of successive locking process (SLP) by which unchanged grid-block dynamically during Newton-Raphson iteration are excluded and the use of the domain decomposition method for parallel computing (Toselli et al., 2005) help achieve an efficient and practicable computation time.

4.5.2 Initial conditions

4.5.2.1 Field initialisation procedure

The initial state of fluid distribution is achieved through field initialization process and other phenomena can be analysed afterward. The current distribution conditions of the groundwater levels and flow rates are quite unknown, but we need them for simulation. To create the current conditions in the objective area, we took the following procedures. This procedure consists on considering first fully saturated condition in underground without any surface water on land surface. Calculating from this initial condition and under the annual averaged precipitation and temperature, air-water two phase flows was traced by transient simulation for long period of time. During this computation, groundwater level around the mountainous area gradually decreased, and unsaturated zone is developed, by groundwater discharge (air intrusion) to the surface. At the same time, groundwater discharge formed river networks. Eventually, the conditions of fluids flow reach to an equilibrium state in which the precipitation and runoff out of the system balances under topographic and geologic/hydraulic structures (Figure 4-4).

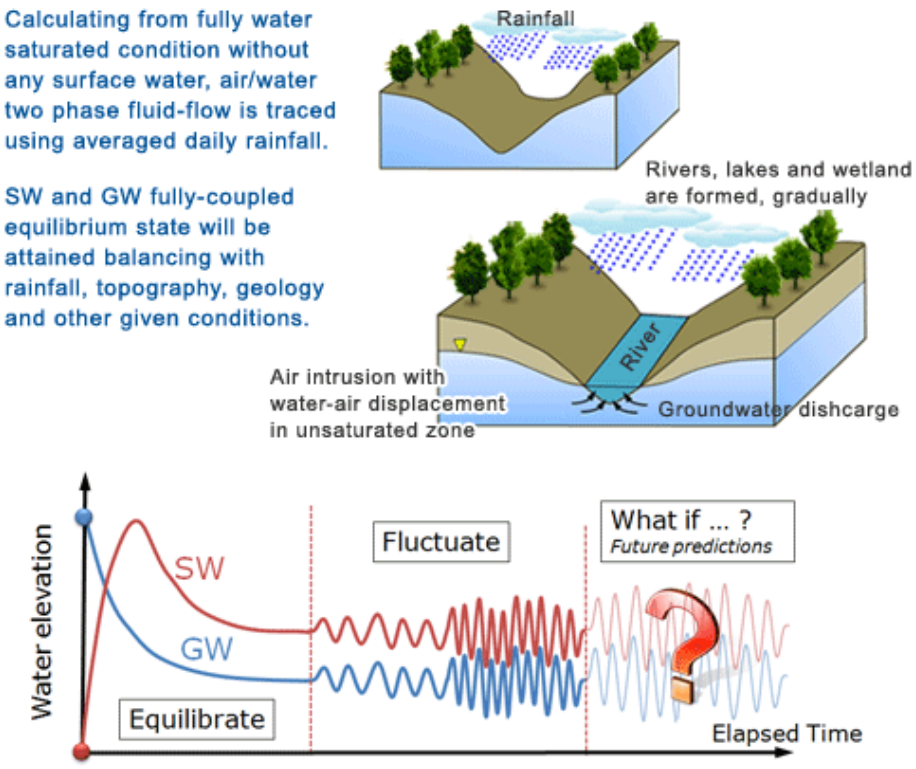

Figure 4.5: Field initialization procedure (Cited from: GET Corp.)

4.6 Input and output data

The primary input data necessary for running GETFLOWS are categorized into:

(1) Physical properties pertaining to the fluids and the substance composition that define the target terrestrial fluid system;

(2) Ground conditions, such as weather and land use;

(3) Structure of geological strata; and

(4) human-related factors, such as water use and building construction.

Hydrological observation data, such as river flow rates, groundwater levels, water quality, and water temperature, are not necessary as input data except in special cases (for instance, when used as boundary conditions). Such observation data can be compared with analysis results and used as field information to verify the model's faithfulness

The numerical output of GETFLOWS consists of a primary output, produced for each grid element, and secondary output calculated from the primary output. The primary outputs include various quantities that obey conservation laws (Pressure, water saturation level, concentration and temperature), which are analyzed directly as numerical solutions. The secondary output consists of quantities obtained analytically from the primary variables. This includes the fluid potential (calculated from grid pressure) and liquid phase flux (calculated from water depth and fluid potential difference between grid elements).

Table 4.1 Primary numerical output

Primary output	Secondary output calculated from the primary output
Pressure Saturation level Concentration Temperature	Fluid flux (mass, volume) Heat flux Sediment flux Surface water depth Fluid potential Fluid mass Fluid velocity Coordinates of fluid trajectory Residence time Terrain elevation

4.7 Model calibration

The purpose of calibration of any model of a physical system is to identify the values of some parameters in the model which are not known a priori (Solomatine et al., 1999). During calibration, input data such as geometry and properties, initials and boundary conditons, and stresses are changed so that the model output variables matches the variable values measured in the physical system. Many of the model inputs that are changed are

called “parameters” (Hill et al., 2007). Their difference should be minimized by solving an optimization problem, with independent variables being the unknown model parameters.

In the trial-and-error calibration of groundwater models, the model parameters such as hydraulic conductivity (K) and specific storage are assigned to each node and the model calculates values of piezometric heads. The calculated heads are then

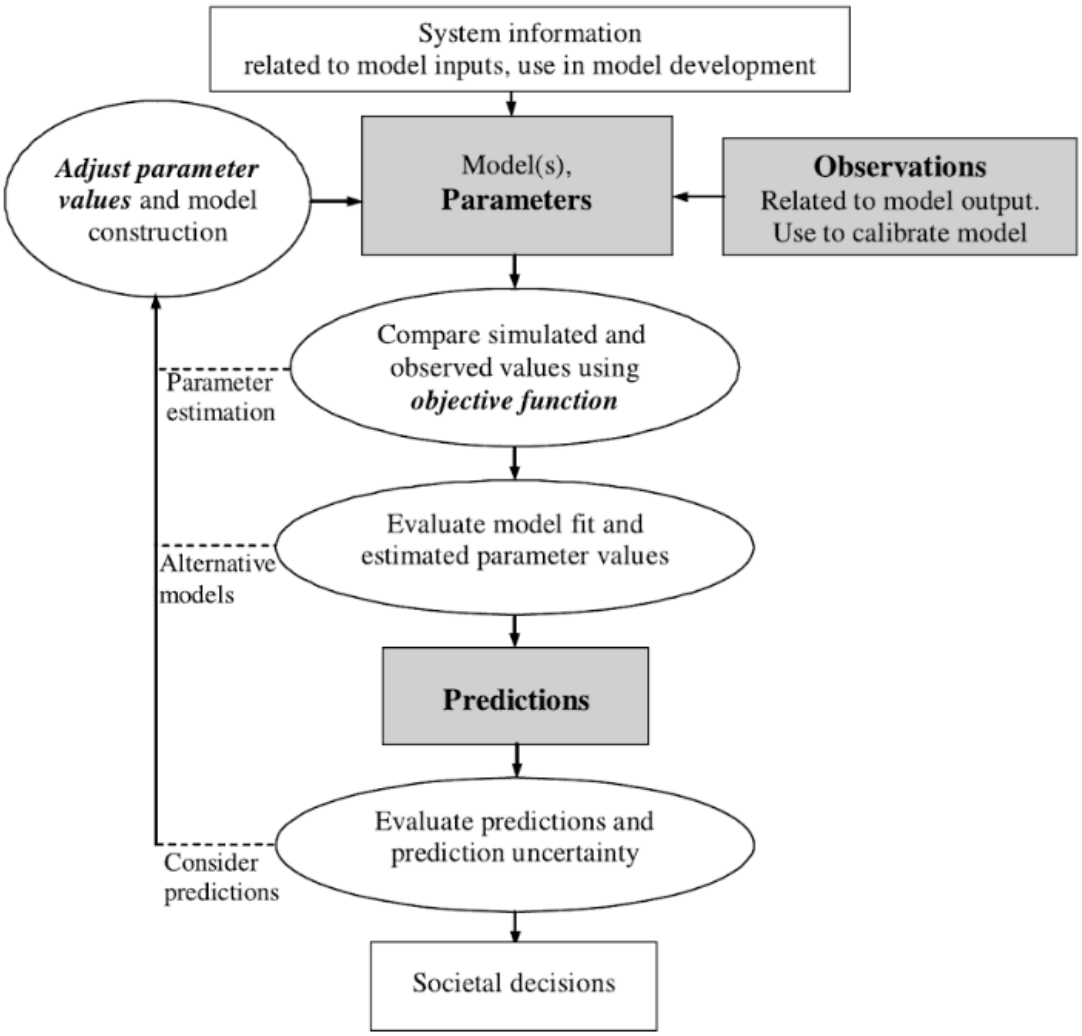

Figure 4.6: Flowchart showing the major steps of calibrating a model and using to make predictions.

compared with measured values and the model parameters are adjusted according to a modeller's judgement, in order to provide a better match. The calibration is repeated until an adequate match (with acceptable error) is obtained. The amount of error that is

allowable is highly dependent on the data available and the use to which the model will be put. A regional model in a data-poor area that will be used for water resources planning can have a much larger acceptable mean error than can a site chemical transport model that is used for litigation support, for example. Therefore, there are no solid rules for the level of error that is acceptable in a given situation; it is a determination that must be made by the individual modeler. Hill et al. (2007) states that the residual standard deviation divided by the range of observed groundwater head elevation values should be less than 10 percent for a good calibration.

The Root Mean Square Error (RMSE) (also called the root mean square deviation, RMSD) is a frequently used measure of the difference between values predicted by a model and the values actually observed from the environment that is being modelled. These individual differences are also called residuals, and the RMSE serves to aggregate them into a single measure of predictive power.

The RMSE of a model prediction with respect to the estimated variable $X_{model,I}$ is defined as the square root of the mean squared error:

$$RMSE = \sqrt{\frac{\sum_{i=1}^{n} (X_{obs,i} - X_{model,i})^2}{n}}$$

Figure 4.7 RMSE error equation

where X_{obs} is observed values and X_{model} is modelled values at time $_i$. Models are designed and built to meet specific objectives and must be critically evaluated to ensure that there are no data input errors and that the conceptual model does indeed accurately represent the actual ground-water system sufficiently to meet the objectives of the study. The evaluation of the model is intended to ensure that the model program and numerical representation of the important aspects of the system are sufficient to meet the objectives of the study.

4.8 Conclusion

GETFLOWS numerical modeling enables to compute and visualize comprehensive terrestrial water circulation under the direct representation of temporal fluctuation and spatial heterogeneity. It is a physically based model that solves flows in a fully unified way by employing generalized flow formula that gives a common numerical description of the surface and subsurface without decoupling them. In GETFLOWS flows is solved in a unified way by using a generalized flow formula which uses common numerical description of the surface and subsurface.

Reference

Aarnes J, Krogstad S and Lie K.A. (2006). Multiscale Mixed/Mimetic Methods on Corner Point Grids

Doummar J., Sauter M., Geyer T. (2012). Simulation of flow processes in a large scale karst system with an integrated catchment model (Mike She) - Identification of relevant parameters influencing spring discharge. Journal of Hydrology, 426-427, pp. 112-123.

Gleeson, T., J. VanderSteen, M.A. Sophocleous, M. Taniguchi,W.M. Alley, D.M. Allen, and Y. Zhou. (2010). Groundwater sustainability strategies. Nature Geoscience 3, no. 6: 378–379.

Gonçalves, T.D., Fischer, T., Gräbe, A. et al. (2013). Groundwater flow model of the Pipiripau watershed, Federal District of Brazil. Environ Earth Sci 69: 617. https://doi.org/10.1007/s12665-013-2400-5

Grabe A, Rodiger T, Rink K, Fischer T, Sun F, Wang W , Siebart C, Kolditz O (2013) Numerical analysis of the groundwater regime in the western Dead Sea escarpment, Israel + West Bank Environ Earth Sci 69:571-585.

Hill, M.C. (1998), Methods and guidelines for effective model calibration: U.S. Geological Survey Water-Resources Investigations Report 98-4005, p90.

Hill, Mary Cassandra, and Claire R Tiedeman (2007). Effective Groundwater Model Calibration : with Analysis of Data, Sensitivities, Predictions, and Uncertainty. Hoboken (N.J.): Wiley-Interscience.

Horton, R.E. (1933). The Role of Infiltration in the Hydrologic Cycle. Transactions of American Geophysical Union, 14, 446-460.

Jalludin M, Razack M. 1994. Analysis of pumping tests in fractured Dalha and Stratoid basalts with regard to tectonics, hydrothermal effects and weathering, Republic of Djibouti. J. Hydrol, 155, 237–250.

Jalludin, M. (1997). Hydrogeological features of the Afar Stratoid basalts aquifer on the Djiboutian part. International Symposium on flood basalts, rifting and paleoclimates in the Ethiopian rift and Afar Depression, Addis Ababa, Djibouti, 3–14/02.

Maxwell, R. M., Condon, L. E., and Kollet, S. J. (2015). A high-resolution simulation of groundwater and surface water over most of the continental US with the integrated hydrologic model ParFlow v3, Geosci. Model Dev., 8, 923-937, https://doi.org/10.5194/gmd-8-923-2015.

Mori, K. Tada, et al: A high performance full-3D nutrient transport modeling based on the surface water and

groundwater coupling technique for the water quality assessment: An application to the lake Kasumigaura, Japan, Int. symp. on Hydro Change 2008

Reilly, T.E and Harbaugh, A.W., (2004). Guidelines for evaluating groundwater flow models. U.S. Geological Survey Scientific Investigations Report 2004-5038, version1, 01, Reston, VA, 30pp.

SOLOMATINE, D.P., Y. B. DIBIKE & N. KUKURIC (1999.) Automatic calibration of groundwater models using global optimization techniques, Hydrological Sciences Journal, 44:6, 879-894, DOI: 10.1080/02626669909492287

Sun, F., Shao, H., Kalbacher, T. et al. (2011). Groundwater drawdown at Nankou site of Beijing Plain: Model development and calibration. Environ Earth Sci., 64: 1323. https://doi.org/10.1007/s12665-011-0957-4

Tosaka, H., Itho, K., Furuno, T. 2000. Fully coupled formation of surface flow with 2-phase subsurface flow for hydrological simulation. Hydrological Process, 14, 449– 464.

Tosaka, H., Mori, K., Tada, K., Tawara, Y., and Yamashita, K. 2010. A general-purpose terrestrial fluids/heat flow simulator for watershed system management. In: IAHR International Groundwater Symposium.

Wu, Y., Wang, W., Toll, M. et al. Development of a 3D groundwater model based on scarce data: the Wadi Kafrein catchment/Jordan. Environ Earth Sci (2011) 64: 771. https://doi.org/10.1007/s12665-010-0898-3

Zhou Y, Li W, 2011. A review of regional groundwater flow modeling. Geoscience frontiers vol 2 , no 6: 205-214.

CHAPTER V:

USING GETFLOWS FOR SURFACE WATER FLOW : APPLICATION ON KOURTIMALEI

CHAPTER V: USING GETFLOWS FOR SURFACE WATER FLOW : APPLICATION ON KOURTIMALEI

5.1 INTRODUCTION

For a period of two years (May 2012-August 2014) the local government put in place a pilot farm project in the area investigating suitable of irrigation techniques and cultivation techniques. In this project, source of the irrigation water was set to be a pond collected from surface runoff of the catchment water. In this chapter we present a study is to integrate the free available satellite products within a distributed hydrologic model (GETFLOWS) to characterize the spatial extent of pond use for irrigation purpose.

5.2 BACKGROUND

The Government of Djibouti has set a policy to improve that livelihood of the local pastoral people through agricultural activities. With the help of JICA, a Master plan regarding sustainable irrigation and farming in southern Djibouti was formulated. Those set of policy were to be tested in the form of pilot farm. Kourtimalei catchment at Grand Bara desert is a one of the pilot farm where implementation of those policies was to verify applicability of irrigation and cultivation techniques in the formulated master plan

Intensive rainfall has sometimes caused abrupt runoff on bare land surface, resulting in heavy flood damages along the alluvial fan. When such rainfall occurs in the closed

watershed, rainfall water accumulates at the lowest point in the watershed and the ponding area can stay up for several months sometimes. Usually that ponding water is lost through evaporation and seepage in a three to six months period. Kourtimalei catchment at Grand Bara desert is a good example of a closed watershed where ponding water appears during intensive rainfall. Annual mean precipitation of the southern Djibouti is extremely low, around 100 – 200 mm, like in the rest of the country. It has two peaks of monthly rainfall in March and during the period from August to September. Precipitation is low in any months, therefore precipitation is not enough for crop cultivation in Djibouti.

5.3 KOURTIMALEI PILOT PROJECT SITE

The pond resulting from rainfall runoff was planned to be used as water source for the pilot farm in Kourtimalei. To utilize the pond more effectively, improvement works including excavation of the pond bed and construction of filter zone were implemented as a part of the pilot project (Figure 5.2). The excavation of the pond bed (2.5m in depth and 5,400m3 in volume) was aimed at reducing the evaporation from the water surface by collecting the water into the excavated portion when water volume of the pond becomes small. On the other hand, construction of the filter zone was aimed at alleviating soil inflow during floods

A pilot farm of about one (1) ha was established just beside an existing farm constructed with financial assistance of FAO. Irrigation network was also set up in the pilot project. Intake work was newly built inside the pond. Water is pumped up from the pond to an existing water tank with an engine pump which was placed on the intake work (Figure 5.3). After that, the water is conveyed by gravity through the pipeline from the water tank to the pilot farm. For the monitoring of water amount consumed at the pilot farm, a flow meter was installed close to the water tank downstream.

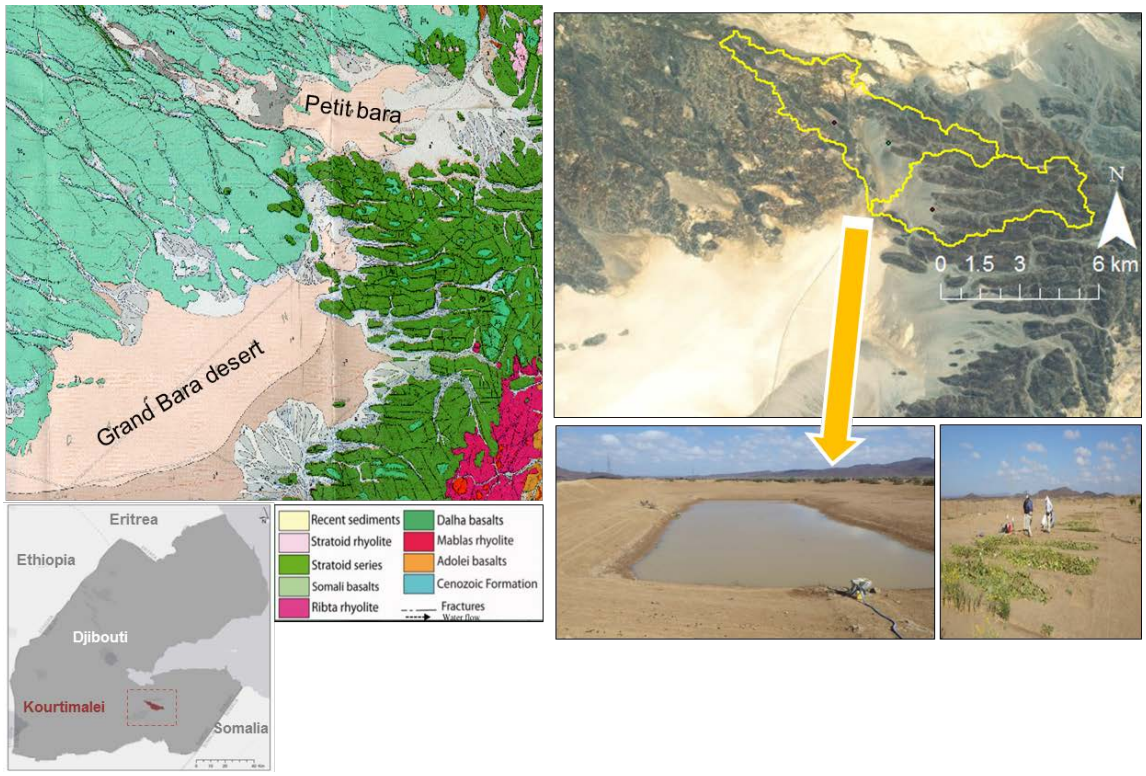

Figure 5.1: Geology of Location of the Kourtimalei pilot farm

Figure 5.2: Improvement Work of Kourtimalei Pond (June 2012)

Figure 5.3: (A) water pump engine. (B) Water tank

Figure 5.4: Pilot form setup

The pilot farm has 0.64ha in total and 16 plots with an area of 400m^2. In regard to the irrigation method, furrow irrigation was applied to Kourtimalei pilot farm. The construction work of Kourtimalei pilot farm was completed in September 2012 (Figure 5.4). In order to monitor the fluctuation of water level of the pond, pressure type of water level sensors with data logger were placed in Kourtimalei pond. Water depth could be traced on a time series basis by calculating the deference of water level recorded at intervals of 15 minutes by two

water level sensor(one was for atmosphere pressure, and the another was for water pressure). Decrease of water level was estimated to be 24.5 to 42.0 mm/day (from August 2012 to December 2012) due to negative effect of pond bed excavation. After that, it was reduced to be 19.3 to 21.1 mm/day (from January 2014 to March 2012).

5.4 Satellite Remote Sensing Data for flooded area mapping

In this study, we used LANDSAT images for flooded area mapping. LANDSAT satellite images offer a unique combination of 16 days coverage with acceptable spatial resolution. These capabilities are being utilized for flood monitoring at the Kourtimalei watershed. Sadiq et al, 2011 and Seemanta et al, 2017 demonstrated that satellite data can be used to distinguish between flooded and non-flooded areas with suitable spatial resolution. This can be very crucial in regions where no other means of flood monitoring are available.

4 LANDSAT-8 images (July 28, September 14 and 30, and December 03) were used for the flooding area (Kourtimalei pond extent) mapping and the area measurements. The images represent also a crucial part of the validation phase of the simulation. It offers a good combination of two months coverage with an acceptable spatial resolution of 30 m. (Figure 5.5). The pond extent were delimited using an unsupervised classification method ISODATA which uses the Euclidean distance in the feature space to assign every pixel to a cluster through a number of iterations.

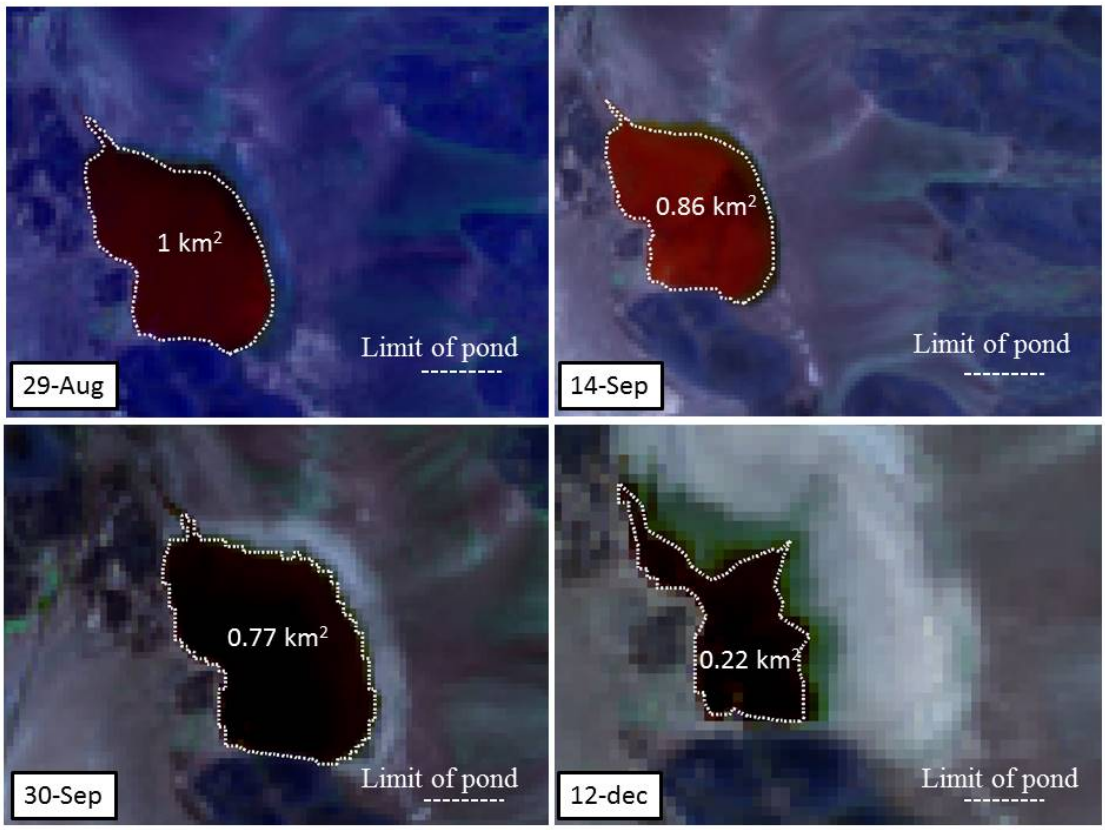

Figure 5.5: LANDSAT-8 (in false color 5:4:3) pond extents in August 29th, September 14, September 30 and December 12, 2013

5.5 Hydrological model

The General purpose terrestrial fluid-flow simulator (GETFLOWS), developed by Tosaka *et al*. (2000), was used to simulate rainfall runoff events at the study site. It is a physically based model that solves both the surface and subsurface systems simultaneously by employing an integral finite difference method approach for solving the governing equations. The natural system is discretized into small cells in order to obtain exact solutions (Magnus et al., 2011). The governing equation for air/water two-phase fluid flow in GETFLOWS is expressed by the following equation of mass conservation (Eq. 1).

$$-\nabla(\rho_p u_p) - \rho_p q_p = \frac{\partial}{\partial_t}(\rho_p \emptyset S_p) \qquad (p = water, air) \qquad (1)$$

Where u_p is the fluid flow velocity (m s^{-1}), ρ_p is the fluid density (kg m^{-3}), q_p is the production and/or injection rate (m^3 m^{-3} s^{-1}), $\emptyset$ is effective porosity (-), S_p is saturation degree (m^3 m^{-3}) and p is a subscripts that indicate quantities on each fluids phases. In the surface GETFLOWS solves the Manning's equation for the horizontal surface water flow by using the linearized-diffusion-wave approximation equations (Tosaka et al., 2000).

The flow in the subsurface and the vertical flow in the surface are expressed with the Darcy's equation. GETFLOWS solves the saturated, unsaturated subsurface flow and surface flow in a continuum approach within a single matrix. Nonlinear interactions between all components of the system are simulated without a priori specification of the coupling between surface and subsurface flow. Therefore, streams formations are purely based on hydrodynamic principles governed by recharge, topography, hydraulic.

The key datasets enabling the implementation and testing of the numerical model are:

1) ASTER GDEM data (30 m resolution DEM) published by NASA and The Ministry of Economy, Trade, and Industry (METI) of Japan was used as elevation data for the watershed area. The vertical accuracy was improved by modifying with point elevation data from ground survey in the reservoir area.
2) Observed precipitation records at different location in the watershed indicating an average of less 100 mm month-1. Although the small scale of the area, it was found that the amount of rainfall isn't homogenously distributed (Toyoda et al., 2015). Evapotranspiration was estimated from potential evapotranspiration and represents 84% of the annual average precipitation.

3) Hourly record of the water level of pond collected from sensors within Kourtimalei reservoir.
4) The surface geology is from the national geology map (ORSTOM, 1986)
5) The land cover map with 3 classes (rock, soil and vegetation) was derived from LANDSAT-8 images by unsupervised classification.
6) The fluid properties of water and air are represented by the typical value in the standard conditions. The soil is mainly comprised of loamy and sandy loam. The loam soil hydraulic conductivity ranges from 50 to 100 mm h^{-1}, while for the sandy loam soil texture, larger ranges (160-190 mm h^{-1}) were recorded (Toyoda et al., 2015). The permeability of basaltic rock, weathered rock on the surface was estimated by pumping test and considered to be small as shown in Table 1 (Jalludin and Razack, 1994).

Table 5.1 Hydraulic parameters used parameters used

Geology	Intrinsic Permeability (cm s^{-1})	Porosity (%)
Loamy soil	5.63 x 10^{-2}	40
Alluvium deposit	1.00 x 10^{-2}	40
Weathered rock	1.00 x 10^{-6}	10
Basalts	1.00 x 10^{-5}	10

Table 5.2 Manning roughness coefficient

Land use	Manning Coefficient
Alluvial fan	0.040
Rock layer	0.027

The study area was discretized spatially in 2D plane by grid blocks of approximately 60 m. The secondary data (i.e., elevation, geology, land cover) were assigned into the corner-point coordinate of the 2D grid. Then the 2D plane grid was enlarged into depth

direction and discretized again along Z axis to generate the 3D grid-block system. The total number of grid cells recorded to be 100,890 cells (Figure 5.6).

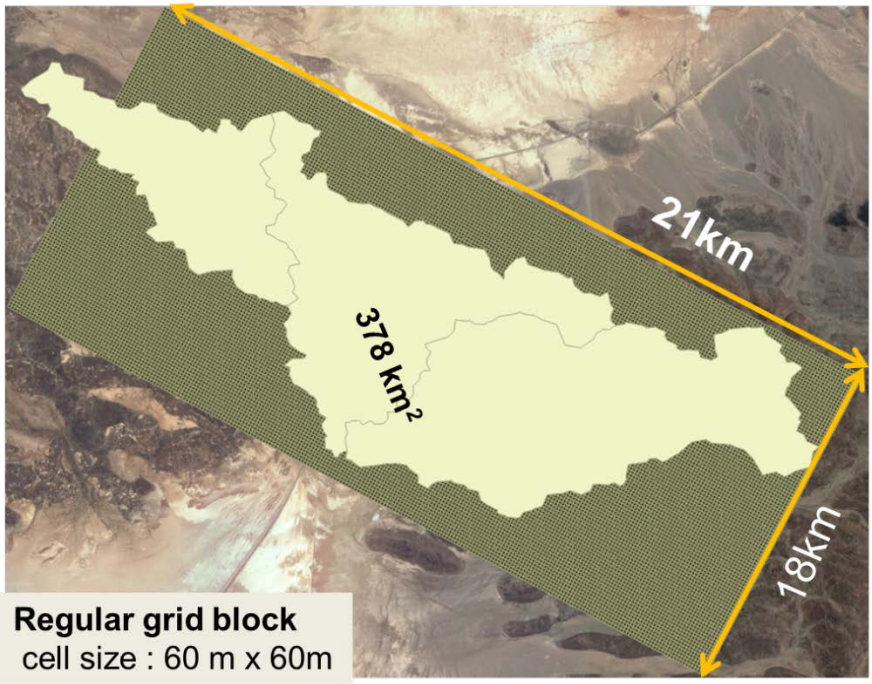

a)

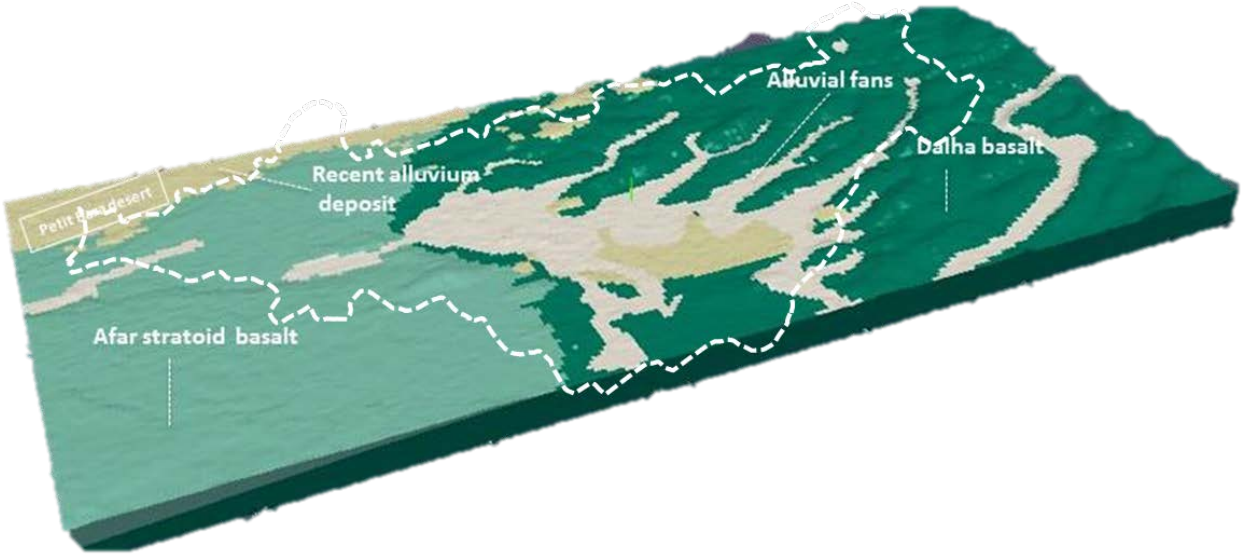

b)

Figure 5.6: a) 2D grid discretization of Kourtimalei watershed. b) 3D structural hydrological model (Geology).

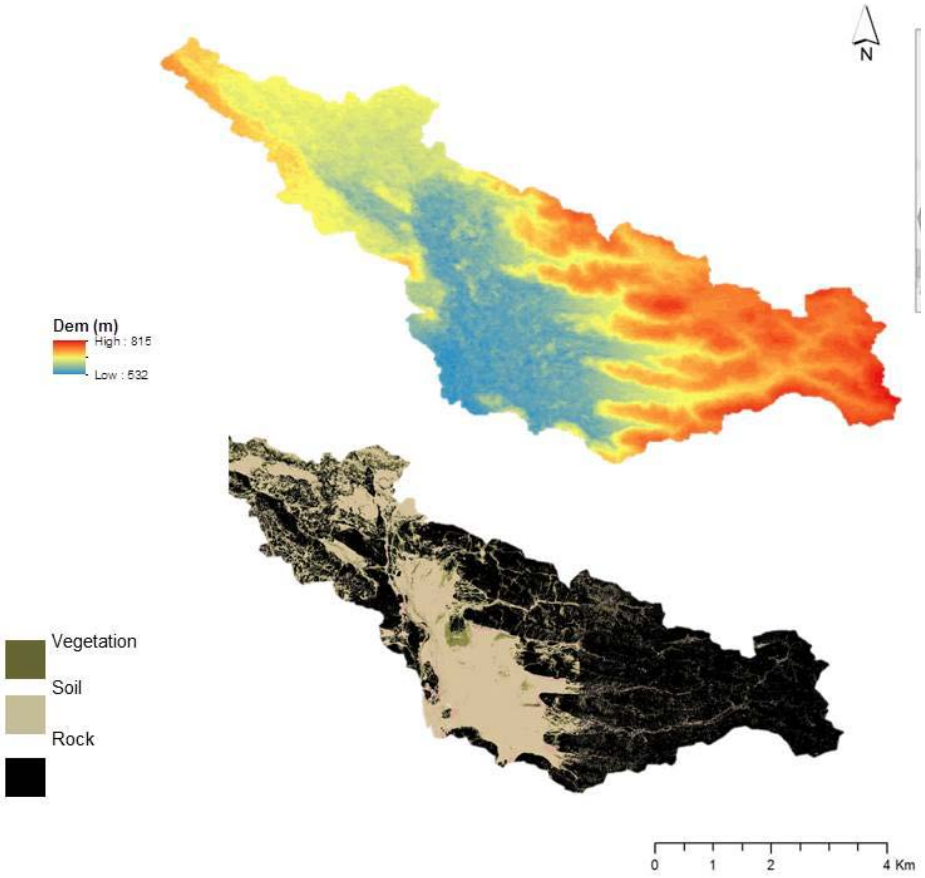

Figure 5.7: Aster GDEM elevation and land cover of Kourtimalei.

Our aim is to analyze the runoff characteristic of the watershed that creates the Kourtimalei pond during intense precipitation events. Thus the model was used for a short-term reproduction of the rainfall events of August 01 to December 03, 2013. Recorded daily fluctuations of meteorological conditions were constrained onto the model. Then, GETFLOWS was calibrated using the available daily pond water elevations observations for the period between August 01 and December 03, 2013 in Kourtimalei. RMSE indicator is used to assess model accuracy in matching the model-simulated runoff with observations of the differences in water level records of the pond. The criterion is used as an objective functions for the calibration. Furthermore the Kappa coefficient is used to assess the accuracy of the model by comparing the pond area extent derived from

LANDSAT-8 satellite images during the simulated period with GETFLOWS simulation result.

5.6 Results and discussions

In this section, we present the results of the calibration process of GETFLOWS. The Root mean squared error (RMSE) has been used for comparison of simulated pond water levels with observed water levels for the period of August to December.

The trial and error method yielded for an optimized parameter combination that had a RMSE of 0.40 m (Figure. 5.7). The Comparison of GETFLOWS-simulated spatial extent of the pond with satellite-based observations images (LANDSAT-8) was to provide a further evaluation of the GETFLOWS performance in simulating the spatiotemporal evolution of the pond extent during the calibration period. (Figure. 5.8) shows the statistical comparison between GETFLOWS and LANDSAT-8 which indicates that a rather good agreement between the obtained pond spatial extents of GETFLOWS and LANDSAT-8.

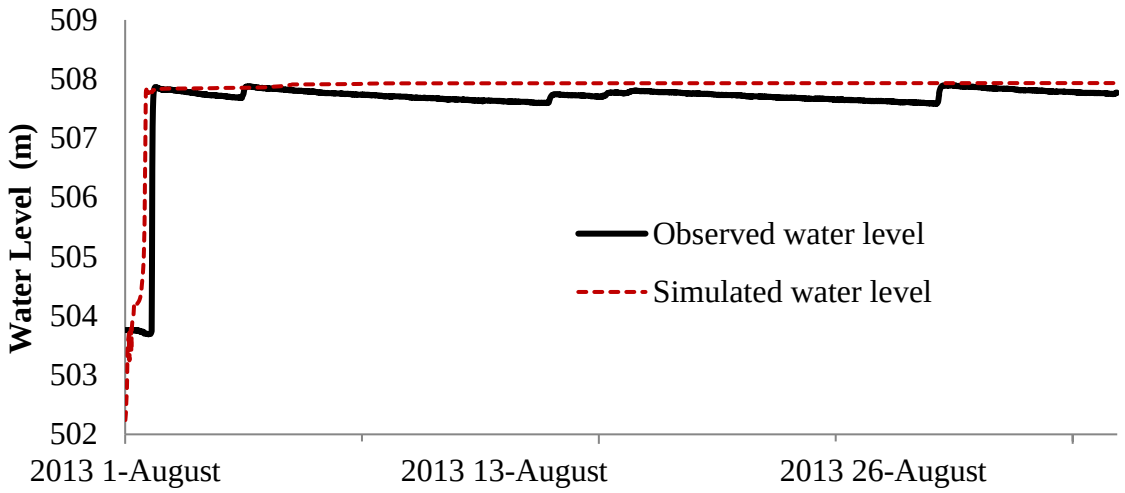

Figure 5.8: Comparison between the observed and simulated Water levels during the month of August, 2013.

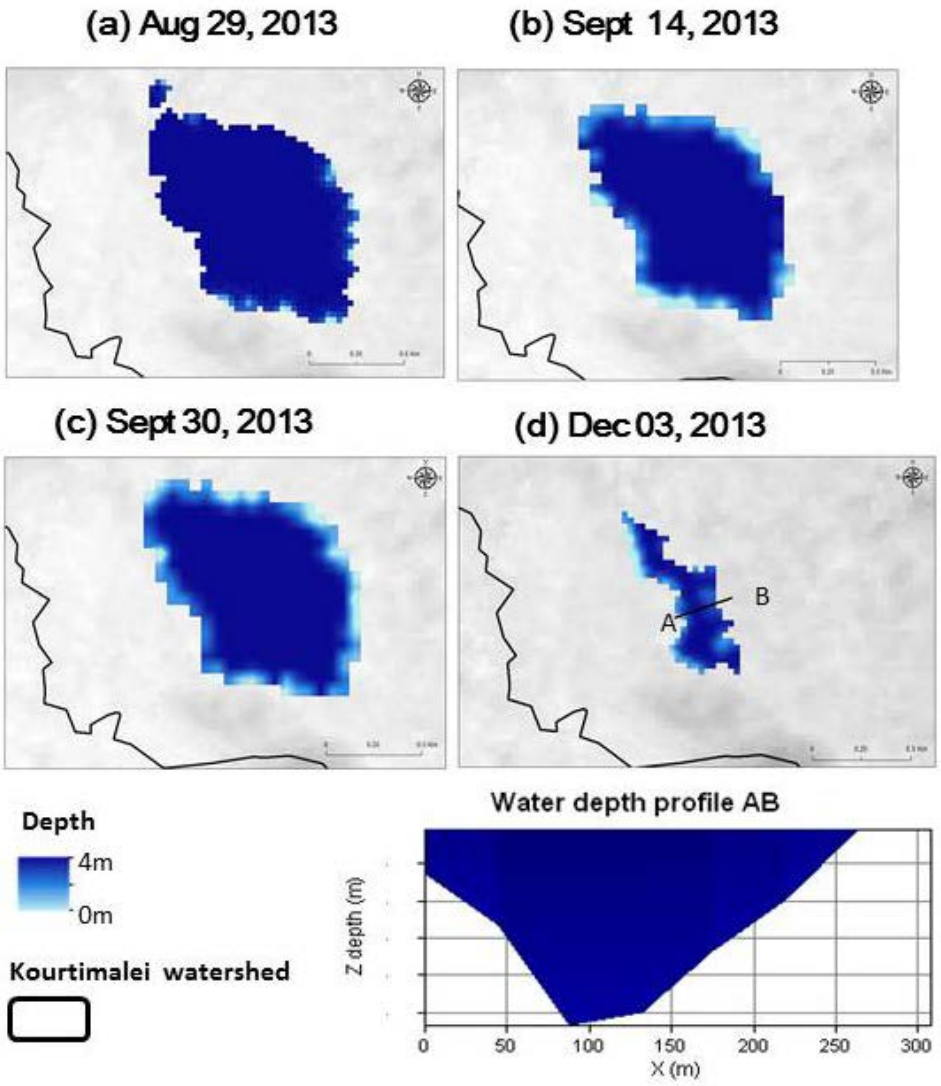

Figure 5.9: Simulated water depths of Kourtimalei pond at four time step with pond profile on 03 December (a) pond extent of 29 August, 2013; (b) pond extent of 14 September, 2013; (c) pond extent of 30 September, 2013; (d) pond extent of 03 December, 2013.

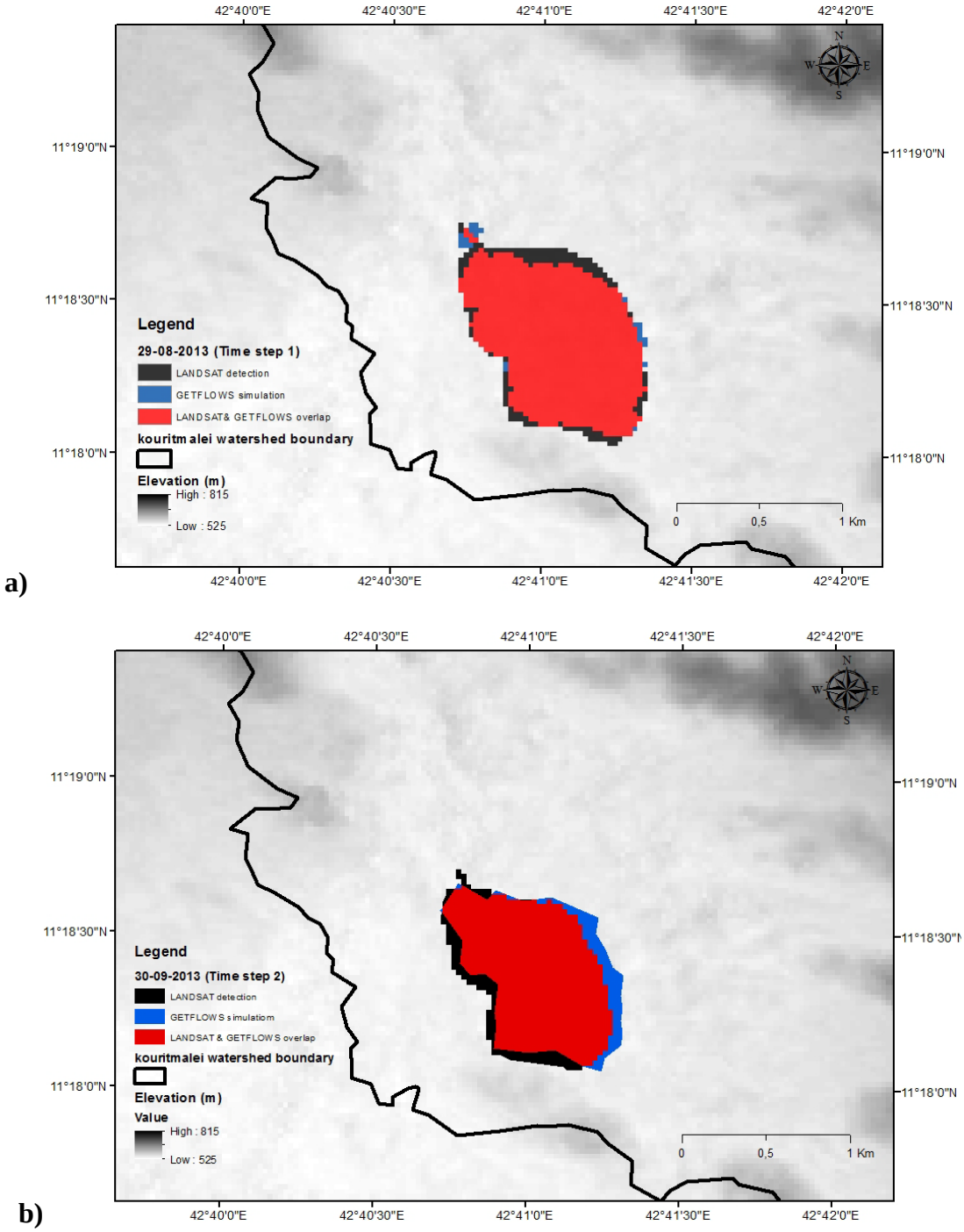

Figure 5.10: Comparison of LANDSAT satellite-based and GETFLOWS-simulated surface pond area extents: a) 29 August, 2013; b) 30 September, 2013.

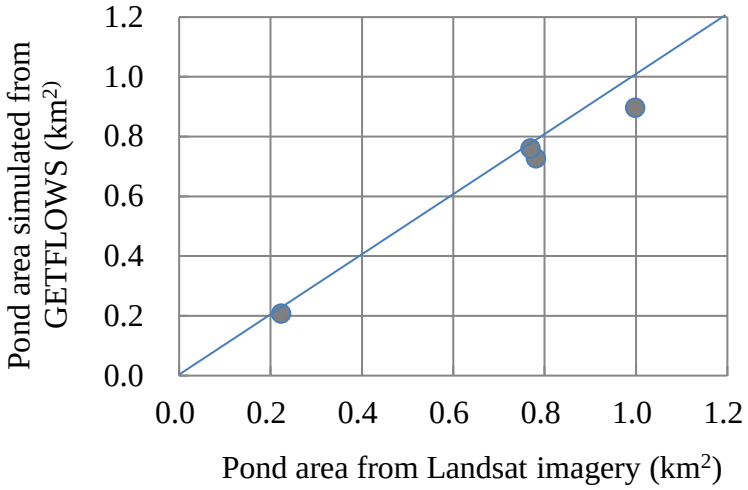

Figure 5.11: Comparison between the surface pond area extents derived from LANDSAT vs GETFLOWS

For further verification of GETFLOWS simulations results, the objective function selected to guide to assess the agreement fit between satellite-based pond extent and GETFLOWS modeled extents was the Kappa coefficient as shown in Table 5.3. Overall, GETFLOWS could recreate the rainfall-runoff process successfully for each of the date. More than 80% of the simulated pond extent matches the spatial extent detected by LANDSAT-8 at the given date. Less than 20% of the simulated spatial extent of the pond was either misclassified as flooded area (false) or either classified as non-flooded not all (missed)

Table 5.3 Comparison between GETFLOWS and LANDSAT area

Date of events	LANDSAT detected area (km^2)	GETFLOWS				Kappa Statistic K
		Simulated area (km^2)	Correct (%)	Missed (%)	False (%)	
29/AUG	1.00	0.90	85.64	12.16	2.20	0.88
14/SEP	0.86	0.73	80.00	13.16	6.83	0.84
30/SEP	0.77	0.76	78.86	11.03	10.10	0.83
12/DEC	0.22	0.21	71.22	6.80	21.99	0.82

5.7 Conclusion

In this work, we have run a rainfall-runoff simulation with GETFLOWS of the Kourtimalei watershed, and calibrated the model by using both water levels observations data, and then validated with satellite derived datasets of the spatial extents of Kourtimalei pond. GETFLOWS model was able to reproduce the rainfall-runoff process of the watershed fairly with RMSE of 0.40 m and a coefficient of determination of r^2= 0.989. This approach is in contrast with the conventional method of runoff modelling technique. The proposed approach implements a distributed hydrologic model and further calibrates the model parameters through satellite derived datasets that are freely available in the public domain. The impact of such a demonstrated technique is to provide a cost-effective tool in poorly gauged or ungauged watershed like in this case study.

REFERENCES

Jalludin, M. (1997). Hydrogeological features of the Afar Stratod basalts aquifer on the Djiboutian part. International Symposium on flood basalts, rifting and paleoclimates in the Ethiopian rift and Afar Depression, Addis Ababa, Djibouti, 3–14/02.

Jalludin M and Razack M. (1994). Analysis of pumping tests in fractured Dalha and Stratoid basalts with regard to tectonics, hydrothermal effects and weathering. Republic of Djibouti. J. Hydrol, 155, 237–250.

JICA/NTC International (2014). The master plan study for sustainable irrigation and farming in southern Djibouti: Final report. Republic of Djiboouuti Ministry of Agriculture, Water, Fisheries, Livestock and Marine Resources, Deccember 2014, Japan International Cooperation Agency/ NTC International Co., Ltd.

Magnus, U., Igboekwe, Achi, N.J. 2011. Finite Difference Method of Modelling Groundwater Flow. Journal of Water Ressource and Protection, 2011, 3,192-198.

ORSTOM (1986). Carte Geologique de la Republique de Djibouti a 1:100,000. Institut Francais de Recherche cientifique pour le Development en Cooperation.

Sadiq I. Khan, Yang Hong, Jiahu Wang, Koray (2011). Satellite Remote Sensing and Hydrologic Modeling for Flood Inundation Mapping in Lake VictoriaBasin: Implications for HydrologicPrediction in Ungauged Basins.

Seemanta S. Bhagabati and Akiyuki Kawasaki (2017); Consideration of the rainfall-runoff-inundation (RRI) modelfor flood mapping in a deltaic area of Myanmar.

Shimada S, Malow FA, Hotta T, Menjo M, Hirokane T, Suzuki S, Watanabe F (2014). Retrieving of the land surface information of a catchment in Djibouti. Journal of Arid Land Studies (Vol. 23-4, 247-250, 2014)

Tosaka, H., Itho, K., Furuno, T. (2000). Fully coupled formation of surface flow with 2-phase subsurface flow for hydrological simulation. Hydrological Process, 14, 449– 464.

Tosaka, H., Mori, K., Tada, K., Tawara, Y., and Yamashita, K. (2010). A general-purpose terrestrial fluids/heat flow simulator for watershed system management. In: IAHR International Groundwater Symposium.

Toyoda, H., Shimada, S., Hirokane, T., Ismael, T.M., Hotta, T., and Menjo, M. (2014). A study on effective use of surface runoff for irrigation in Djibouti: Watershed analysis using GIS and trial on runoff parameters estimations. Journal of Arid Land Studies, 24, 253-256.

Toyoda, H., Shimada, S., Hirokane, T., Sekiyama, A., Malow, F.A., Menjo, M., Suzuki, S.,Watanabe, F. (2015) Soil and Hydrological Survey for Retrieving the Characteristics of Surface Runoff on Kourtimalei Reservoir Watershed in Djibouti. Journal of Arid Land Studies (Vol. 25-3, 241-244)

CHAPTER VI :

DEVELOPMENT OF 3D NUMERICAL MODEL OF AMBOULI WATERSHED

CHAPTER VI : DEVELOPMENT OF 3D NUMERICAL MODEL OF AMBOULI WATERSHED

6.1 Introduction

In this chapter we present the result of the use a groundwater flow model is developed using surface and subsurface fully-coupled fluids code GETFLOWS (Tosaka et al., 2000) to investigate the hydrological processes in the Ambouli watershed. The hydrogeological system is reproduced according to sparsely distributed boreholes data and based on available geological, hydrogeological, geomorphological, climatological and pedological data. Groundwater levels measured in 2010 are used for the steady state calibration and are employed then as initial conditions for the transient simulations.

6.2 Background

The wadi Ambouli is of particular importance in the Republic of Djibouti though the catchment area (about 600 km^2) represents less than 2.5% of area of the national territory. In fact, this hydrographic unit has two physical characters that are closely associated with the country's activity and more especially to the development of its capital, Djibouti town.

Firstly, the delta of the wadi in the Indian Ocean is a large cone flattened extended by a coral peninsula on which is located the city of Djibouti. The presence of a good water resource in the alluvial terraces lining the last kilometers of the wadi before its delta is one of the primary causes of the installation then the development of the city (and the port) for more than a century by the French colonial power. This beneficial aspect has setbacks, the most serious of which is the risk of inundation by floods, rare and brief (a few hours) but very violent and more and more harmful as urban infrastructures become denser and more valuable. Several disasters have taken place over the past decades, the most recent on April 13, 2004, with loss of life and serious material and economic damage.

Secondly, the underground of the entire lower part of the watershed consists of basaltic rocks of several tens of meters thickness which contains an abundant aquifer of good quality. It has been exploited for several decades by means of many boreholes for almost all the water needed to supply the city of Djibouti (more than 13 Mm^3 per year at present, with rapid growth in needs and a steady deterioration of water quality).

On the other hand, many activities, traditional or recently rapidly expanding, are practiced more or less intensively in this watershed: pastoralism, extraction of construction materials, transports along the main road to Ethiopia, or even urbanization and irrigated agriculture (especially in the PK 20 sector).

6.3 Hydrological feature

The wadi Ambouli drains a watershed of about 600 km^2 upon arrival in the City of Djibouti where it flows into the Indian Ocean at the entrance to the Gulf of Tadjourah.

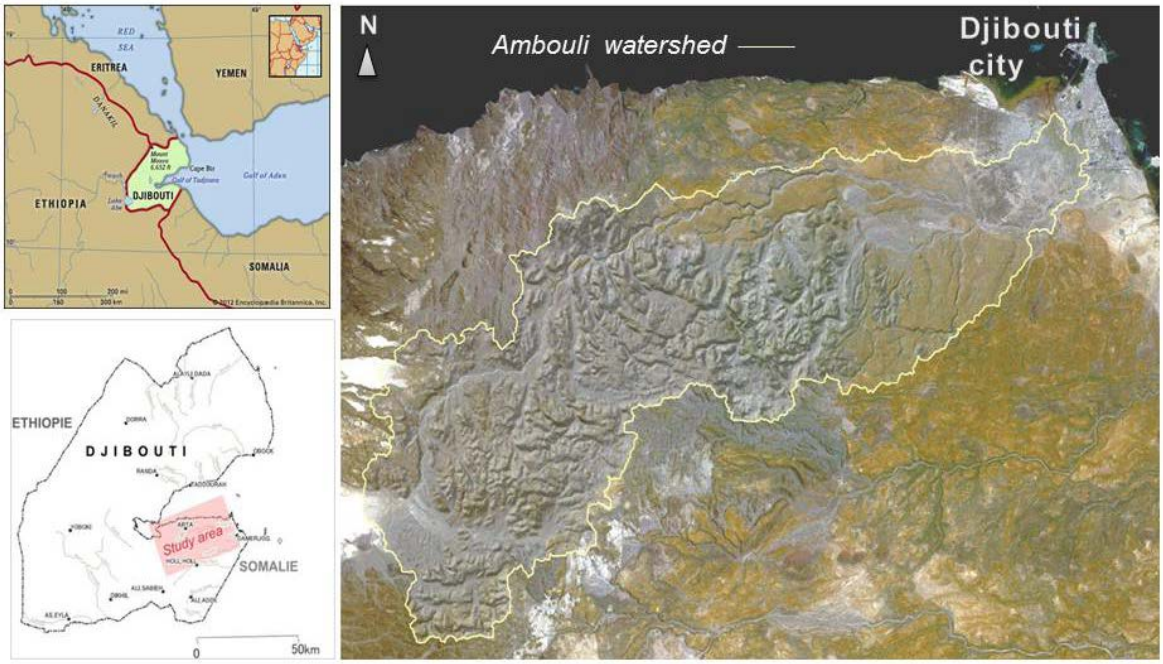

Figure 6.1: Location of Ambouli watershed

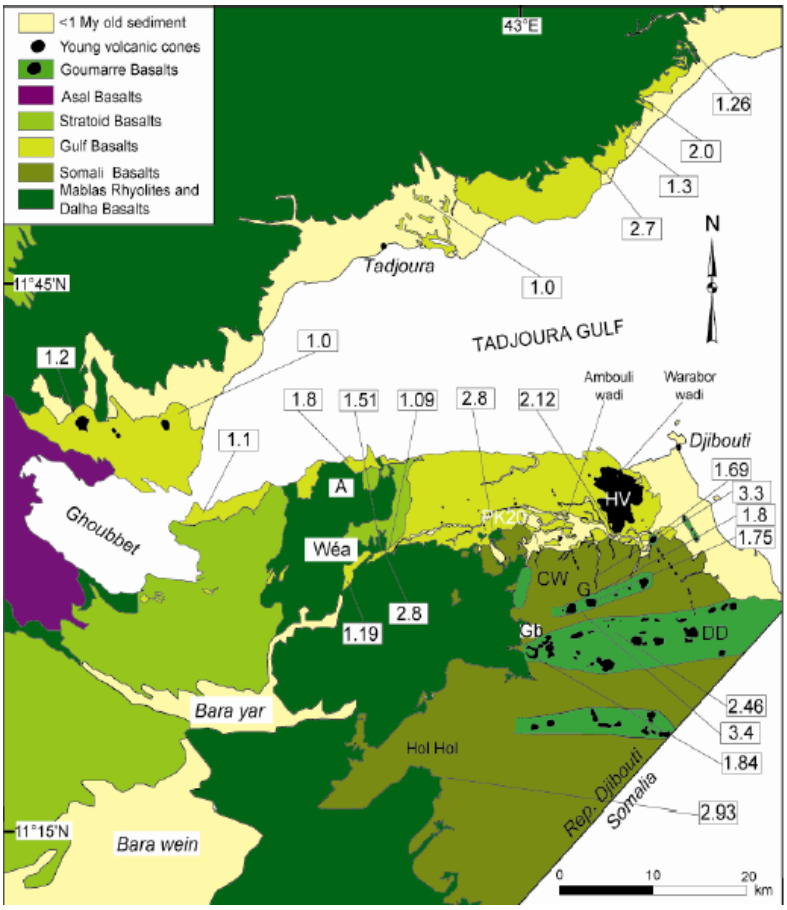

Figure 6.2: Geological map of Gulf Tadjourah (Daoud, 2008)

The main stream, wadi Ambouli (which takes the name of wadi Oueah on the most of its upstream course), cut the watershed on its western and northern parts for about 60 km long. The main tributary wadis lead to the right bank of the wadi Oueah. They drain a significant proportion (31.3%) of the total watershed; these are, from downstream to upstream: the wadi Chabelley (24.7 km^2 at the confluence), the wadi Boullé (85.7 km^2), wadi Kalaloho (48.5 km^2) and wadi Langobalé (19.3 km^2), which all join wadi Oueah within 23 km upstream of the terminal delta at Nagad.

In the intermediate and upstream areas of the watershed, we find several tributary sub-basins between 20 and 50 km^2 (Wadi Bod, wadi El Bahay, wadi Hilbaley-Sagar), they are subject to different rains (continental) than the oceanic rains prevailing on the downstream part of the watershed. On the left bank of wadi Oueah, the hydrography is broken up into a multitude of small sub-basins (a few km^2 at most) drained by very steep ravines (Figure 6.1).

6.4 Topography

The main geomorphological groups composing the watershed are in number six, from upstream to downstream:

- The upper watershed extends on the Bour Ougoul Mountain that reaches the highest altitudes of the watershed but a large part of the area consists of plains (notably the Petit Bara) with slow flows, which are characterized by an aptitude for intense runoff significantly less than other parts of the watershed.
- The ravines descending from the Arta massif on the left bank of wadi Oueah.
- The central massif (Bour Ougoul), divided into about thirty small basins area between 3 and 12 km^2. It is composed of a backbone of trays oriented South West - North East and peripheral valleys with transverse profile in V rather flared. The altitude ranges from 600 to 900 m on the summit and about 150 m to the outlet on the piedmont.

- The alluvial peneplains areas (Petit Bara desert area)
- The plateaus and canyons of Basaltic rocks with a very characteristic facies in the landscape.
- The terminal delta of the Ambouli River, forming a very flattened cone of alluvium coarse about 6 to 8 km long (Figure 6.2).

6.5 Geological feature

The watershed's entire substratum consists of basalts, of relatively recent origin (between the Tertiary middle and early Quaternary). The basaltic aquifer, including Gulf and Somali basalts, cover an area of 600 km².The basalts are in the form of a series of plateaus that rise up to 200 m. Several major wadis (Ambouli, Atar, Damerdjog, Douda) cut these basalts by forming canyons with cliffs which can exceed several tens of meters. Many volcanic cones of different sizes are situated on the plateaus, particularly in the South. Gulf and Somali basalts are composed of basaltic flows with intercalation of sedimentary strata, scorias and palaeosoils. They are characterized by an important surface alteration in bowls. The age of the Gulf basalts is 2.8-1 Ma, while the Somali basalts are older (9-3.4 Ma). The thickness of the Gulf basalts was determined after the mineralogical analysis of the cores of the only well that entirely cut these basalts (Daoud, 2008). This well is part of the PK20 wells field. A thickness of 250m was determined. The Gulf basalts lie on Somali basalts in the South and Dalha basalts (9-3.4 Ma) and Mabla rhyolites (15 Ma) in the West. On the East Coast, there is a coastal plain forming a band of a few kilometers wide, related to alluvial cones of different wadis. These formations date from the Pleistocene and the Holocene (Gasse et al. 1986). Several fractures networks affect the Gulf basalts. The East-West fractures direction is the most important one and is probably related with the first deformations associated with the setting up of the basalts (Arthaud and Jalludin, 1990). This main fracture strike would have been reactivated until recently. The other fracturing directions are N140-150

and NS-N040. Outcrops are characterized by varying degrees of alteration and hydrothermalism. Hydrothermal activities result in deposits of secondary minerals and thus reduce the permeability of the basalts (Jalludin and Razack 1993, 1994). Infiltration mainly occurs in sedimentary formation in the wadis beds. The recharge of the wadi-alluvial aquifers then allows the recharge of the underlying volcanic aquifers. Most of the wells in the Ambouli area were designed for pumping purposes and are not well distributed. The water table is known with sufficient accuracy in the east and lest precisely in the west of the watershed. Given the fracturing affecting the basalts, the groundwater flow is assumed to be continuous.

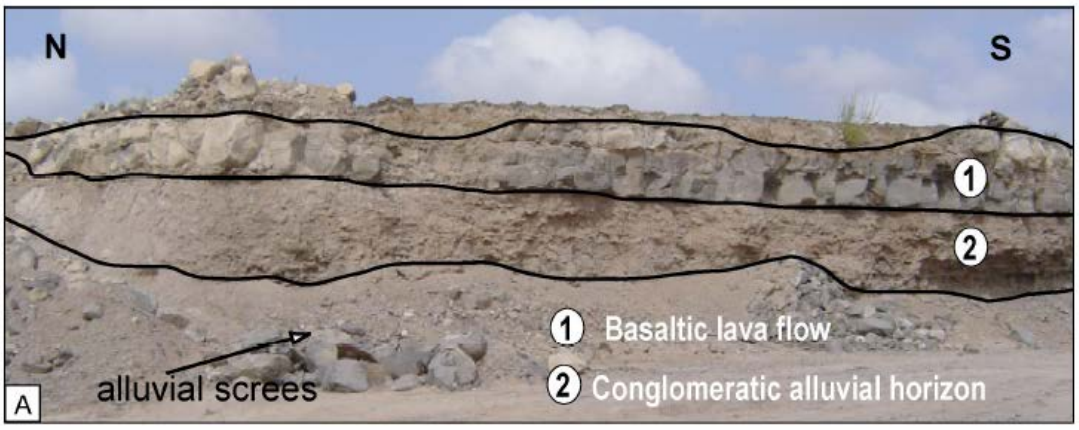

Figure 6.3: Alluvial conglomeratic horizon interdigitated with a thin basaltic lava flow of Gulf Basalts in the Ambouli-Chabelley area (Daoud, 2008)

The primary discharge in the study area is the groundwater abstraction. The Gulf/Somali basalts aquifer is intensively exploited for the supply of fresh water for the Djibouti city. The boreholes are operated continuously with a total daily average discharge of 52,250 $m^3 day^{-1}$ (ONEAD).

6.6 Materials and numerical methods

6.6.1 3-D grid corner point representation

In order to implement the numerical simulation model, a spatial description of the problem

domain must be developed through 3D structural model. A 3D grid-block system for which each nesting level have different spatial resolution were constructed. First the basic data such as topographic features, land use/land cover and important geological features such as channels and thickness variations in different geological strata were pre-processed in Geographic Information System (GIS) then used to define the topology and boundary of the 3D model. The wadi Ambouli watershed along with the adjacent sea area is discretized in the grid-block system. It covers an area of 800 km^2 with total number of grid-blocks of 33,410 horizontally and 18 for vertical layering.

The aquifers of the Ambouli watershed are characterized by a complexes boundary condition with anisotropy and heterogeneity. Although some areas with little or no hydrogeological data (e.g., the western Ambouli basin) exist within the watershed because few or no wells have been drilled in these areas, a reasonable representation (Figure 6.2) was developed. Groundwater flows are influenced by the presence of faults. However, the locations of faults remain unknown so therefore the hydraulic influences of faults are unknown. The water recharge occurs downward by the porous domain of the wadi-alluvial aquifers then allows the recharge of the underlying volcanic aquifers.

6.6.2 Field initialisation procedure

The current distribution conditions of the groundwater levels and flow rates were recreated through the field initialization procedure. This procedure consists on considering fully saturated condition in underground without any surface water on land surface. Eventually, the conditions of fluids flow reach to an equilibrium state in which the precipitation and runoff out of the system balances under topographic and geologic/hydraulic structures.

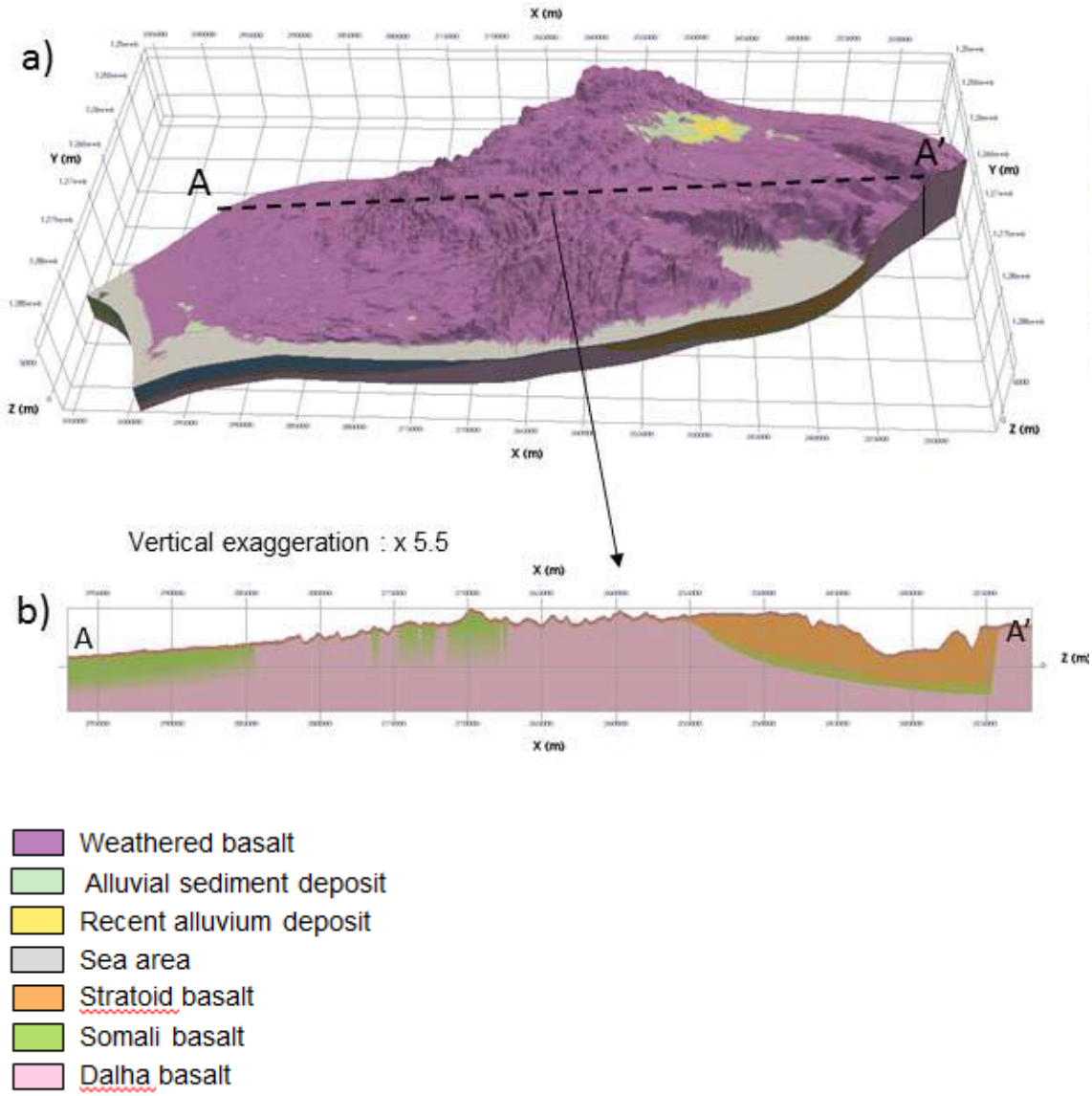

Figure 6.5: (a) Geological units in the heterogeneous model, (b) vertical cross-section through the model .The vertical exaggeration for all figures is 5.5x

The calibration aims at obtaining an optimal fit between the calculated and the measured data, which is also an important measure for the reliability of the operational model. In the current groundwater model, it involved two sequential steps: At first, the steady state model representing the state of the aquifer system before water resources development was calibrated using the measured water level data from observation wells in order to understand the trend of groundwater level in the whole domain. Then based on the preliminary hydrogeological properties obtained from the steady-state calibration, a transient flow model is developed to simulate the groundwater level changes in the time period of between 1999–2007.

6.7 Analysis Conditions

6.7.1 Precipitation and Evapotranspiration

The effective precipitation, which can be obtained by removing the evapotranspiration from the total precipitation, is used as the average precipitation for the initialization process. The annual precipitation of the study area is totally 150 mm yr^{-1} to 200 mm yr^{-1}. It is extremely small compared to the annual evapotranspiration that is estimated by Harmon's method which is over 1,850 mm yr^{-1} (BGR1982).

6.7.2 Fluids Properties

The fluid properties of water air and is represented by the typical value in standard condition as shown in Table 6-1.

Table 6-2 Fluid Properties

Surface water flow		Linearized diffusion wave approximation
Groundwater flow		Generalized Darcy's law
Freshwater	**Density**	1.0 g cm^{-3}
	Viscosity	1.0×10^{-3} Pa·s
	Compressibility	0.45 GPa^{-1}
Air	**Density**	1.3×10^{-3} g cm^{-3}
	Viscosity	1.82×10^{-5} Pa·s
	Compressibility	Table function of formation volume factor

6.7.2.1 Soil and rock properties

Jalludin and Razack, (2004) conducted an analysis of the data from pumping tests conducted since the 1960s in the sedimentary and volcanic aquifers in the Republic of Djibouti. It has showed that measured transmissivity data collected on the sedimentary aquifers range between very low (T=0.4 m^2 h^{-1}) and relatively high values (T=163 m^2 h^{-1}). These formations are quite heterogeneous and the variable clay content in sediments and also to hydrothermal effects as observed in the field is the reason behind the extended transmissivity range.

Similarly, the extend range was observed in the transmissivity values of the Gulf and stratiform basalt aquifers range that were between 0.5 and 1,130 m^2 h^{-1}. The transmissivity values of the Dalha basalt aquifers are found to be lower than those of the recent basalt aquifers, and range between 0.5 and 36 m^2 h^{-1}. The transmissivity values of

the Somali basalt aquifers range between 1 and 219 m^2 h^{-1}. Table 6-2 shows the summaries of the soil and rock properties. The permeability of outcrops of basalt, weathered rock and bedrock was considered to be small according to (Jalludin and Razack, 2004)

Table 6- 3 Soil and Rock Properties

Density		$28m^{-3}$
Compression ratio		10^{-5} GPa^{-1}
Absolute Permeability	Alluvium Deposit	1.16×10^5 md
	Gulf/Stratiform Basalt	7.43×10^4 md
	Dalha Basalt,	1.37×10^3 md
	Somali Basalt	9.33×10^3 md
	Weathered basalt,	1.0×10^2 md
Effective Porosity	Alluvium deposit	0.40
	All basalt	0.10
Roughness coefficient		Bare soil: 0.033

6.8 The steady state model

Figure 6.4 shows the computed hydraulic head distribution after the field initialization procedure. It can be seen that the general groundwater flow pattern is clearly represented, i.e. from the highlands area to the lower plain. Water tables are deeper in the western regions, and shallower in the eastern regions of the model (Figure 6.4). Next, we compare the results of the numerical experiment to observations. The observed water levels of wells

are available and they are poorly distributed in different parts of the study area (locations of the observation wells. To obtain the best match between the calculated and the observed groundwater levels from the observation, the parameters values were adjusted until the deviation are reduce to a minimum in the model calibration process (Table 6.3).

We see a very close agreement between observations and model simulations (Figure 6.5). The RMSE error between observation heads and computed heads is 11.37 m while the correlation coefficient r^2 is around 0.9. This can be considered acceptable (Hill 1998), but the difference between the measured and calculated water level of the 17 wells varied between 20 and 30 m. The computed hydraulic heads are a bit higher than observed heads values. This phenomenon may be due to the pumping activities at those locations. To reflect these local intensive pumping activities, the equal distribution of pumping rates shall be changed once the data on such activities are available.

Table 6.4 Optimized hydraulic conductivities values

Geology	***Initial values K*** ***(m^2)***	***Optimized values K*** ***(m^2)***
Alluvium deposit	1.37×10^{-10}	1.37×10^{-10}
Gulf/Stratiform basalt	7.33×10^{-10}	9.14×10^{-5}
Dalha basalt	1.36×10^{-11}	1.01×10^{-6}
Somali basalt	9.21×10^{-11}	3.49×10^{-6}

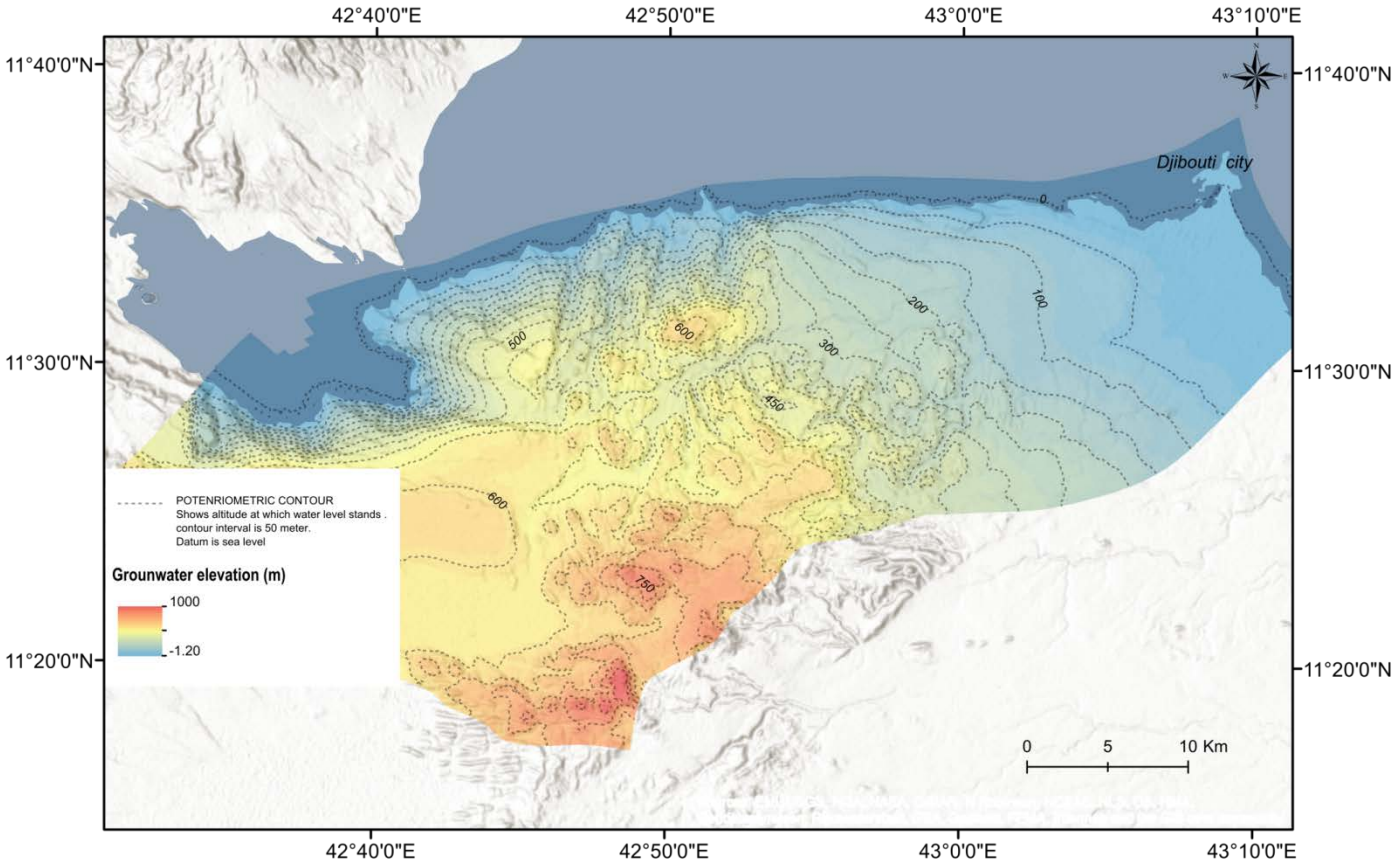

Figure 6.6: Groundwater elevation (m) resulting from the simulation.

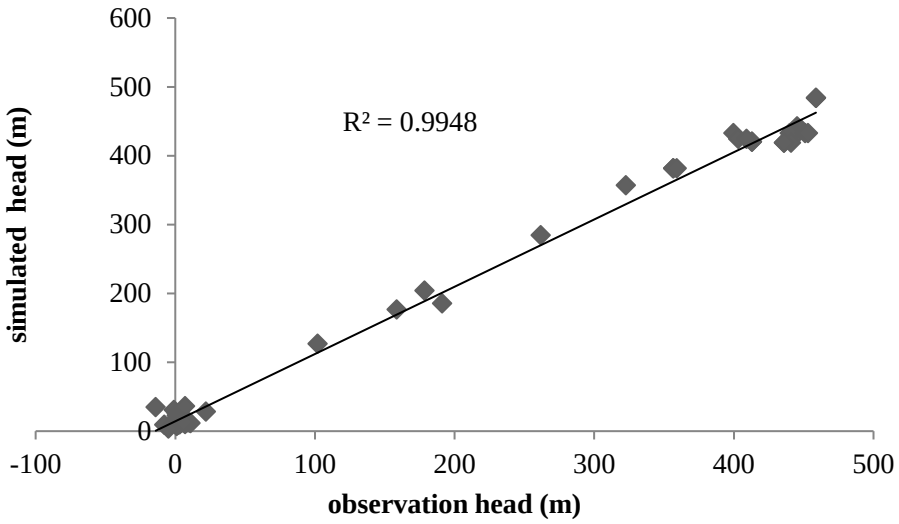

Figure 6.7: Comparison of the observation head and the simulated head

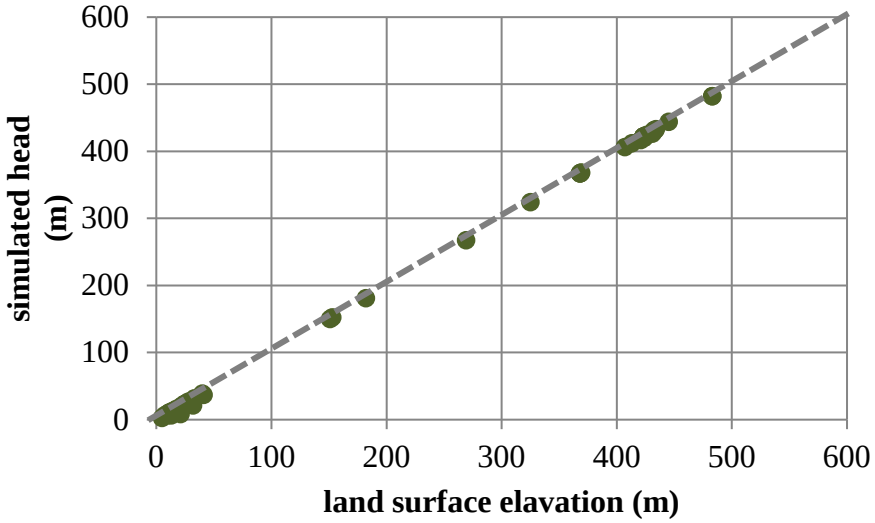

Figure 6.8: Plot of simulated hydraulic head vs. surface elevation

6.9 The transient state model

Based on the preliminary hydraulic conductivities and boundary conditions obtained from the steady-state calibration, a transient flow model is developed to simulate the groundwater level changes. The resulting flow field of the calibration is used as the initial condition for the next transient simulation in response to the dynamic recharge. The calibration period of time is determined as 40 years from 1960 to 2010 according to the available rainfall data (Figure 6.6), which is given in the unit of year. In the simulation, the time step size is fixed to a year and time and space-dependent source terms are imposed on the top surface according to the yearly average rainfall over the simulation period. The transient model calibration is accomplished by simulating hydraulic head change in response to changes in recharge. With regard to the time series data of water level, only

1 borehole (RG3) has records which cover part of the simulation period. For this borehole, the groundwater abstraction integrated into the model was fixed at 245 $m^3 d^{-1}$ according to the available historical record of the borehole. The comparison of the calculated versus measured groundwater levels of the well is shown in Figure 6.7. It is

noticeable from the measured water level in observation well a continuous decline during the available records. Figure 6.8 indicate overall the same trend observed in the measured well. Root mean square error (RMSE) was also used as criteria to check the calibration results. For the observation well, RMSE is 0.88 m. The slight differences between the calculated water levels and the observed ones exist because of the uncertainty of the abstraction representing the pumping activity in the study area

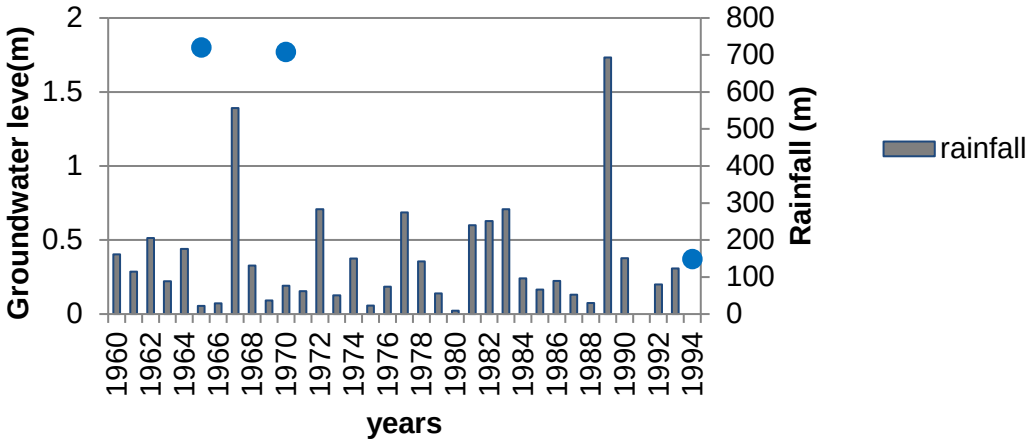

Figure 6.9: Rainfall recorded at the Djibouti aerodrome station

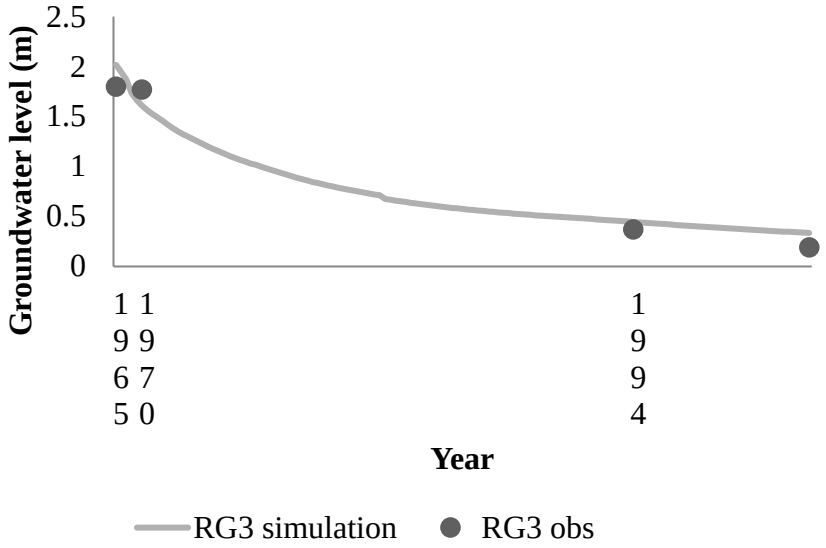

Figure 6.10: Trends in groundwater level reproduced over time in RG3 borehole

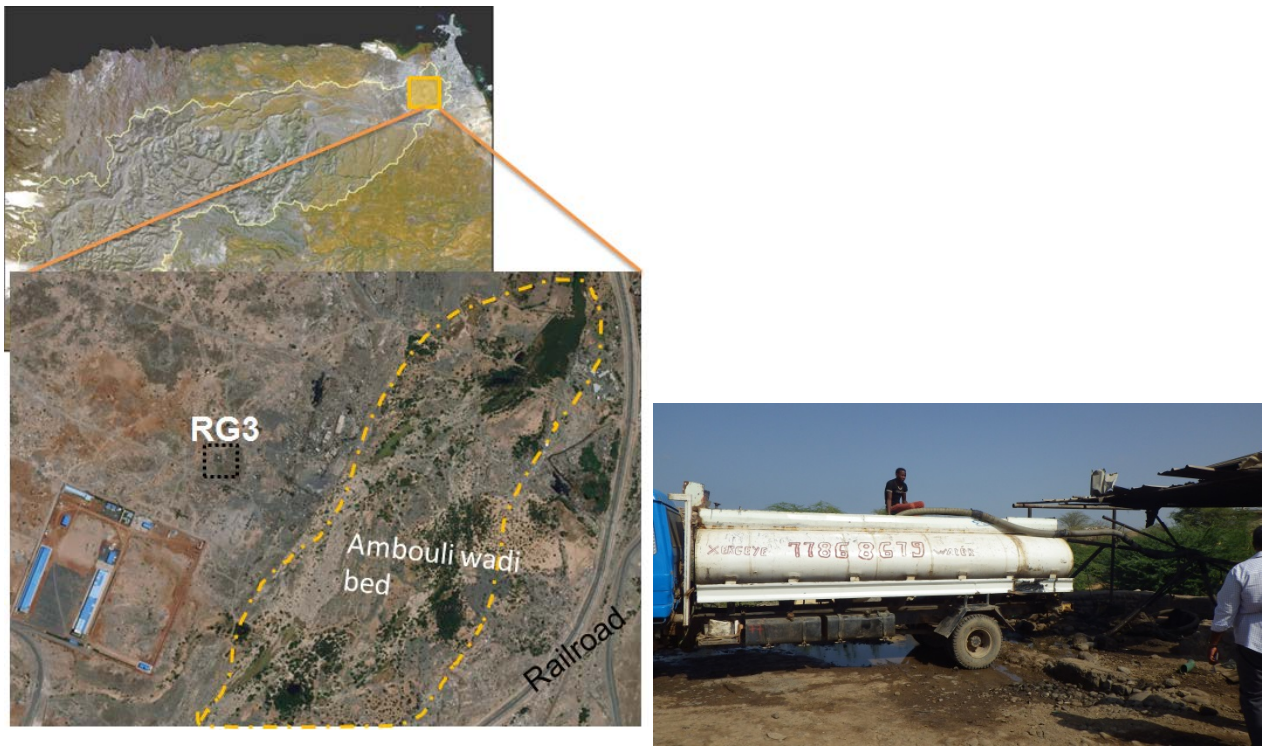

Figure 6.11: Location of the RG3 borehole. Truck used to pump the borehole

6.10 Model limitation

Numerical models of groundwater flow are limited in their representation of the physical system because they contain simplifications and assumptions that may or may not be valid. Results from groundwater flow models have a degree of uncertainty primarily because of uncertainties in many model input parameters (most importantly hydraulic conductivity and transmissivity) and boundary conditions applied. The various steps in the modelling process may each introduce errors, converting the real world into conceptual model and converting conceptual model into3D model.

The built model of the present research is associated with a number of uncertainties. First of all, the hydro-geological heterogeneity caused difficulties in the conceptual simplification of the field condition due to lack of detailed description of the heterogeneity. Despite the complex and heterogeneous nature of the aquifer system,

assumptions and simplifications were made during the conceptualization of the system. Definitely uncertainties will be introduced as the result of these assumptions and simplifications of the field conditions. Various forms of heterogeneity in the porous media properties can be very different from the fluid flow behaviour in the individual zones (Das and Lewis, 2007). There are generally few locations where observations are available, and the geological structure of the aquifer is only partially known. Lack of proper site characterization may result in a model that is calibrated to a set of conditions which are not representative of actual field conditions.

The main constraints in the modelling process were data gaps and poor quality of the available data. The data which have a key role in defining the model geometry (aquifer thickness) are not well documented. The available records of the water level measurements are not continuous and mostly are only single measurements. Furthermore, calibration values (heads) are highly associated with measurement errors. The available hydraulic head data is applied for model calibration, thus there was insufficient independent data for model validation. Another area of uncertainty is resulting from defining the boundary conditions of the model domain. The boundary conditions were defined based on the surface physical features such as impervious geology and surface water divide. Hence additional uncertainty may be introduced as the result of this assumption.

6.11 Conclusion

There is a dramatic deterioration of groundwater in the Djibouti city area where groundwater is the most important resource for drinking water supply. In this chapter, a 3D groundwater model was developed for the semi-arid to arid Ambouli watershed area in Djibouti. The challenge was to develop and to apply a methodology for a typical situation of data scarcity i.e. data or information is only available in a few locations. Using methods of interpolation, scientific interpretation and expert knowledge, a comprehensive data

network was established which was used to generate a groundwater flow model on the basis of high precision data (DEM) and scarce and partly inadequate hydraulic and hydrogeological data (hydraulic parameters) as well as spatial clustered data (boreholes). The model was calibrated with all available data and the groundwater flow regime was investigated under steady and transient conditions. It was found that the groundwater level changes are due to anthropogenic activities (groundwater abstraction)

The present model cannot be regarded as validated yet because of inadequate data (Insufficient information) however it helped understand locally the natural groundwater behaviour. It can be seen that the decreasing trend of ground water levels in the study area shows that the current groundwater utilization scheme is unsustainable under the climate conditions. In order to reduce the uncertainties, the model will need to be improved in the future by developing appropriate monitoring strategies and collecting more detailed data when available. This is the first step toward a comprehensive effort to the scenario analysis for a sustainable water resources management in the area, including climate change, land use, and social-economic factors.

References:

Appleyard, J.R.I. (1983). Nested factorization. Society of Petroleum, SPE12264

Arthaud F. and Jalludin M. 1990. Mapping of fractured hydrogeological reservoir in a volcanic environment from SPOT field-controlled data (Miocene basalts). of Djibouti). 4th Scientific Remote Sensing Days. Montreal. 1991.

Gasse F., Varet J., Mazet G., Recroix F. and Ruegg J.C. 1986. Geological map of the Republic of DJibouti at 1: 100,000. Ali Sabieh. Instructions. ISERST, French Ministry of Cooperation, ed. ORSTOM, Paris, p. 104.

Grabe A, Rodiger T, Rink K, Fischer T, Sun F, Wang W, Siebart C, Kolditz O (2013) Numerical analysis of the groundwater regime in the western Dead Sea escarpment, Israel + West Bank Environ Earth Sci 69:571-585.

Harbaugh, A.W., Banta, E.R., Hill, M.C., and McDonald, M.G., (2000). MODFLOW-2000, The U.S. Geological Survey Modular Ground-Water Model - User guide to modularization concepts and the ground-water flow process: U.S. Geological Survey Open-File Report 00-92, 121 p.

Hill M.C. (1998) Methods and guidelines for effective model calibration with application to UCODE, a computer code for universal inverse modelling: U.S. Geological Survey Water Resources Report 98–4005. Tech rep

Horton, R.E. (1933). The Role of Infiltration in the Hydrologic Cycle. Transactions of American Geophysical Union, 14, 446-460

Jalludin M, Razack M. (1994). Analysis of pumping tests in fractured Dalha and Stratoid basalts with regard to tectonics, hydrothermal effects and weathering, Republic of Djibouti. J. Hydrol, 155, 237–250.

Jalludin, M. (1997). Hydrogeological features of the Afar Stratoid basalts aquifer on the Djiboutian part. International Symposium on flood basalts, rifting and paleoclimates in the Ethiopian rift and Afar Depression, Addis Ababa, Djibouti, 3–14/02/1997.

Mori, K. Tada, et al (2008): A high performance full-3D nutrient transport modeling based on the surface water and groundwater coupling technique for the water quality assessment: An application to the lake Kasumigaura, Japan, Int. symp. on Hydro Change.

Reilly, T.E and Harbaugh, A.W., 2004. Guidelines for evaluating groundwater flow models. U.S. Geological Survey Scientific Investigations Report 2004-5038, version1, 01, Reston, VA, 30pp.

Tosaka, H., Itho, K., Furuno, T. 2000. Fully coupled formation of surface flow with 2-phase subsurface flow for hydrological simulation. Hydrological Process, 14, 449– 464.

Tosaka, H., Mori, K., Tada, K., Tawara, Y., and Yamashita, K. 2010. A general-purpose terrestrial fluids/heat flow simulator for watershed system management. In: IAHR International Groundwater Symposium.

Toselli, A. and O.Widlund. (2005). Domain Decomposition Methods: Algorithms and Theory.

Wu, Y.; Wang, W.; Toll, M.; Alkhoury, W.; Sauter, M.; Kolditz, O., 2011: Development of a 3D groundwater model based on scarce data; the Wadi Kafrein catchment/Jordan.

CHAPTER VII:

CONCLUSION AND RECOMMENDATIONS

CHAPTER VII: CONCLUSION AND RECOMMENDATIONS

7.1. Conclusion

Water shortage and groundwater degradation have become two primary environmental concerns to Djibouti since the 1990s. The local aquifers in the capital city, as the dominant sources for domestic and agricultural water supply, are depleting due to groundwater abstraction and continuous drought in recent years with rapid urbanization and increasing water consumption.

The country, especially the capital city, has to face continuously difficulties in its water supply which is derived by 95% from groundwater. First, the arid climatic conditions in the recent years had led to a recurrent drought period. The economic development programs and population growth in Djibouti city increased groundwater demand leading to an overall overexploitation of the resources and water quality degradation. Future water requirement (2020, 2030) estimated to three times more than the present production rate. The new phase of water resource development must inevitably be followed by management and protection of the aquifers systems and not just the search for the new groundwater resources

Therefore, understanding the hydrogeological system is fundamental for a sustainable water resources management. This work focused on the use of Groundwater models in for sustainable management of the watershed with a focus on two watersheds specifically (Ambouli and Kourtimalei) because of the available information.

This first work was focused on the simulation of a surface terrestrial water flow process model in the area of Kourtimalei in Djibouti using GIS, RS and GETFLOWS, a physics-based surface and subsurface fully coupled fluids flow code. A trial and error method were used to calibrate the model using observed surface water level of the pond. The manual calibration was performed until the surface water level of the pond RMSE to be 0.40 m with r^2=0.99. Furthermore, kappa coefficient was used to evaluate the agreement between the pond areas extents derived from available LANDSAT-8 images during the simulation period with the pond area extents results of GETFLOWS simulation. The analysis showed that GETFLOWS successfully simulated the surface water flow process. We conclude that the use satellite derived datasets can help calibrate and evaluate GEFTLOWS hydrologic model for an ungauged watershed like in the present case.

The second work was a research in order to investigate the hydrological processes in the Ambouli watershed. A 3D groundwater flow model was developed using surface an GETFLOWS (Tosaka et al., 2000). The hydrogeological system is reproduced according to sparsely distributed boreholes data and based on available geological, hydrogeological, geomorphological, climatological and pedological data. Groundwater levels measured in 2010 are used for the steady state calibration and are employed then as initial conditions for the transient simulations. Good agreement between simulated and observed groundwater heads with r^2 of 0.9 is obtained. The transient groundwater flow simulations reflect the observed drawdown of the last 40 years and show the formation of a depression cone in an intensively pumped area.

Despite the lack of information, the model was able to reproduce correctly the main behavior of the system with a reasonable accuracy for both surface and subsurface level. However, some additional improvements should be made for the model to increase in the representativeness of the system. In the future this tool can be used as part of an

integrated watershed management tool

7.2. Recommendations

This present work should not be the end of groundwater flow modeling in the area rather it is a good starting work for detailed modeling in the future. With additional data, further refinement of the model is possible, which is expected to improve the accuracy of the model.

Further extensive field-based observations combined with down whole geophysical well logging and hydraulic testing techniques, detailed delineation of fractures and other secondary porosity is required to compile the hydro-geologic framework for each geological sequence. Prior to detail groundwater modeling, detail structural mapping is required which will have a great importance in aquifer characterization and definition of boundary conditions.

The transmissivity to which the model is highly sensitive requires better future characterization. The cell size applied in the discretization of the problem domain is not small enough to adequately represent the drawdown in the wells. Thus the model can be further developed by integrating additional data and by applying finer grids in the pumping areas.To improve calibration values, groundwater level should be monitored at a set of monitoring wells that are evenly distributed in the sub-catchment. In this study only one well had the adequate times series documentation. In the future the time series documentation of the abstraction rates of the all the boreholes should be further improved and extended.

Once an improved steady-state model is obtained, transient simulation should be carried out for better predictions of pumping effect and for better recharge modeling (response of groundwater levels to good/bad raining seasons).

Future groundwater resource development plans should take into account the

balance between the groundwater recharge and the intended abstraction rates to ensure the sustainability of the resource in the catchment.

ANNEXES

Annexes

Monthly Relative Humidity, Temperature, Sunshine Hour and Wind Speed in Djibouti (1961-2007)

	Month	Jan	Feb	Mar	Av	My	Jun	Jul	Aug	Sep	Oct	Nov	Dec
Tmin (^{O}C)	ave	19,1	19,5	20,9	22,7	24,1	26,4	27,7	27,1	25,9	22,5	20,7	19,4
	Max,	23,9	24,4	26,2	31,0	27,0	28,9	30,8	36,3	30,5	27,9	22,8	23,5
	Min,	16,0	16,2	17,0	18,5	19,8	21,4	23,3	23,6	23,1	17,2	17,8	16,8
Tmax (^{O}C)	Av	30,0	30,7	32,6	34,7	39,1	44,0	44,6	44,0	42,4	35,9	32,6	30,5
	Max,	33,8	33,4	36,8	38,1	44,8	46,5	46,1	45,8	44,6	40,3	38,5	32,6
	Min,	25,2	26,8	26,8	28,5	29,2	33,0	35,4	33,0	31,6	29,0	26,1	25,6
Humidity Max (%)	Av	94,5	94,0	94,0	94,2	93,9	91,0	84,5	87,0	92,4	92,8	94,1	94,5
	Max,	100	100	99,0	100	99,0	99,0	100	98,0	100	100	100	100
	Min,	84,0	85,0	88,0	88,0	80,0	80,0	66,0	66,0	78,0	82,0	82,0	88,0
Humidity Min (%)	Av	47,3	46,5	44,9	36,4	28,0	14,6	15,3	18,3	21,1	32,9	42,7	47,0
	Max,	59,0	62,0	70,0	63,0	51,0	35,0	23,0	25,0	30,0	53,0	55,0	63,0
	Min,	38,0	29,0	17,0	15,0	5,0	2,0	9,0	10,0	11,0	11,0	23,0	39,0
Radiation	Av	235,3	229,6	259,0	274,1	310,1	270,7	250,5	270,6	275,7	295	282,9	277,2
	Max,	310	294	316	326	347	323	290	307	320,9	327	310	360,5
	Min,	138,0	105	171	213	253	143,3	190	224	241	209	158,1	194
Potential Evaporation (mm)	Av	46,2	38,6	55,2	59,4	60,4	73,6	90,2	100,3	71,7	58,6	55,3	46,4
	Max	67,4	71,8	79,6	84,8	92,6	124,0	155,0	151,9	113,3	96,0	84,2	76,5
	Min	5,6	3,5	6,7	7,4	7,8	9,8	10,7	10,7	9,3	7,5	4,6	5,8

N°I	Région	Localité	Nom-Pt d'eau	X(m)	Y(m)	Z(m)	Date	Réa.	Type O	Etat	Prof (m)	NS (m)	ND (m)	Conductivity.	Q (m3/h)	T(°C)
	Djibouti	Chebelley	Wehad2	291391	1273484	62	2010	DE	Forage	Fonctionnel	140	----	----	3900	----	43
	Djibouti	Djibouti	DOUDA	300332	1275927	22	2002	DE	Forage	Forage positif	61	----	16.5	4420	88	38.6
	Djibouti	Camp Lemonier	Camp Lemonier	298256	1276593	----	2002	DE	Forage	Forage positif	61	16,05	15	42500	80	42,7
	Djibouti	Djibouti	E 15b	297908	1273867	21	2006	DE	Forage	Onead	29,5	----	20	3800	----	38
	Djibouti	BASE AERIEN	BASE AERIEN	297347	1278374	3	1988	DE	Forage	HS	----	----	----	----	----	----
	Djibouti	EDD	EDD	297302	1280680	3	1990	DE	Forage	Forage positif	22	----	8	10000	13	35
	Djibouti	nagad	E 6b	297135	1274934	23	2003	DE	Forage	Onead	34	----	----	----	----	----
	Djibouti	nagad	E 6	297114	1275118	23	1964	DE	Forage	Fonctionnel	38	----	21	----	36	----
847	Djibouti	nagad	E6 (bis)	297100	1275108	27	----	DE	Forage	HS	41	22,73	26,95	----	----	----
125	Djibouti	nagad	E6 (bis)	297100	1275108	27	----	DE	Forage	Fonctionnel	41	26,95	22,73	3060	----	----
	Djibouti	nagad	E 1	297025	1275457	21	1962	DE	Forage	Onead	31	----	19	3625	56	40
	Djibouti	douda	E 3	296845	1275673	21	1963	DE	Forage	Onead	37	----	18	----	39	40
	Djibouti	douda	E 13	296810	1274674	22.5	1972	DE	Forage	Onead	39,1	----	21	----	48	38
883	Djibouti	douda	Douda E3	296748	1274838	27	----	DE	Forage	Forage positif	37	18	----	----	----	----
160	Djibouti	douda	Douda E3	296748	1274838	27	1986	DE	Forage	Fonctionnel	37	----	18	2820	13	----
	Djibouti	nagad	E 5b	296733	1275030	----	----	DE	Forage	Onead	----	----	----	----	----	----
846	Djibouti	nagad	Nagad E5 (bis)	296725	1275216	27	----	DE	Forage	HS	38	23,81	26,05	----	----	----
124	Djibouti	Nagarro	Nagad E5 (bis)	296725	1275216	27	----	DE	Forage	Fonctionnel	38	26,05	23,81	1680	----	----

	Djibouti	nagad	E 2	296693	1275551	23	1962	DE	Forage	Abandonné	30	----	22	2725	40	39
	Djibouti	nagad	E 2b	296693	1275551	23	2003	DE	Forage	Onead	40	----	----	----	----	----
	Djibouti	nagad	E 5	296691	1275275	24	----	DE	Forage	Abandonné	37	----	23	2740	35	39
	Djibouti	nagad	E 12	296632	1275515	23	1966	DE	Forage	Onead	46,5	----	22	3375	36	40
	Djibouti	Plateau	PL.DU SERP. 2	296436	1278073	10	1940	DE	Forage	Forage positif	79	----	----	1005	80	----
	Djibouti	douda	RG 1	296377	1276567	16	1972	DE	Forage	Onead	35	----	15	3450	34	41
	Djibouti	Djibouti	RG 5	296341	1277398	17	1966	DE	Forage	Abandonné	38	----	16	5300	28	38
	Djibouti	Djibouti	MOBIL	296172	1284067	6	1988	DE	Forage	HS	42	----	----	----	----	----
	Djibouti	Djibouti	RG 4	296129	1277399	12	----	DE	Forage	Abandonné	40	----	10	----	----	----
	Djibouti	Djibouti	RG 6	296125,358	1276876,57	26	1966	DE	Forage	Abandonné	51	----	19	----	36	45
	Djibouti	Djibouti	RG 2	296121	1276231	11	1972	DE	Forage	Fonctionnel	51	----	19	2850	74	42
	Djibouti	Djibouti	RG 2b	296121	1275992	----	2003	DE	Forage	Onead	----	----	----	----	----	----
	Djibouti	Djibouti	E 4	296086	1275494	27	1962	DE	Forage	Abandonné	37	----	26	2040	29	39
	Djibouti	Djibouti	RG 3	296002	1276478	20	1972	DE	Forage	Fonctionnel	46	----	20	3100	47	41
	Djibouti	Djibouti	Torobora (Défilé)	295993	1276783	----	2007	DE	Forage	Forage positif	----	----	----	----	----	----
	Djibouti	Djibouti	BOELAYYAL	295869	1282294	54	1990	DE	Forage	HS	228	----	----	----	----	----
	Djibouti	Djibouti	RG 7	295642,315	1277156,31	26	1966	DE	Forage	Abandonné	51	----	26	5000	----	42
	Djibouti	Djibouti	DORALE	290394	1280879	19	1988	DE	Forage	Forage positif	28	----	13	2780	1	35
	Djibouti	Djibouti	Forage Lootha	289480	1276686	78	2007	DE	Forage	Forage positif	----	----	----	----	----	----

	Djibouti	Djibouti	AWRLOFOUL	287329	1275675	116	1990	DE	Forage	HS	128	----	76	1200	----	----
	Djibouti	Djibouti	Awrolofoul	287091	1276018	110	2007	DE	Forage	Forage positif	----	----	----	----	----	----
	Djibouti	Djibouti	Forage-ZAMZAM	284904	1278882	140	2009	DE	Forage	Forage positif	----	----	----	----	----	----
	Djibouti	pk20	PK 20 -17	283759	1 278 873	140.18	1996	DE	Forage	Forage positif	170	----	106.9	1228	7	----
	Djibouti	pk20	PK 20 - 1	282970	1276443	157	1980	DE	Forage	Fonctionnel	161	----	94	1990	41	44
	Djibouti	pk20	PK 20 – 12	282637	1276537	150	1982	DE	Forage	Forage positif	135	----	----	1300	26.3	42
	Djibouti	pk20	PK 20 – 6	282331	1276171	150	1982	DE	Forage	Forage positif	89	----	----	----	----	----
	Djibouti	pk20	PK 20 – 7	282331	1276171	150	1982	DE	Forage	Forage positif	152	----	96	----	45	42
	Djibouti	pk20	PK 20 – 4	282126	1277125	150	1982	DE	Forage	Abandonné	158	----	----	----	----	----
	Djibouti	pk20	PK 20 – 5	282126	1277125	150	1982	DE	Forage	Forage positif	146	----	94	----	18	----
	Djibouti	pk20	PK 20 - 3	282126	1277125	157	1981	DE	Forage	Forage positif	156	----	94	----	40	----
	Djibouti	pk20	PK 20 -16	281923	1278468	171.76	1996	DE	Forage	Forage positif	202	----	118.79	1080	24	46
	Djibouti	pk20	PK 20 -14	281372	1277972	187.5	1996	DE	Forage	Forage positif	265	----	133.57	1049	50	43
	Djibouti	pk20	PK 20 -15	280122	1278352	170.59	1996	DE	Forage	Forage	241	----	113.9	1089	40	----

										positif						
	Djibouti	Arta	PK23	277864	1277864	220	2008	US	Forage	Fonctionnel	----	----	----	----	----	50

N°I	Région	Poste administratif	Localité	Nom-Pt d'eau	X(m)	Y(m)	Z(m)	Date	Réa.	Type O	Etat	Prof (m)	NS (m)	ND (m)	Conduc tiviyt	Q (m3/h)	T(°C)
	Arta	arta	arta	E16	298735	1271966	735	2006	DE	Forage	Forage positif	----	----	----	----	----	----
134	Arta	arta	douda	E10	298144	1273361	30	----	DE	Forage	HS	66	----	33	2000	----	----
126	Arta	arta	douda	E13	296809	1274843	32	----	DE	Forage	Fonctionnel	39,1	22,96	21,71	3150	----	----
130	Arta	arta	douda	E9	296555	1273999	32	----	DE	Forage	HS	51	----	30	3850	----	----
129	Arta	arta	douda	E8	296554	1274588	30	----	DE	Forage	Fonctionnel	----	----	----	----	----	----
135	Arta	arta	douda	E11b	296410	1273403	20	2005	DE	Forage	Onead	42,7	----	30	2700	----	----
	Arta	arta	arta	E 8b	296230	1274387	29	1965	DE	Forage	Onead	44	----	28	1800	31	38
	Arta	arta	arta	E 9	296076	1273927	31	1965	DE	Forage	HS	51	----	30	3850	18	41
	Arta	arta	nagad	E 10	296013	1273589	34	1965	DE	Forage	HS	66	----	33	2000	36	44
	Arta	arta	arta	AGADER 1	295343	1273163	43	1986	DE	Forage	Forage positif	61	----	44	1350	12	42
	Arta	arta	arta	AGADER 2	293679	1273481	59	1989	DE	Forage	Forage positif	67	----	----	1350	112	42
	Arta	arta	agader	AGADER 3	293679	1273481	59	1990	DE	Forage	HS	97	----	52	2300	20	----
	Arta	arta	wea	Weha 14	290 951	1273499	61	1986	DE	Forage	Piézo	108	----	60	1070	----	57
	Arta	arta	Arta	CHABELLEY 1	290025	1271047	150	1990	DE	Forage	Fonctionnel	150	----	----	1194	6	48
121	Arta	Arta	chabeley	Chabeley F2	289944	1271494	106	----	DE	Forage	Fonctionnel	150	----	91	1230	----	----
842	Arta	arta	Chabeley	Chabeley F1	289926	1271527	108	2006	FORACO	Forage	Fonctionnel	149	94,8	94,53	1194	17,6	----
	Arta	arta	Chebelley	CHABELLEY 2	289110	1270131	150	1983	DE	Forage	Fonctionnel	150	----	91	1230	20	48
	Arta	arta	Wea	Weha 2	283759	1272357	415	1971	DE	Forage	Fonctionnel	25	----	2	1470	18	35
	Arta	arta	arta	PK 20 - 8	283370	1273029	150	1983	DE	Forage	Forage positif	157	----	98	1250	30	45
	Arta	arta	arta	PK 20 - 9/1	283370	1273029	150	1983	DE	Forage	HS	151	----	87	1700	15	47
	Arta	arta	arta	PK 20 - 2	282686	1274847	170	1981	DE	Forage	HS	172	----	107	1600	----	43
	Arta	arta	arta	PK 20 -9/3	281848	1272025	150	1985	DE	Forage	Fonctionnel	154	----	----	----	----	----

	Arta	arta	arta	PK 20 - 4 Bis	281848	1272025	150	1985	DE	Forage	HS	----	----	----	----	----	----
	Arta	arta	pk20	PK 20 - 9/2	281848	1272025	150	1983	DE	Forage	HS	154	----	87	1700	40	47
	Arta	arta	pk20	PK 20 – 10	281848	1272025	162	1983	DE	Forage	HS	160	----	100	----	----	----
	Arta	arta	pk20	PK 20 – 11	281848	1272025	150	1982	DE	Forage	Forage positif	143	----	----	----	----	----
	Arta	arta	pk20	PK 20 – 13	281848	1272025	148	1984	DE	Forage	Forage positif	133	----	97	----	36	----
	Arta	Arta	wea	Weha 4	265784	1272295	415	1977	DE	Forage	Piézo	27	----	12	----	12	37
	Arta	Arta	wea	Weha 1	265693	1272357	416	1967	DE	Forage	Fonctionnel	29	----	7	----	14	37
117	Arta	Arta	wea	Weha 12	265656	1272301	422	----	DE	Forage	Fonctionnel	----	----	----	----	----	----
	Arta	arta	Wea	Weha 11	265647	1272171	416	1995	DE	Forage	Onead	118	16,24	25,2	1284	10	37,2
	Arta	Arta	wea	Weha 3	265510	1272204	417	1971	DE	Forage	HS	24	----	4	1400	25	36
	Arta	Arta	wea	Weha 9	265479,4767	1272143,171	461	1989	DE	Forage	HS	130	----	21	1270	20	39
	Arta	Arta	wea	Weha 6	265479	1272143	461	1983	DE	Forage	Fonctionnel	50	----	10	1250	16	34
	Arta	Arta	wea	Weha 7	265479	1272143	461	1983	DE	Forage	Fonctionnel	48	----	8	1150	20	34,0
118	Arta	Arta	wea	Weha 13	265434	1273210	420	----	DE	Forage	Onead	61	7,2	10,28	1252	62	----
	Arta	Arta	wea	Weha 5	265419	1272205	420	1976	DE	Forage	HS	27	----	7	1380	41	35
	Arta	Arta	wea	Weha 10	265373	1272113	461	1990	DE	Forage	Onead	132	18,78	26,52	----	20	37
	Arta	Arta	wea	Weha 8	264967	1271862	461	1987	DE	Forage	Onead	70	20,14	21,68	1288	20	38,3
109	Arta	arta	arta	F2	264525	1270240	454	----	DE	Forage	HS	----	----	----	----	----	----
	Arta	arta	arta	ALI - FADEN	264503	1271321	440	1980	DE	Forage	HS	----	----	----	1300	----	37
108	Arta	arta	arta	Ali-Faren F1	264235	1270808	452	----	DE	Forage	Fonctionnel	30	----	8,2	1300	----	----
	Arta	Arta	Arta	ARTA PLAGE 1	262093	1281267	----	1992	DE	Forage	HS	20	----	----	----	----	----
	Arta	Arta	Arta	ARTA PLAGE 2	261898	1279547	200	1992	DE	Forage	HS	20	----	9	----	----	----
	Arta	Arta	pk20	PK - 48	260268	1265518	517	2007	DE	Forage	Fonctionnel	----	----	----	----	----	29
	Arta	Arta	Wea	PETIT-BARA 1	260255,9426	1258965,507	581	1978	DE	Forage	Forage	75	----	----	----	----	----

											Négatif						
	Arta	Arta	Arta	PK 50	257998,6729	1265191,756	528	1972	DE	Forage	Fonctionnel	90	----	68	1320	22	40
115	Arta	Arta	Arta	Wea F10	256330	1272280	418	----	DE	Forage	Fonctionnel	131,5	----	13,55	1120	----	----
	Arta	Arta	Arta	PK51	255734	1263658	551	2007	DE	Forage	Fonctionnel	----	----	----	----	----	----
105	Arta	arta	petit bara	Petit-Bara F3	255087	1259330	570	----	DE	Forage	Forage Négatif	106	----	----	----	----	----
828	Arta	arta	Kourtimaley	F4	255072	1259129	578	----	DE	Forage	Forage positif	161	108	----	----	----	----
106	Arta	Arta	Arta	F4	255072	1259129	578	----	DE	Forage	Fonctionnel	161	----	108	1900	----	----
	Arta	arta	petit bara	PETIT-BARA 3	255010,5502	1259159,342	575	1978	DE	Forage	HS	106	----	----	----	----	----
	Arta	arta	petit bara	PETIT-BARA 4	254859,3892	1259221,989	581	1984	DE	Forage	Fonctionnel	161	----	108	1900	17	41
	Arta	arta	petit bara	PETIT-BARA 2	254857,0099	1258914,621	581	1978	DE	Forage	HS	82	----	----	----	----	----
	Arta	Arta	Arta	Iskoutir	248746	1250293	569	2009	DE	Forage	Fonctionnel	----	----	----	----	----	----
826	Arta	arta	Kourtimaley	Korti-Malay F1	245960	1253566	563	----	DE	Forage	HS	90	39	----	----	----	----
104	Arta	Arta	Arta	Korti-Malay F1	245960	1253566	563	----	DE	Forage	HS	90	----	39	8120	----	----
527	Arta	Arta	Arta	Doudoub Boulaleh F1	243546	1244558	572	2005	DE	Forage	Fonctionnel	102	75	----	2650	25	35
56	Arta	Arta	Arta	Doudoub Boulaleh F2	242795	1246915	560	----	DE	Forage	Fonctionnel	11O	----	67,79	2580	----	----
825	Arta	arta	arta	Gabla-Galan F1(bis)	236184	1249634	552	2006	FORACO	Forage	Fonctionnel	134	84,52	84,23	1118	13	----
	Arta	arta	arta	Gabla-Galan F1	236184	1249634	552	1989	Italie	Forage	HS	156	84,08	84,57	2790	10,14	41,6
	Arta	Arta	Wea	KARTA 2	232986,6549	1265947,157	458	1987	DE	Forage	Forage Négatif	35	----	----	----	----	----
	Arta	Arta	Arta	Karta F3	232919	1266008	550	2006	DE	Forage	Forage	----	----	----	----	----	----

											Négatif					
	Arta	Arta	Wea	KARTA 1	232675,5791	1265027,5	457	1983	DE	Forage	Forage Négatif	123	----	----	----	----	----
	Arta	Arta	Karta	Forage karta	231080	1268597	492	----	DE	Forage	Forage Négatif	----	----	----	----	----	----
	Arta	arta	Karta	Forage karta 1	230436	1268829	497	1985	DE	Forage	Forage Négatif	----	----	----	----	----	----
119	Arta	arta	Hemed	Karta F1	230434	1268828	494	----	DE	Forage	Forage Négatif	123	----	----	----	----	----
	Arta	arta	ASSAL	ASSAL 4	226422	1278301	200	1987	DE	Forage	Forage Négatif	2013	227	----	175644	----	36
	Arta	arta	ASSAL	ASSAL 2	225259	1276990	180	1975	DE	Forage	Forage Négatif	1554	----	----	----	----	----
	Arta	arta	ASSAL	ASSAL 3	225050	1277391	180	1987	DE	Forage	Forage Négatif	1316	----	----	----	----	50
	Arta	arta	ASSAL	ASSAL 1	224775	1277117	----	1974	DE	Forage	Forage Négatif	1147	----	----	----	----	----
	Arta	arta	ASSAL	ASSAL 6	224296	1277859	182	1988	DE	Forage	Forage Négatif	1761	240	----	----	----	----
	Arta	Arta	Wea	KARTA 3	223150,9828	1268337,977	458	1987	DE	Forage	Forage Négatif	31	----	----	----	----	----
	Arta	Assal	ASSAL	ASSAL1	225259	1276990	2	1975	DE	Forage	Forage Négatif	1154	----	----	----	----	----
	Arta	Assal	ASSAL	ASSAL3	224775	1277117	1	----	DE	Forage	Forage	146	----	----	----	----	----

											Négatif						
137	Arta	Damerjog	Damerjog	E23	301202	1269130	37	----	DE	Forage	HS	40	17	----	2120	----	----
	Arta	Damerjog	Damerjog	ATTAR 1	302678	1268414	21	1979	DE	Forage	Fonctionnel	33	----	23	2250	40	40
	Arta	Damerjog	Damerjog	ATTAR 2	305824	1267258	16	1985	DE	Forage	Fonctionnel	39	----	21	2110	46	39
	Arta	Damerjog	Damerjog	ATTAR 3	305824	1267258	16	1988	DE	Forage	Fonctionnel	40	----	28	4400	40	----
	Arta	Damerjog	Damerjog	ATTAR 4	303280	1267734	59	1988	DE	Forage	Fonctionnel	50	----	29	1740	70	41
	Arta	Damerjog	Damerjog	ATTAR 5	303815	1265979	140	1989	DE	Forage	Fonctionnel	110	----	70	9000	50	43
	Arta	Damerjog	Damerjog	ATTAR 6	304724	1265974	54	1991	DE	Forage	Fonctionnel	70	----	----	----	----	----
	Arta	Damerjog	Damerjog	ATTAR 7	303805	1269268	27	2002	DE	Forage	Fonctionnel	37	----	25.5	5580	----	27.7
	Arta	Damerjog	Damerjog	ATTAR 7	303653	1269084	22	2002	DE	Forage	Fonctionnel	34	----	16.5	1947	----	35.4
	Arta	Damerjog	Damerjog	ATTAR YAR 1	303805	1271420	13	1986	DE	Forage	Fonctionnel	45	----	13	5200	----	39
	Arta	Damerjog	Damerjog	DAMERJOG	301397	1271895	35	1990	DE	Forage	Fonctionnel	38	----	17	2020	64	36
138	Arta	Damerjog	Damerjog	Damerjog E21	301965	1269001	25	----	DE	Forage	Fonctionnel	3 3,30	----	21	1950	----	----
122	Arta	Damerjog	Damerjog	Damerjog F1	302720	1268432	27	----	DE	Forage	Fonctionnel	38	----	17	2020	----	----
123	Arta	Damerjog	Damerjog	Damerjog F2	302935	1269770	20	----	DE	Forage	HS	34	16,05	----	1947	----	----
	Arta	Damerjog	douda	E 11	296410	1273403	32	1970	DE	Forage	Onead	49,8	----	30	2700	35	40
	Arta	Damerjog	douda	E 14	297927	1274253	14	1974	DE	Forage	Fonctionnel	33	----	12	----	26	38
	Arta	Damerjog	douda	E 16	298012	1273392	24	1974	DE	Forage	Fonctionnel	35	----	24	3850	66	39
	Arta	Damerjog	douda	E 17	298978	1272771	24	1977	DE	Forage	Fonctionnel	27	----	23	3800	----	39
	Arta	Damerjog	douda	E 18	299464	1272186	17	1975	DE	Forage	Onead	33,6	----	15	3700	79	38
	Arta	Damerjog	Damerjog	E 21	302001	1268843	16	1990	DE	Forage	Onead	33,4	----	----	1950	20	37
	Arta	Damerjog	Damerjog	E 22	302535	1268538	19	----	DE	Forage	Onead	38,6	----	----	2130	17	38
	Arta	Damerjog	Damerjog	E 23	302859	1268198	28	1978	DE	Forage	Piézo	40	----	17	2120	60	38
	Arta	Damerjog	Damerjog	E 26	305882	1267269	22	1979	DE	Forage	Onead	32	----	21	2840	70	38

	Arta	Damerjog	Damerjog	E 27	304943	1267179	22.5	1985	DE	Forage	Onead	39	----	22	2940	140	39
	Arta	Damerjog	Damerjog	E 28	303763	1267332	22.8	1988	DE	Forage	Piézo	41	----	28	4400	50.4	----
	Arta	Damerjog	Damerjog	E 31	301254	1268485	28.3	1990	DE	Forage	Fonctionnel	47	----	28	2010	61	----
	Arta	Damerjog	Damerjog	E 32	305028	1266033	28.4	1990	DE	Forage	Forage Négatif	70	----	----	----	----	----
	Arta	Damerjog	Damerjog	E 38-LOYADA	308187	1267059	15	1981	DE	Forage	Piézo	20	----	14	2900	39	36
	Arta	Damerjog	douda	E 7	296596	1274630	28	1965	DE	Forage	Abandonné	43	----	27	2450	36	38
	Arta	Damerjog	douda	E 7b	296578	1274419	28	2003	DE	Forage	Onead	----	----	----	----	----	----
	Arta	Damerjog	douda	E 9 BIS	296582	1273868	29	1972	DE	Forage	Onead	45	----	27	----	41	40
854	Arta	Damerjog	douda	E1	298940	1269141	53	----	DE	Forage	Fonctionnel	67	46	----	1920	----	----
	Arta	Damerjog	douda	E15	297863	1273853	32	2006	DE	Forage	Forage positif	----	----	----	----	----	----
	Arta	Damerjog	douda	E17	299046	1272740	27	2006	DE	Forage	Forage positif	----	----	----	----	----	----
	Arta	Damerjog	douda	E17b	299046	1272740	27	2006	DE	Forage	Onead	31	----	----	----	----	----
139	Arta	Damerjog	Damerjog	E22	302511	1268605	26	----	DE	Forage	Fonctionnel	34,5	----	18,3	2130	----	----
861	Arta	Damerjog	Damerjog	E22b	302548	1268552	26	2006	DE	Forage	Onead	34	18,3	----	----	----	----
862	Arta	Damerjog	Damerjog	E24	304654	1267377	24	1978	DE	Forage	Onead	31	22	----	----	----	----
863	Arta	Damerjog	Damerjog	E25	305136	1266564	27	1976	DE	Forage	Onead	29	18	----	----	----	----
146	Arta	Damerjog	Damerjog	E27	302930	1268176	35	----	DE	Forage	HS	39	22	----	2940	----	----
	Arta	Damerjog	Damerjog	E29	302969	1268037	34	1988	DE	Forage	HS	41	28	----	4400	50	----
	Arta	Damerjog	Damerjog	E29b	302969	1268037	34	1995	DE	Forage	Onead	51	----	----	----	----	----
869	Arta	Damerjog	Damerjog	E31	301241	1268967	34	1993	DE	Forage	Onead	47	28	----	----	----	----
	Arta	Damerjog	Damerjog	E33b	298904	1269147	53	2006	DE	Forage	Onead	65	----	----	----	----	----
131	Arta	Damerjog	Damerjog	E9 (bis)	302932	1268150	38	----	DE	Forage	HS	52	----	30	1940	----	----
	Arta	Damerjog	Damerjog	EM1	303867	1267417	36	2006	DE	Forage	Fonctionnel	----	----	----	----	----	----

	Arta	Damerjog	Damerjog	EM2	303853	1267439	38	2006	DE	Forage	Fonctionnel	----	----	----	----	----	----
	Arta	Damerjog	Damerjog	EM3	303843	1267461	38	2006	DE	Forage	Fonctionnel	----	----	----	----	----	----
	Arta	Damerjog	Damerjog	EM4	303832	1267425	36	2006	DE	Forage	Fonctionnel	----	----	----	----	----	----
	Arta	Damerjog	Damerjog	EM5	303823	1267444	38	2006	DE	Forage	Fonctionnel	----	----	----	----	----	----
757	Arta	Damerjog	Damerjog	F3	298904	1268688	53	----	DE	Forage	HS	----	----	----	----	----	----
	Arta	Damerjog	douda	GODCHABEL 1	296972	1267160	96	1986	DE	Forage	Forage positif	120	----	0	1572	17	42
756	Arta	Damerjog	Damerjog	God-Chabel F2	298940	1269141	53	----	DE	Forage	HS	----	----	----	----	----	----
	Arta	Damerjog	Damerjog	Loyada1	306169	1268059	16	2008	DE	Forage	Fonctionnel	----	----	----	----	----	----
	Arta	Damerjog	Damerjog	Loyada2	305660	1268195	21	2008	DE	Forage	Fonctionnel	----	----	----	----	----	----
	Arta	Damerjog	Damerjog	Loyada3	305560	1268195	21	2008	DE	Forage	Fonctionnel	----	----	----	----	----	----
	Arta	Damerjog	Damerjog	MIGDAOUNE 1	303569	1265428	62	1986	DE	Forage	HS	69	----	46	482	----	38
	Arta	Damerjog	Damerjog	MIGDAOUNE 2	305509	1265354	62.1	1986	DE	Forage	Piézo	85	----	48	8394	----	37
	Arta	Damerjog	Damerjog	MOGUARADA	306050	1264583	149	1992	DE	Forage	Piézo	66	----	49	4850	14	----
	Arta	Damerjog	Damerjog	NAASLEY	301245	1271896	35	1986	DE	Forage	Forage positif	34	----	7	3235	----	36
	Arta	Damerjog	douda	E 20	300843	1270577	13.5	1972	DE	Forage	Piézo	31	----	22	2600	59	38
	Arta	Damerjog	douda	E 19	300312	1270921	21	1977	DE	Forage	Onead	33,6	----	22	3650	53	38
136	Arta	Damerjog	douda	Douda-Yar E18	299046	1272747	32	----	DE	Forage	Fonctionnel	30	15	15	3700	----	----
	Arta	Damerjog	Douda	E 33	298985	1269083	50.5	1991	DE	Forage	Fonctionnel	67	----	50	2120	65.3	----
	Arta	Damerjog	Douda	E 36	298330	1258897	50.5	1998	DE	Forage	Onead	185	----	----	----	----	----
	Arta	Damerjog	douda	GALILE	297918	1272839	15	1986	DE	Forage	Fonctionnel	56	----	----	2920	----	36
	Arta	Damerjog	Douda	E 35	297038	1259545	----	1998	DE	Forage	Onead	198	----	----	----	----	----
	Arta	Damerjog	douda	DOUDA TP	296408	1273771	22	1986	DE	Forage	Fonctionnel	28	----	----	----	13	----
128	Arta	Damerjog	douda	Douda E7(bis)	296243	1274233	34	----	DE	Forage	Fonctionnel	42,6	29,72	28	2580	----	----
161	Arta	Damerjog	douda	Douda E19	296048	1273492	43	----	DE	Forage	HS	35	----	21,2	3230	----	----

	Arta	Damerjog	douda	GUISSI 1	295029	1271475	59	1986	DE	Forage	Fonctionnel	90	58	----	1540	----	42
	Arta	Damerjog	douda	E 30	294248	1273465	30	1990	DE	Forage	Onead	67	----	44	1895	82	----
829	Arta	Djibouti	Pk50	PK 50	258181	1265305	530	----	DE	Forage	Fonctionnel	90	68	----	----	----	32
827	Arta	Djibouti	Petit-Bara	Petit-Bara F3	255087	1259330	570	----	DE	Forage	Forage Négatif	106	----	----	----	----	38